UNIVERSITÀ DEGLI STUDI DI PADOVA

UNIVERSITA' DEGLI STUDI DI PADOVA

Dipartimento di Ingegneria Industriale DII

Corso di Laurea Magistrale in Ingegneria dell'Energia Elettrica

Tesi di Laurea Magistrale

DEVELOPMENT OF A SMART GRID MODELLING TOOL, CONSIDERING OPTIMAL CONTROL OF ELECTRIC VEHICLES

Relatore: Prof. Roberto Turri

Correlatore: Prof. Ghanim Putrus, Northumbria University

Laureando: Manuel Nicoli
[1129607]

Anno Accademico 2017/2018

INDEX

SUMMARY

In the world, power generation industry and transportation sector are still reliant on fossil fuel resources, despite their gradual depletion and the environmental concerns. Moreover, global energy demand is rapidly increasing due to the economic and population growth, leading to higher carbon dioxide emissions and very challenging future choices.
European Union, but also many other Countries of the world, are promoting policies to stimulate the adoption of Renewable Energy Sources (RES) and the electrification of transport in order to reduce fossil fuels use. They expect to combine these two strategies because Electric Vehicles (EVs) can support a high penetration of RES and renewable sources can solve several problems for the EVs. This is true only if charging of electric vehicles is properly managed, otherwise it can lead to severe consequences in the operation of local distribution systems.
In this context, the thesis project aims to create a novel tool, based on a Matlab/Simulink platform, able to model distribution networks and analyse the impact of EV charging, renewable energy generation and the adoption of smart grid technologies. The tool, which is managed through a user-friendly GUI (Graphic User Interface), needs input information, about the characterization of electricity network and connected systems, in order to depict a geographical representation and perform a techno-economic assessment of the modelled system, considering different EV charging strategies.
The tool has been applied to analyse an existing low-voltage distribution network, applying different scenarios according to current and expected operating conditions in the year 2050. Moreover, the simulations of the forecasted ones consider three different charging strategies: uncontrolled, smart and V2G (Vehicle-to-Grid). In the last two typologies, the modelling tool performs a cost function optimization problem that defines the charging profile of each EV, also taking into account battery degradation costs.
The results show the severe consequences related to uncontrolled EV charging, as current and voltage constraints violations and distribution transformer overloading; while vice versa, they demonstrate the technical and economic feasibility of smart charging and V2G technology.
In the next decades, EV penetration is expected to achieve very high targets; therefore, relevant regulations will have to be defined in order to maintain the power system operating.
In conclusion, to ensure a sustainable implementation of EVs in the transportation sector, EV charging will have to be properly controlled and, in addition, V2G technologies, by providing ancillary services, will be able to represent alternative revenue streams to offset the high vehicles initial cost.

SOMMARIO

L'industria della generazione di energia elettrica e il settore dei trasporti sono, tuttora nel mondo, dipendenti dai combustibili fossili, nonostante il loro progressivo esaurimento e le crescenti preoccupazioni in tema ambientale. Inoltre, il consumo mondiale di energia è in rapido aumento a causa della crescita economica e demografica, comportando, quindi, da un lato maggiori emissioni di anidride carbonica, dall'altro scelte future molto impegnative.
L'Unione Europea, ma anche molti altri Paesi del mondo, stanno promuovendo politiche per incentivare l'adozione di Fonti Energetiche Rinnovabili (FER o RES) e l'elettrificazione dei trasporti con l'obiettivo di ridurre l'uso di combustibili fossili. Si prevede, infatti, la combinazione di queste due strategie in quanto i veicoli elettrici (EV) possono sostenere un alta diffusione di FER e le rinnovabili possono risolvere molti problemi correlati all'adozione dei veicoli elettrici. Questo è vero, però, solo se la ricarica dei veicoli elettrici viene gestita opportunamente, altrimenti può determinare gravi conseguenze nel funzionamento dei sistemi di distribuzione.
In questo contesto, il lavoro di tesi si è focalizzato sullo sviluppo di un nuovo software, basato su una piattaforma Matlab/Simulink, in grado di modellare reti elettriche di distribuzione e di analizzare l'impatto della ricarica dei veicoli elettrici, della generazione fotovoltaica e dell'adozione di tecnologie per reti intelligenti. Lo strumento di modellazione, che è controllabile attraverso una semplice interfaccia grafica utente (GUI), necessita di alcune informazioni di input riguardanti la caratterizzazione della rete elettrica e dei sistemi ad essa connessi, al fine di costruire la rappresentazione geografica ed eseguire la valutazione tecnico-economica del sistema esaminato, considerando differenti strategie di ricarica dei veicoli elettrici.
In particolare, lo strumento è stato utilizzato per analizzare una rete elettrica reale di distribuzione a bassa tensione, applicando diversi scenari in relazione alle condizioni operative attuali e previste per l'anno 2050. Inoltre, nelle simulazioni degli scenari al 2050 sono state prese in considerazione tre diverse strategie di ricarica: incontrollata, intelligente e V2G (Vehicle-to-Grid). Nelle ultime due tipologie, lo strumento ottimizza una funzione di costo per definire il profilo di carica di ciascun veicolo elettrico presente, tenendo in considerazione anche i costi relativi alla degradazione della batteria.
I risultati mostrano le gravi conseguenze legate alla ricarica non controllata, come la violazione dei vincoli di corrente e tensione e il sovraccarico del trasformatore di distribuzione; mentre viceversa, dimostrano la fattibilità tecnica ed economica della ricarica controllata (intelligente) e della tecnologia V2G.
Nei prossimi decenni, si prevede che la diffusione dei veicoli elettrici raggiungerà livelli molto importanti; pertanto, dovranno essere definite normative adeguate al fine di mantenere operativo il sistema elettrico.
In conclusione, per garantire un'implementazione sostenibile dei veicoli elettrici nel settore dei trasporti, la loro ricarica dovrà essere gestita adeguatamente e, inoltre, le tecnologie V2G, fornendo servizi ancillari, saranno in grado di rappresentare fonti di reddito alternative per compensare gli ancora elevati costi iniziali dei veicoli.

1. INTRODUCTION

University of Northumbria at Newcastle, which received me for six months of Erasmus program, is one of the main partners of SEEV4-Grid consortium. This thesis project comes as an attempt to meet the needs of SEEV4-Grid project, described below.
In the current stage of the plan, the main targets concern modelling and simulations; therefore, the purpose of this thesis is to create a new tool, based on Matlab/Simulink platform, able to model distribution networks and analyse their operating conditions. It takes into account passive loads, photovoltaic generation and the implementation of different EV charging strategies, which are settable among uncontrolled, smart or V2G methods.

1.1. Background

In the world, power generation industry and transportation sector are mainly based on fossil fuel resources. Their energy consumption has grown rapidly over the last decades. Moreover, International Energy Agency projects significant growth in world energy demand [1]. It is expected to increase by 40% until 2040.
Electricity generation and transportation are responsible for about 60% of all energy use in the world [2], so the promotion and adoption of Renewable Energy Sources (RES) and electrification of transport are essential for future power systems [3] and they offer a great potential for reducing fossil fuel use.

The deployment of RES is expected to speed up not only in Europe, in order to reach the targets promoted by the EU Member States, but also in many other Countries of the world, where many researches are aimed to achieve high RES implementation, especially after Fukushima accident [4]. Indeed, as shown in the following Fig. 1.1.1 and Fig. 1.1.2, the trends of annual additions of global photovoltaic (PV) and wind generating capacity [5] reflect what was stated before.

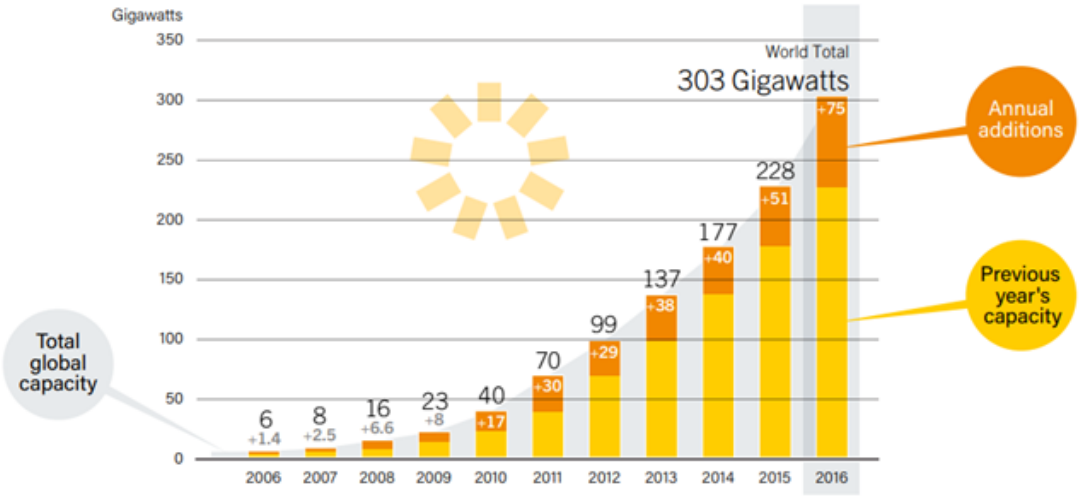

Fig. 1.1.1 Solar PV global capacity and annual additions, 2006-2016 [5]

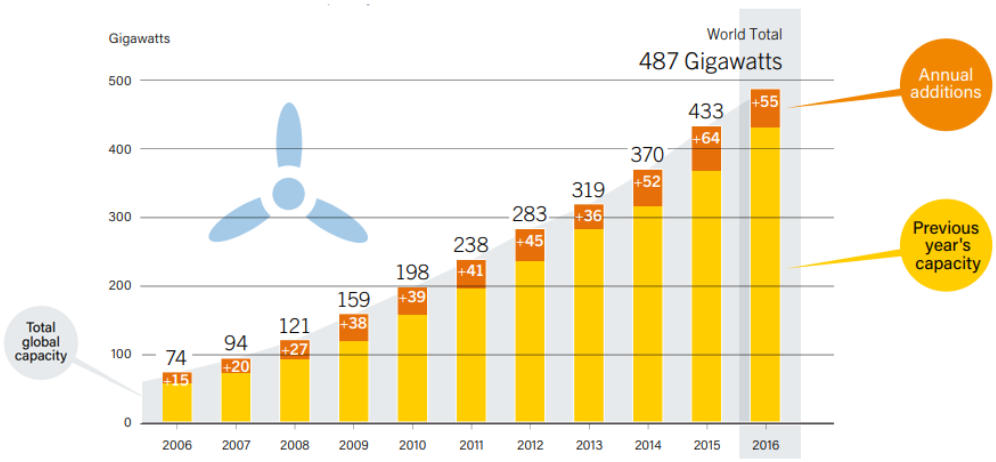

Fig. 1.1.2 Wind Power global capacity and annual additions, 2006-2016 [5]

European Union (EU) has set up a challenging 2050 low-carbon roadmap in order to reduce by 80% Greenhouse Gas (GHG) emissions by that year. Fig. 1.1.3, provided by European Commission in [6], illustrates the planned path to reach the intended goal. The red line projection shows how GHG emissions would develop according to current policies.

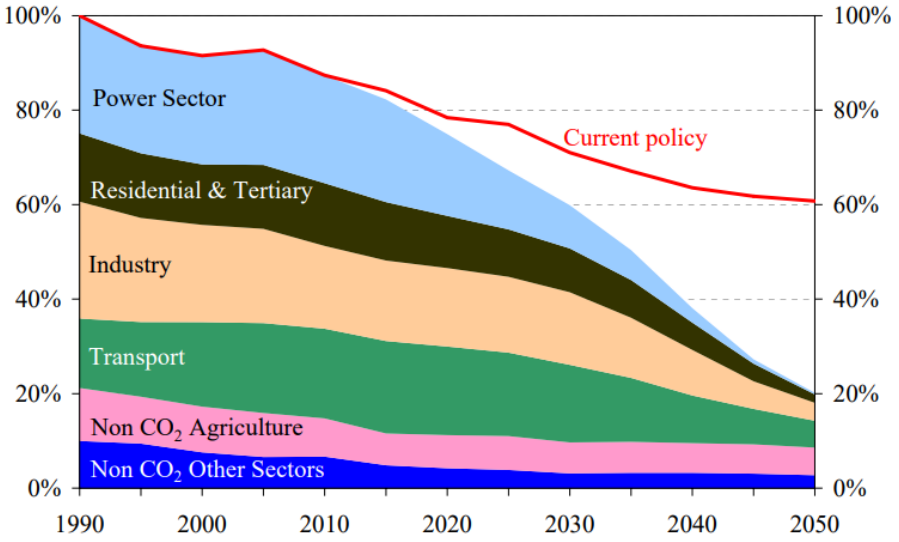

Fig. 1.1.3 EU GHG emissions towards an 80% domestic reduction (1000% = 1990) [6]

However, it considers two intermediate climate and energy targets for the years 2020 and 2030 to put the EU on the way to achieve the aforementioned low-carbon economy.
European leaders set for 2030 [7]:

- A 40% reduction in greenhouse gas emissions compared to 1990 levels;
- A 27% share of RES in the energy mix;
- A 27% increase in energy efficiency.

Of course, from an electricity generation point of view, these targets are reachable mainly through a massive deployment of Photovoltaic (PV) panels and wind farms, if we ignore nuclear power plants; while, plug-in Electric Vehicles (EVs), moved by electric motors and powered by electrochemical batteries, represent a promising solution from a transportation sector point of view [7].

Indeed, EVs have higher efficiency and lower operating costs compared to the conventional Internal Combustion Engine (ICE) vehicles [8]; the constant research on lithium-ion batteries and fast charging technology will be the major facilitator for EVs roll out, though high initial price, limited driving range and limited charging facilities may represent limitations.
For this reason, many Countries have taken specific policy initiatives to encourage RES implementation and EVs introduction [9].

International Energy Agency (IEA) reports that the global number of EVs has exceeded 2 million in 2016 [10] with a global evolution, until 2016, shown in the following Fig. 1.1.4.

Electric-power industry forecasts that the number of EVs in the world would increase by 5 million per year by 2020 [11] and will be more than 2 hundred million by the year 2050 [12].

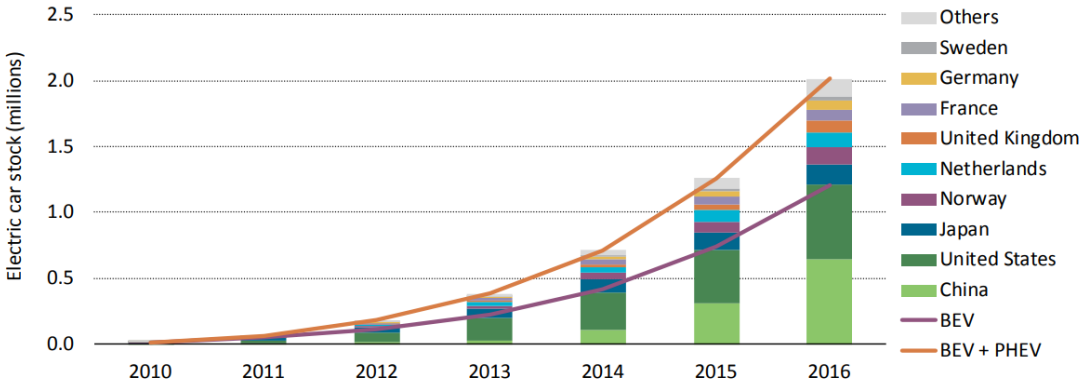

Fig. 1.1.4 Evolution of the global electric car stock, 2010-2016 [10]

However, both RES and EVs have heavy downsides:

- Most of renewable energy sources are characterized by an intrinsic intermittency and unpredictability, so a large-scale penetration can cause severe challenges in energy generation and load balance maintenance to ensure power network stability and reliability [13]. A further huge problem arises when many Distributed Generation (DG) plants are located in areas where energy demand is low. In this case Power Quality problems, like reverse power flow and line overvoltage, can occur [14]. DG can also lead to higher fault currents, network protection system failure and phase imbalances [15];
- A high EVs penetration can considerably increase the electricity demand and its daily peak if EV charging is uncontrolled. Random charging profiles and large scale of EVs can cause high voltage deviations, distribution losses and degradation in term of power quality. Moreover, they can reduce lifetime of the transformers due to overload and instability [16].

EV charging can lead to synergies with distributed generation and smart demand-side technologies; it can be scheduled to charge the vehicles when green power production is high with energy cost savings for users and system. So, EVs can be an important participant in Demand Response (DR) strategies [3]; as well as EVs can become electricity storage and providers, if they are managed in bulk by an intermediary entity, called aggregator [17].
Hence, the large scale of grid-connected EVs can be considered as a huge energy storage distributed in the power grid and controlled charging schedules can arrange a charging when the grid has a surplus of RES generation and a discharging at the time when grid has less capacity, in order to provide a storage facility for supply/demand matching [14]. Therefore, the potential of EVs to share energy with the power network has created a new opportunity to

improve the system reliability and sustainability, allowing a large-scale integration of RES [12]. This concept, called Vehicle-to-Grid (V2G) technology, was firstly adopted by Kempton in [18].
In the retail energy market, the storage, provided also by EV batteries, can decrease energy costs through load levelling and avoiding renewable electricity spillage. In fact, it is possible that renewable generation can be spilled during valley hours if no storage is available on the electricity network [4].

Traditionally, power systems include some large generating power plants, linked together by a high voltage transmission system, which supplied electricity to consumers via medium and low voltage distribution networks [14]; they have no storage, therefore generation must be continuously managed in order to match the fluctuating customer consumption, maintaining a constant frequency value in the electricity grid.
With RES spread, the direction of power flows into the grid is not as obvious as it was before; so, if energy storage infrastructures were not implemented in the electricity network, power system regulation would become much trickier and a worsening of power quality could be occurred.

A reliable wide scale energy storage technology already exists, Pumped Hydroelectric Energy Storage (PHES) is the main and most developed form of energy storage available so far in the world, but its available energy capacity is inadequate and, moreover, new suitable locations to build up new PHES plants are limited [19]. Other energy storage technologies are currently available [3], but they are not economically sustainable because of their capital and operational costs.
However, the capital cost can be avoided if EV batteries are exploited when electric vehicles are plugged in, so from this point of view, many researchers assert that V2G implementation can lead many potential benefits to the power grid. For example, peak load shaving and load levelling, but it can also support the grid by ancillary services such as spinning reserve, voltage and frequency regulations. In conclusion, energy regulation services improving energy efficiency and mitigation of RES intermittency.
V2G concept is part of Smart Grid technologies, which involve EVs to make positive change in the power system operation.

For these reasons, a very large implementation of new entities in the electricity grid, such as small-distributed generators and electric vehicles, has imposed a redefinition of power systems concept.
The European Technology Platform for Electricity Networks of the Future has defined the concept of Smart Grid (SG) as: "An electricity network that can intelligently integrate the actions of all users connected to it (generators, consumers and those that do both) in order to efficiently deliver sustainable, economic and secure electricity supplies" [14].
In the recent years, users that are both producers and consumers are conventionally called prosumers (combining *pro*-ducers with con-*sumers*).
SG will have to integrate EVs, renewable generations and distributed generation into the traditional power network, exploiting real-time communication in order to coordinate bidirectional power flows, through intelligent control strategies. To realize this, fundamental infrastructures need an overall upgrade; indeed, both actual power grid infrastructures and EVs charging stations are not so developed to manage bidirectional power flows [11].

Recapping, it has been introduced that large scale adoption of EVs will permit a much bigger implementation of renewable energy generation into the grid than those would have been

possible without their energy storage [14], considering the high costs of the electricity storage technologies.
The economic feasibility of EVs depends on the availability of cost-effective batteries with high power and energy density [20]. As reported in [21], Lithium-ion batteries are a key technology for actual and coming energy storage applications.
Nowadays, batteries cost covers a significant fraction of the overall cost of many applications, but many studies, including [7] and [20], report that batteries cost is expected to decrease with high-volume of cell production and the upcoming improvements of manufacturing technologies.

Automotive manufactures recommend battery replacement when the remaining energy capacity reaches (70 ÷ 80) % of the nominal value [20]. That is because the energy capacity left in the battery is not enough to guarantee the EV's designed range.
Nevertheless, a new economic opportunity arises. Decommissioned batteries still have significant power and energy capacity, so they can be used in bulk, so in large-scale BESSs (Battery Energy Storage Stations) connecting several units in series and parallel arrangement, or in distributed scale to provide important grid-balancing services.
These ancillary services, provided by second use or second life of EV batteries, can represent alternative revenue streams to offset their high initial cost [20], also because, BESS control strategies are not influenced by the EV user transportation needs anymore.
In this way, exploiting both EVs and BESSs, the Automatic Generation Control (AGC) could, for example, perform frequency regulation (FR) on both generation and load sides simultaneously to help traditional generating units [3].

The expected development of EV market requires a corresponding progress in the charging facilities sector. Next to the batteries, the availability and reliability of chargers are extremely important. Many studies are aimed to improve chargers efficiency, to make them more versatile and to reduce charging costs.

Statistics, reported in [7] and [18], show that personal vehicles are used, in average, for transportation about only 4% of the time, for an average daily commuting trip of 24 km, about 15 miles; so, they are parked for more than 22h every day. However, considering a fleet of vehicles, the share of those being parked never falls below 75%. Consequently, V2G technology appears as a promising innovative solution.
However, V2G technology requires frequent charging and discharging cycles which cause extra battery degradation of EVs. This problem can create a strong social barrier for V2G implementation. A very important research area concerns the assessment of the impacts of V2G services on the battery life in Battery Electric Vehicles (BEVs) and Plug-in Hybrid Electric Vehicles (PHEVs), all referable to the acronym EVs [22].
The battery degradation is a function of the number of charging/discharging cycles, the operating temperature, the depth of discharge (DOD) or State Of Charge (SOC) and of the total energy exchanged.
Batteries used in the EVs are usually charged between an upper limit of (80 ÷ 90) % of their State of Charge (SOC) and a lower limit of (20 ÷ 30) % of SOC [20]. However, battery capacity degradation is inevitable as the battery is used to meet transport needs, but V2G strategy can make it worse.

It is also true that nowadays, there are two different payments for the power plants providing ancillary services, the first one is for the power capacity contracted, the second one concerns

the energy actually provided to the grid [22]. Therefore, by the same token, there may be payments to vehicles that will provide ancillary services.

As mentioned before, some studies [23] revealed that, most of the vehicles are currently parked more than 90% of their time, so, if they were electric vehicles, they could make available their battery capacity on the electricity network.
In this case, they could remain plugged-in and ready to store or provide energy from/to the grid. As aforementioned, to guarantee the needed power capacity for ancillary services an intermediate system, called aggregator, is necessary. It allows to break down the dependence on EVs plug-in uncertainties and, finally, to handle small-scale power of EVs in order to provide the regulation services on the large-scale network [24].

The basic idea is that, the owners of EVs, participating in ancillary services, would not change their vehicle usage, but they only have to notify the aggregator, through a dashboard interface, the expected plug-out time and the wanted battery level for every plug-in [24]. The aggregator would then manage the EV battery charging and discharging in order to, of course charge the battery, but also provide the power capacity to the electricity grid. Meanwhile, the aggregator would make a contract with the grid operator to provide regulation services with the contracted power capacity of EVs.

1.2. Electrification of road transport system

Electrification of transport combines a high energy efficiency method to move vehicles with the opportunity of using different sources than fossil fuels, indeed, to generate the electricity, required by the Electric Vehicles (EVs), Renewable Energy Sources (RES) can be exploited.
The power is supplied to the EV by on-board battery, which is charged by power grid when plugged in, or by on-board generator, if the EV uses regenerative braking technologies [11].
In the recent years, EVs are gaining high popularity and attention because they promise economic and environmental benefits; in fact, just from an economic point of view, International Energy Agency (IEA) expects a substantial increase in the price of crude oil in the coming decades [25].

EVs can be classified, as shown in Fig. 1.2.1 below, into the following four categories [25]:

- Battery Electric Vehicle (BEV);
- Hybrid Electric Vehicle (HEV);
- Plug-In-Hybrid Electric Vehicle (PHEV);
- Extended Range-Electric Vehicle (EREV).

The first category of EVs is BEVs, which are completely powered by electrochemical batteries. This feature makes BEV zero emission vehicles. However, drivers must beware of BEV driving range, as their refuelling is not as immediate as approaching a nearest fuel station.

Then, HEV is a combination of BEV and traditional Internal Combustion Engine (ICE). The vehicle uses the energy stored in the battery below speed of 40 mph (65 km/h) with zero emissions, while it uses the combustion engine at higher speeds. Hence, ICE extends driving range of BEVs.

The third category is PHEVs, which are similar to HEVs, but they can be also charged, through a plug, from power grid and renewable energy sources while parked. They have greater fuel efficiency and less environment impact than HEVs.

The last category is EREVs. They are a combination of BEV and PHEV with more improved fuel efficiency and reduced emissions.

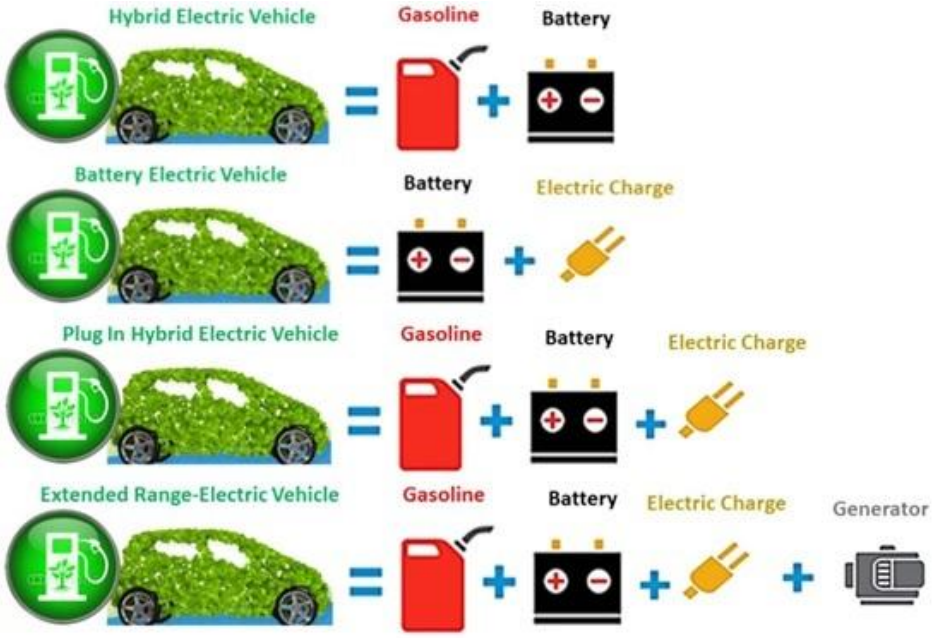

Fig. 1.2.1 Types of EVs [25]

Hybrid energy technologies can be used in two different approaches: battery charge-sustaining (CS) mode or battery charge-depleting (CD) mode [11]. In CS mode, fossil fuel is the major energy source. In CD mode, the PHEV's operation depends on the electricity provided by the battery and gasoline consumption can be substantially reduced.

The prices of EV batteries are considerably high, even though the average price of lithium-ion (Li-ion) battery pack is decreasing every year [11].
Nowadays, PHEVs are generally more competitive than BEVs in terms of driving range and price. In fact, BEVs with longer-range features have usually a higher price. Since PHEVs can rely also on ICE, they have small capacity battery packs (less than 25% ÷ 33% of those equipped by BEVs), so lower final price [11].

Properties of Rechargeable Batteries

As reported in [11], the EVs in the current market are equipped with Li-ion batteries because they have many important properties, such as, for example, high energy density, slow self-discharge and less environmental influence.
However, Li-ion battery charging requires advanced voltage and current controls of charger output, because large fluctuations can cause severe damages to the battery. Hence, interaction between EVs and Smart Grids (SG) must ensure proper charging quality in order to maintain a long EV batteries lifetime.
The following list shows the key properties of rechargeable batteries suitable for EVs [11].

- Charging power controllability: nowadays, the three charging standards currently in use (Sec. 1.3) cannot provide continuously controllable charging power especially since battery packs require very smooth DC voltage and current. Some targets, such as flattening loads, can be reached only through controllable charging power, which means through more advanced batteries.
- Battery charging rate: current Li-ion batteries show a nonlinear relationship between charging time and battery State of Charge (SOC). The time elapsed to complete the final stage of charging is usually much longer than that taken for the initial part. According to Fig. 1.2.2, the last 1/3 of the charging cycle is characterized by a decrease in the charging current since the battery cell open circuit voltage increases; therefore, the SOC increases more slowly.

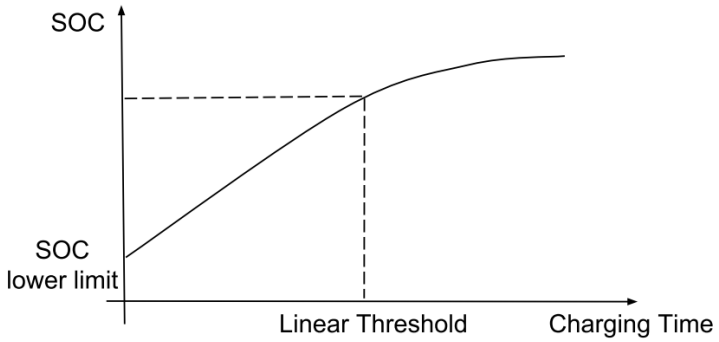

Fig. 1.2.2 Battery SOC/Charging time curve [11]

However, the related discharging cycle shows a linear dependence between SOC and discharging time, therefore this discrepancy between charging and discharging leads to complications in the determination of charging needs with different initial SOCs.

- Battery aging: speaking about EV charging, another factor needs to be taken into account in the overall cost, in fact Battery Life is a significant aspect since batteries cost comprises a large percentage of today's EVs' price. Conventionally, battery life is the minimum between Calendar Life and Cycle Life. The first one is the elapsed time before a battery becomes unusable, while the latter is the number of complete battery charge-discharge cycles before its nominal capacity falls under 80% of its original capacity. The temperature of the battery mainly influences the Calendar one, while usage patterns and Depth of Discharge (DOD) affect the Cycle Life, indeed for many batteries and chemistries, deep cycles cause more significant aging compared to small cycle depths [21].

  Different types of Li-ion batteries imply different aging effects, thus it is impossible to build a universal model to simulate aging mechanisms; but, as aforementioned, they are also affected by different operating conditions, such as daily driving cycles, charging schedules and strategies.

  Frequent charging and discharging reduce battery life; therefore, it is also important to evaluate the effect of battery aging resulting from providing ancillary services.

1.3. Charging infrastructures

One of the most critical components for global EV implementation is charging infrastructure. According to [25], the most challenging target is to develop a nationwide network of charging points rather than producing batteries at affordable costs.
Nowadays, there are some standard chargers and plugs based on three levels of power and voltage values, but they depend on the locations. For instance, International Electrotechnical Commission (IEC) defined the standards for Europe, while SAE International for North America.
In order to describe EV chargers, the first distinction is between AC (Alternating Current) and DC (Direct Current) types. Of course, in both cases, the EV battery pack receives DC current, but in the former, the EV has an on-board rectifier that converts AC to DC, while in the latter case, the conversion is directly performed in the DC charging station.
As aforementioned, IEC defines three different levels for AC charging type, which are Level 1, 2 and 3; while for DC charging type, it considers only one level (Tab. 1.3.1).
The first level of AC typology is an on-board charging facility, which means the charger is located inside the vehicle, so the user can directly plug it to a conventional outlet. It does not require additional facilities and it is usually performed at home during the night. Because of the limited size and weight and thermal constraints, the AC Level 1 charging current, and consequently power, are very low, leading to long charging time.
The second level is the most widespread charging point; it requires a dedicated charging infrastructure, due to its higher ratings and it can have a single-phase or a three-phase connection.
The last AC Level ensures fast charging thanks to its very high performances, but as reported in [16] it is yet to be implemented.
The DC fast charging facilities are the most promising candidates for a widespread installation; in fact, thanks to the high power ratings they can solve the problem of charging time. They can be installed in highway rest areas, car parks of shopping areas, restaurants, etc. or in city refuelling points, where users can quickly charge their vehicles.
The EV charging time depends on three factors: size of battery pack, power rating of the charger and number of EVs connected to the same charger at the same time.

Tab. 1.3.1 IEC Standards for EV charging [16]

Level	**Max power rating [kW]**	**Max ampere rating [A]**
AC Charging		
- Level 1	4 ÷ 7.5	16
- Level 2	8 ÷ 15	32
- Level 3	60 ÷ 120	250
DC Charging		
- DC Fast Charging	100 ÷ 200	400

As reported in [26], EV battery charging can be classified according to the energy transfer mode in conductive, inductive and battery swapping methods.

Conductive charging relies on a power transfer through direct contact, which means it uses an electrical cable to connect the electronic devices to the electricity source. This type of charging is very simple and efficient; it can rely on an on-board or off-board method.
Inductive charging (wireless charging) is based on an electromagnetic coupling to transfer electricity from the source to the EV. This type of charging is the safest one under all-weather conditions. At the current state of the art, it has low efficiency with high power loss.
Battery swapping is a method where EV users can swap their empty battery with a fully charged one, approaching a specialized "refuelling" station called Battery Swapping Station (BSS). This method has several benefits, such as long battery lifetime and minimal management costs, given that batteries can be managed in a centralized way. Furthermore, it can give the chance to avoid the peak demand related to uncontrolled charging. On the other hand, BSSs require huge initial investments to purchase batteries and huge space to operate.

There are different available techniques to charge an EV battery, by which charging time depends on. They are based on traditional methods or advanced technologies.
The former are related to slow charging concepts and they rely on Constant Current (CC) or Constant Voltage (CV) methods.
CC technique, for example, is the simplest one and it provides a single low-level current to the discharged battery. Usually, the charging current is set as 10% of the maximum rated capacity of the battery, but it can lead to gassing and overheating if the battery is overcharged.
Fast charging is based on advanced technologies, such as CC-CV and Pulse Current (PC) techniques. Its advantages include limited charging current and voltage thanks to battery control systems, which prevent over-voltages and thermal stress. CC-CV technique starts implementing CC charging until a pre-set voltage level is achieved, then it applies a CV charging to complete the charging cycle.
In [26], a method with some rest periods during battery charging are implemented in order to reduce battery temperature and therefore battery degradation.
Some researchers are considering PC technique for fast EV charging because it can double the speed of standard CC-CV charging. It uses pulses to supply charging current to the EV battery. It relies on sophisticated systems to generate and control pulses.

1.4. Impact of EVs on Power System

Electrification of transport system has been proposed both to address environmental concerns and to increase energy security of transportation sector. However, the achievement of these goals will depend on the management of the overall system. In fact, the targets of reducing atmospheric emissions and increasing energy security are obviously related to the mix of sources for electricity generation, but also to EV charging management.
EV charging could negatively affect power and distribution systems if uncontrolled battery charging is adopted. Indeed, since EV owners tend to charge their vehicle as soon as they get home from work, the evening peak load can result significantly increased. Therefore, it causes, according to [27], transformers heating and overloading, voltage deviations and increased fault currents and losses in the distribution system.
EV charging causes a huge power consumption for short periods, hence it has significant impact on voltage stability and it can lead to network constraints violations if a large number of EVs are simultaneously connected to a distribution grid.

The current power system is based on a three-phase framework, but single-phase charging infrastructures are more practical, in fact, they are the majority. Therefore, they can lead to unbalances because of unequal load distribution in the three-phase system.
Moreover, power electronic converters are required to transfer power to the EV battery packs, thus, since they are highly non-linear devices due to their operating principles and the presence of switching power semiconductors elements [15], harmonic currents, dc offset, phantom loading, required reactive power [16] can contribute to the degradation of the power quality. Harmonic currents lead to additional Joule heating in the power transformer windings and cables, while increased eddy current loss in the transformer core induces a higher temperature, reducing the transformer efficiency [16].
Nowadays, converters are usually based on PWM control, so thanks to high frequency switching, they ensure harmonics cancellation.
On the other hand, if EV charging is properly controlled from a power system point of view, EVs can bring significant advantages for power system operation. For example, EV charging can decrease the cycling of the power plants and increase the capacity factor of base load plants.
Smart Grids are networks of electrical components used to supply, transmit and consume electricity. They enable bidirectional flows of energy that allow new operations and opportunities, with the support of a coordinated control [11]. Therefore, considering the advanced and challenging concept of V2G (Vehicle-to-Grid), introduced by Kempton and Tomic in [18], EVs will have the capability of providing power to the electricity network, through bidirectional charging infrastructures.
Following sec. 1.6 gives further explanations.

1.5. Electric Vehicles management

The implementation of a large number of EVs in an electricity network involves many challenges that require a severe forecasts and assessments in terms of economic impacts, operation and control conditions. In both case of home and off-home charging, EVs directly affect the electric power distribution system. As aforementioned, a control of EV charging is a key point for a sustainable deployment of this new transportation concept.
The literature proposes many approaches to integrate large EV fleet into the electricity network, but the most common are reported in [11].
EV charging coordination can be categorized into three typologies: centralized, decentralized and hierarchical.
Centralized coordination assumes the existence of a central controller that directly manages all participated EVs, but this approach is far from viable because of the need of accurate acquisition of EV status data and poor scalability. Moreover, the current electricity market does not provide support for direct control contract, since the minimum power capacity threshold is significantly higher than that of an individual EV.
In the decentralized coordination, the EV owners have complete control over their vehicles and they individually interact with the grid operator through price-based mechanisms. But also this case seems no feasible, since the current electricity market does not provide support for this kind of contracts.
The last and most promising approach for short-term implementation of coordinated EV charging is the hierarchical one. It is a hybrid solution of the previous ones and considers an aggregator, in a price-based mechanism, which intermediates between the grid operator and EV owners.

However, at the current state of the art, all these approaches are only at a conceptual level because they require novel systems of communication, interfaces and control algorithms, which must be designed and built up.

1.6. V2G technology

According to [26], V2G (Vehicle-to-Grid) technology increases the reliability and decreases the costs of power system. When EVs are connected to the distribution grid, they store energy during charging time, but they can also perform as generating sources when V2G is enabled. Hence, EV owners can benefit by providing V2G services because they can play a very useful role in order to mitigate voltage fluctuations and line losses in distribution grids; they can participate in frequency control, load shifting and peak-load shaving.
If we take into account only one electric vehicle performing V2G services, nothing relevant happens for the distribution network; but if we consider a large number of EVs properly managed, their operations involve several benefits in terms of environment, economics and smart grids development. However, EV owners are more concerned about initial cost, charging time, driving range, battery lifetime and reliability.
As explained in sec. 1.5, considering the hierarchical approach, the aggregator obviously controls the EV fleet in order to charge their batteries, but it manages them also to provide ancillary services. The aggregator makes profits by contracting with EV owners and grid operator.
The aggregated EVs, which are like a large electricity source, can provide [25] voltage and frequency regulation, spinning reserve and also non-spinning reverse for load flattening by tracking intermittent RES (Sec. 1.8). In fact, V2G mainly aims to store the exceeding renewable generation during the day and feed the surplus energy back to the grid during the hours of peak demand. Therefore, V2G can lead to considerable reductions in the operating costs of power system and increase distribution network security.
However, the most common battery chargers do not have technical features for V2G implementation, indeed, they do not allow bidirectional power flows and therefore they do not consider EV battery discharging.
With the current state of the art, if V2G services were provided by EVS, they would affect battery life cycle, but the authors of [26] state that through improved charging/discharging systems, also battery life can be preserved. Another practical solution and immediately adoptable, proposed by the authors of [11], is that EV owners can take advantage from exploiting their EVs without causing severe battery degradation, providing only voltage regulation instead of frequency regulation. In fact, the latter causes frequent battery charging and discharging that lead to significant degradation.
The authors of [26] state that innovative lithium-sulfur batteries show promising advantages over lithium-ion batteries, such as higher energy density, wide temperature range, improved safety and lower costs due to the availability of sulfur, but they are characterized by higher self-discharge and capacity degradation with higher number of charging/discharging cycles.
The success of V2G implementation is intrinsically dependent on the development of a sustainable business model for the different players involved in V2G services, but nowadays it is highly uncertain.
Something more feasible in the short term could be Vehicle-to-Home (V2H) solutions, where EVs are part of a home energy management system. These solutions are nearer because the management of electricity demand is limited to the single home, therefore no direct interfaces

between vehicle and grid are required. Communications and controls have only to be implemented between vehicle and home.

1.7. SOC Control

According to [28], in every moment of the day, only a small percentage of cars are driving on the roads in comparison to the overall number of cars. Therefore, this situation is expected to be the same in future with a large deployment of EVs. Because of their shorter driving range and easy charging, it is expected that EV owners will charge their vehicles frequently. Thus, parked EVs will be usually plugged in and near their full SOC. From this points, Kempton and Tomic in [18] established their innovative concept of V2G.
The functional block, which manages the battery charging and discharging, is the Battery Management System (BMS). It protects the battery against deep discharging or overcharging by estimating the SOC and SOH (State Of Health) of the EV battery. Overcharging is dangerous for Li-ion batteries, since it causes a reduction of lifetime and safety, decomposition of electrolytes and formation of lithium dendrites; while, deep discharging oxidizes the negative electrode copper that dissolves in the electrolyte. [16] Therefore, precise measurements of cell voltages, battery current and thermal state are required.
In general terms, it is possible to describe the behaviour of a plugged EV, as follows [12]:

$$SOC \leq SOC_{min}, only\ charging\ allowed$$

$$SOC_{min} \leq SOC \leq SOC_{max}, charging\ and\ discharging\ allowed$$

$$SOC \geq SOC_{max}, only\ discharging\ allowed$$

Where SOC_{min} allows to reserve a certain amount of energy for EV travel usage, while SOC_{max} prevents battery overcharging issues.
The EVs, once the minimum SOC value has been reached, can be managed in bulk in order to provide ancillary services.

1.8. RES integration with EVs

In the last decade, the global penetration of Renewable Energy Sources (RES) into the electricity system is considerably increased, as described in sec. 1.1, but the power system must daily deal with unpredictable and intermittent supplies, especially of wind and PV solar energy. The RES generation can be very high, sometimes also more than power demand, sometimes very low, inadequate compared to power demand, depending on the availability of energy sources. Therefore, the only way to match green power generation to the power demand is the use of stationary Energy Storage Systems (ESS), which absorb or supply electricity in relation to the surplus or lack of renewable generation. However, this solution implies too high initial investments. Therefore, as a significant increase in the use of EVs is expected over the coming years, some researchers have proposed to exploit these vehicles as dynamic energy storage devices.
As reported in [23], the EVs can be aggregated and absorb the excess RES generation through different charging profiles or supply power to the electricity network in the case of low generation, in order to support grid operation through V2G services. In this case, the aggregated EVs play the role of energy buffer for network regulations and ancillary services.

Integrating the distributed RES generation, wind and PV solar, with the adoption of EVs with V2G services (Fig. 1.8.1) we can maintain energy security, while reducing GHG (greenhouse gas) emissions. Obviously, to reduce both GHG emissions and overall costs, an optimized utilization of EVs and RES is essential.
We can state that EVs can support high RES penetration, but also RES can solve problems for EVs. In fact, if EVs are charged by fossil fuels, they do not lead to any improvement in the environment, we are just shifting the emissions from the city to somewhere else, but if EVs exploit renewable energy, they reduce the emissions related to the transportation sector.
Therefore, EVs can support renewable generation and RES can support EVs. However, EVs can also support autonomous energy operation in the case of losing the grid, because we can rely on the renewable energy generation to satisfy electricity demand, while on the energy stored in the EVs to control grid voltage and frequency, allowing the operation in islanding mode.
Nowadays, we are not allowed to operate in islanding mode because we cannot keep the values of frequency and voltage constant. What the research is interested in is not the operation in islanding mode, but the operation in a way to minimize the dependence on the grid in order to reduce network losses and improve energy autonomy. However, if everybody does this, we do not need the grid anymore, it becomes as a backup just to balance the system. In this way, we can make the system more efficient because we are using local renewable energy rather than energy from the power system.

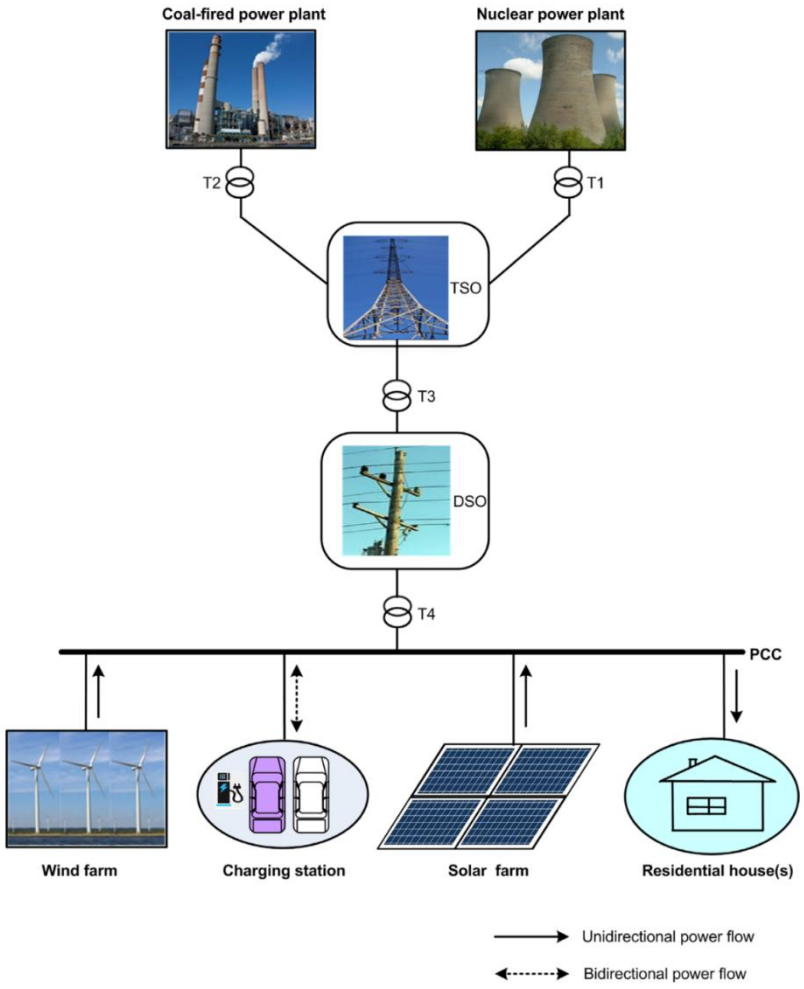

Fig. 1.8.1 Wind and PV solar energy sources integration into the electricity grid with EVs [23]

1.9. SEEV4-City project

SEEV4-City (Smart, clean Energy and Electric Vehicles for the City) is an Interreg Europe project co-founded by North Sea Region Programme and financed by European Regional Development Fund for the period 2014-2020. Interreg Europe helps regional and local governments across Europe to develop and deliver better policy [29].
As reported in [30], the aim of this project is making a huge step forward in green city development thanks to a smart integration of Electric Vehicles (EVs), Renewable Energy Sources (RES) and Information Communication Technologies (ICT) solutions. In fact, a top priority is stimulating clean transport solutions powered by clean renewable energy.
In the cities of the UK, plug-in electric cars are growing fast, from 3500 units in 2013 to almost 95000 in March 2017. However, charging EVs during the evening, after working day, involves a significant increase in the evening peak load. Therefore, EV charging does not exploit renewable energy and does not act as a clean transport solution; moreover, the higher peak needs expensive grid adjustments in order to meet the new power demand.
The challenge is to structure a new policy in order to perform EV charging through locally produced renewable energy, rather than through electricity supplied by the power system, by achieving a high-performance operation of the electricity grid, a significant reduction in emissions and an increase in energy autonomy.
Anyway, ICT solutions are essential to maximize the integration between EVs and local renewable energy generation and therefore optimize the electricity grid operation.

It consists of 6 operational pilots [30], located in 5 cities of 4 European countries, aimed to achieve the same three targets:

- An increase in energy autonomy;
- An increase of ultra-low emission kilometers;
- Avoid additional investments to make the existing electricity network suitable for the effects of uncontrolled charging and high renewable energy generation.

Beyond the main common goals, each pilot has its own individualities [30]:

1. Leicester (Vehicle2Business) – United Kingdom
   This operational pilot assesses the effects of relatively small V2G implementation in large systems; the target is to evaluate the overall cost-effectiveness, considering a limited number of EVs in a depot where council vehicles are currently parked. This depot has a solar PV generating system that already produces more than a third of the energy consumed.
2. Loughborough (Vehicle2Home) – United Kingdom
   This project focuses on a single household with PV generation, which regularly produces more electricity than the consumption, excluding EV charging. Thanks to ICT integration, when the EV is plugged in, it charges and discharges in relation to the household's electricity demand and solar energy production forecast.
3. Kortrijk depot (Vehicle2Business) – Belgium
   This depot hosts the vehicles of forty workers, therefore, it must deal with their different mobility needs. It has different charging points, some for cars, two slots for electric bikes and three for electric forklifts. The depot is connected to a nearby sports centre that consumes the surplus of the production of a rooftop PV system. The target is to manage the energy stored in the EVs in order to optimize the overall operation.

4. Amsterdam (Vehicle2Neighbourhood) – Netherlands
   This operational pilot wants to optimize the interaction, at district level, between prosumers and EVs. The chosen area has preliminary conditions in terms of EV usage, PV installations and therefore potential grid constrains problems. The main point is that the EV owners do not have to change their electricity usage habits, but they should only plug in their vehicle when parked. The ICT solutions forecasts electricity generation and consumption in order to manage properly EV charging and discharging.
5. Amsterdam Arena (Vehicle2Business) – Netherlands
   It considers a different order of magnitude for V2G services. It has to deal with an energy consumption comparable to a district of 270 households. It has PV installations that produce about 10% of consumption. It is focused on energy storage and V2G implementation because most of the energy consumption is during the evening.
6. Vulkan Project (Vehicle2Neighbourhood) – Oslo, Norway
   This project is on the Vulkan Estate Building, a housing development currently under construction. It has geothermal, solar and PV systems. In order to tackle renewable energy unpredictability and intermittency, it will rely on a smart grid that includes energy storage and EV implementation. In fact, it will serve more than 400 EVs per day and is expected to shave 20% of peak demand during the evening.

Another important challenge is about the creation of a feasible business model, because if you do not take care of the benefits of EVs, aggregator, grid operator, community, environment and therefore all the benefits of stakeholders, nobody will be interested in this.
SEEV4-City partners have good knowledge and experience in the field of energy forecasting systems, monitoring and modelling tools and, in addition, they are currently working on the development of energy management systems to be applied to the Operational Pilots.
The project results will be a key factor for the development of innovative cities that integrate clean electric transport services and renewable energy generation.

Fig. 1.9 SEEV4-City Project

1.10. Contents of the thesis

The first chapter has reported an introduction on the state of the art. Sec. 1.1 starts explaining, in general terms, the background issues, opportunities and challenges about all the topics that this thesis is based on. It reports the trends of RES global capacity and global EV stock, also introducing V2G technology with its opportunities and limitations. Then, in sec. 1.2, it explains the opportunities related to the spread of electric vehicles, instead of Internal Combustion Engine (ICE) vehicles, and classifies the four conventional categories of EVs. Other important pieces of information are about the key properties of rechargeable batteries suitable for EVs and battery aging. Sec. 1.3 describes one of the most critical components for global EV implementation, which are charging infrastructures, listing the standards for EV charging and their characteristics in terms of energy transfer mode and charging profiles.
Sec. 1.4 explains the positive and negative impact that EVs can involve on Power System, differentiating the three different charging strategies. Sec. 1.5 describes several approaches proposed by literature to integrate large EV fleet into electricity networks. Once the EVs are spread in the grid, it is very important to control their state of charge, in fact sec. 1.7 is about it. Sec. 1.8 reports the core point, about integrating RES and EVs. It explains the promising synergies between renewables and vehicles, revealing the future opportunities.
In conclusion, sec. 1.9 describes SEEV4-City (Smart, clean Energy and Electric Vehicles for the City) project, reporting the main aims, the six European operational pilots, the consortium partners and the related current and future challenges.

The second chapter explains the core of the thesis project, the Smart Grid Modelling Tool based on Matlab/Simulink platform. Sec. 2.1 describes the design and coding processes of the GUI (Graphic User Interface) window. It is a kind of user guide, because it explains all GUI functions, commands and procedures, all the input variables and tables and finally the results output. Sec. 2.2 describes the Matlab scripts and functions needed by the modelling tool to create and analyse the geographical representation of the distribution network in the Simulink model. Then, it reports the parameters set to characterise it and the very important information about preliminary assumptions. It also describes the cost function optimization process performed by the tool in order to define the EV charging profiles, from both theoretical and practical points of view. It explains the script performed to obtain the wished results representations and tables.
In conclusion, it lists the most interesting variables available in the workspace output file.

The third chapter reports the case study assessed through the modelling tool. It considers six scenarios applied on an existing electricity grid, whose characterization and representation are reported in sec. 3.1. The last four evaluate expected frameworks in the year 2050. Sec. 3.2 shows the network load typologies with their hourly load profiles. Sec. 3.3 describes the considered economic parameters needed by the modelling tool in order to perform the economic analysis of network operation. Sec. 3.4 reports the parameters related to the EVs considered by the tool, to evaluate the charging profiles through the optimization processes. Sec. 3.5, 3.6, 3.7, 3.8, 3.9 and 3.10 report the information related to the characterization and the analysis results of each scenario.
In conclusion, since the main aim was to compare the three different charging strategies, sec. 3.11 shows a comparison of the results obtained by the evaluation of last three scenarios, considering Scenario 3 as baseline scenario. The comparisons are in terms of three-phase apparent power flowing in the distribution transformer and network operating costs.

2. SMART GRID MODELLING TOOL

This thesis project comes as an attempt to meet the needs of SEEV4-Grid project. In the current stage of the plan, the main targets are about modelling and simulations.
The purpose of this tool is to provide an automatic and user-friendly software based on MATLAB®/Simulink® platform [31], to perform analysis of the effects of traditional passive loads and smart loads, with microgeneration and EV charging, on a distribution electricity network.
The tool, thanks to a simple Graphical User Interface (GUI), allows the user to input all the parameters related to the grid topology, number and type of loads and electrical equipment, and finally load and generation profiles.
The proposed tool allows investigations about advantages and disadvantages of uncontrolled-dumb charging, smart charging and V2G technology. For the last two charging mode, an optimization problem is performed in order to define the charging profile of each EV.
Simulink solver and relevant Matlab scripts evaluate the defined network from an electrotechnical and economic point of view and save the results into output files.
User can find tables and graphical representations of the results directly on the GUI window.

2.1. Graphical User Interface (GUI)

All the analysis, which can be performed by the modelling tool, are accessible from the GUI.
It has been created with Matlab App Designer™ and it is the head of the entire tool. This Matlab toolbox is very practical to use and it allows the creation of customized apps, with standard components, like buttons, check boxes, dropdown lists, editable fields, sliders and text areas; but also instrumentations, like gauges, knobs and besides lamps, switches.
It is a graphic tool, so you can create your own app from a graphical point of view and it automatically translates it into code instructions. In fact, App Designer has two different views: “Design view” and “Code view”.
Following Fig. 2.1.1 shows the GUI window at the launch of the program.
It has been created starting from three main panels: *Input data*, *Evaluation* and *Output data*. Then, they have been gradually filled with the needed parameters or commands.
The buttons, shown in GUI, are internally linked with proper functions in order to call external files, such as Excel files, .csv tables or Matlab script.
Some lines of code are necessary to set up these inner links; therefore, the suitable functions have been called in the relevant sections of the “Code view” of App Designer toolbox.
Moreover, the code, written in the aforementioned toolbox, needed some data saving and loading commands because the app’s execution does not rely on Matlab workspace, thus to import and export variables from and to external functions this process is essential.
Obviously, GUI window has been set up after finishing all the required Matlab scripts; otherwise, it would have been difficult to have a complete view of the relevant input and output needs. All input text fields already show default values. They have been chosen in according to some preliminary assumptions (Sec. 2.2.1).
As can be noticed in Fig. 2.1.1, all output buttons are disabled before grid evaluation process and the feedback text area displays “Ready”, which means that the tool is ready to start the modelling process.
These buttons behaviours are possible thanks to the instruction *app.*“*ButtonName”.Enable.* It can be set to “on” or “off” directly from the “Code view” of App Designer toolbox.

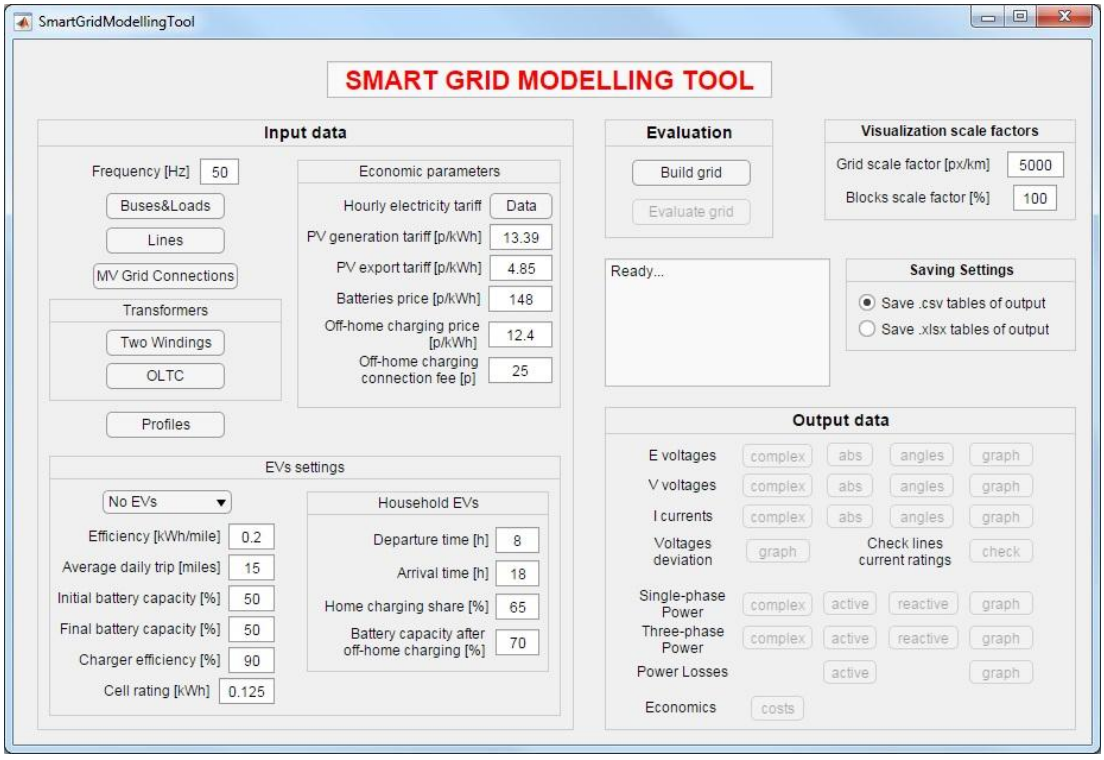

Fig. 2.1.1 GUI Initial Window

Input parameters are all on the left-hand side of the view and some of them can be directly set in the window, others are linked to input Excel tables.

- *Buses&Loads* Button: it refers to an input table for grid buses and loads characterization. Buses of the grid are described by their number, the geographic coordinates expressed in decimal degrees of their position and by the nominal Line-to-Line (L-L) voltage. The latter is selectable among 400V, 11kV and 33kV.
  Loads, instead, can be chosen among households, schools, shops, light industries and car parks. This kind of feature allows us to consider different daily load profiles in another input table, as it has been explained in the following.
  Each category has a smart and a traditional version.
  The traditional one consists of the conventional passive load; the smart one, in addition to the conventional load, implements also photovoltaic (PV) generation and Electric Vehicle (EV) charging.
  An example is shown in Tab. 2.1.1 below.

Tab. 2.1.1 Buses&LoadsData Table

BUSES CHARACTERIZATION				LOADS CHARACTERIZATION								
Buses	Geographic coordinates		Nominal voltage	Households		Schools		Shops		Light Industries		Car Parks
N°	Latitude	Longitude	Vrms	N° Smart	N° Traditional	N° Smart	N° Traditional	N° Smart	N° Traditional	N° Smart	N° Traditional	N° Smart
1	45.406776	11.877277	11000	0	0	0	0	0	0	0	0	0
2	45.409052	11.89461	400	2	0	1	0	0	0	1	0	1
3	45.410845	11.892105	400	0	2	1	0	0	0	1	0	0

- *Lines* Button: it calls an input table for grid lines characterization.
  The starting bus number, the end bus number, the length of the line (expressed in kilometers) and cable type define each line of the electricity network.
  Consequently, thanks to a link between the first and second sheet of the Excel table, it provides the values of line current rating, specific resistance and inductance in according to the cable typology previously set.
  There are 13 available cable types, but others can be easily implemented. They are:

  - Al Consac 300 mm2;
  - Al Consac 240 mm2;
  - Al Consac 185 mm2;
  - Al Consac 150 mm2;
  - Al Consac 120 mm2;
  - Al Consac 70 mm2;
  - Cu 300 mm^2;
  - Cu 240 mm^2;
  - Cu 185 mm^2;
  - Cu 120 mm^2;
  - Cu 95 mm^2;
  - Cu 70 mm^2;
  - Cu 35 mm^2.

  Tab. 2.1.2 presents an example of the input table.

Tab. 2.1.2 LineData Table

From Bus	To Bus	Length	Cable Type	I(max)	Resistance	Inductance
		km		A	Ohm/km	H/km
2	3	0.18	AL Consac 185 mm2	190	0.164	0.000218

- *MV Grid Connections* Button: it is linked to an input table for Medium Voltage (MV) grid connections description.
  This table provides details of the connections between MV grid and Low Voltage (LV) grid to the modelling tool. So, in this table, the user have to write the bus number where the connection is located, the nominal L-L voltage, the nominal frequency, the three-phase short-circuit level at base voltage, the base voltage and X/R ratio.
  The L-L voltage is selectable among 11kV and 33kV.
  If the user had to consider an ideal MV grid connection, he should set an infinite (inf) three-phase short-circuit level.
  The phase-to-phase base voltage is used to specify the three-phase short-circuit level.
  The base voltage is usually the nominal voltage, but as shown in the following example (Tab. 2.1.3), they could also have different values.

Tab. 2.1.3 MVGridData Table

Bus number	Nominal Voltage	Phase angle of phase A	Nominal Frequency	Three-phase short-circuit level at base voltage	Base Voltage	X/R ratio
	Vrms	degrees	Hz	VA	Vrms	
1	11000	0	50	5.00E+08	2.00E+04	10

- *Transformers* Inputs: this slot has two input tables, one for the conventional two windings transformers and the other one for the On Load Tap Changers (OLTC) transformers. Both of them show several parameters that are essential for transformers characterization in the grid model. User have to specify the value of the parameters described below:

Two windings transformer	**OLTC transformer**
- Number of "from" and "to" bus;	- Number of "from" and "to" bus;
- Windings connection;	- Windings connection;
- Nominal power and frequency;	- OLTC position (winding 1 or 2) ;
- Nominal voltage, Resistance and Inductance of winding 1;	- Nominal voltage, Resistance and Reactance of winding 1;
- Nominal voltage, Resistance and Inductance of winding 2;	- Nominal voltage, Resistance and Reactance of winding 2;
- Magnetization Resistance and Inductance;	- Magnetization Resistance and Inductance;
- OCTC value.	- Tap changer parameters;
	- Voltage Regulator parameters.

  Resistance and inductance values, for two windings transformers, can be added in two different way: pu (per-unit system) or SI (from the French Système International d'unités, International System of Units)
  For the first typology, Off Circuit Tap Changers (OCTC) value is considered, so in this way a different value of the nominal secondary winding voltage is settable for the transformer in order to comply with the voltage constraints of the grid. OCTC value is expressed in pu and the user can select a value among: 0.95, 0.975, 1, 1.025 and 1.05.
  On the other hand, for the OLTC transformers type, it is possible to specify the side where OLTC is located, all tap changers parameters and, finally, automatic voltage regulation can be set on the transformer, but it is important to stress that this automation leads to a long processing time during electricity network evaluation performed by Simulink solver.

- *Profiles* Button: it refers to an input table for loads and generation power profiles characterization.
  In this table user can set the array of active powers for each load type (Households, Schools, Shops and Light Industries). This list has 24 values, one for each hour, in order to establish dynamic load profiles.
  Active power absorbed from the grid and power factor (PF) are the two keys to define each load of the electricity network.
  As mentioned before, the table contains also information about generation. It is described by 24 values of specific active power injected in to the grid. This means that the values are expressed as a fraction of the nominal power of the PV power plant.
  These values are dependent on the geographic location and orientation and on the efficiency conditions of PVs. In addition, it is also possible to specify the power factor of PV generation.
  Furthermore, the Excel worksheet shows a graphical representation of the profiles listed in the table. In this way, the user can perform a first data check.
  Following Fig. 2.1.2 shows an example of the input table.

	LOADS				GENERATION
	Households	Schools	Shops	Light Industries	Photovoltaic
	PF				PF
	0.95	0.95	0.95	0.9	1
Time	Active power				Active power
h	W	W	W	W	W/W$_{inst}$
0	370	0	1833	48319	0.0
1	235	0	1670	50000	0.0
2	195	0	1630	42392	0.0
3	190	0	1605	40413	0.0
4	185	0	1457	34499	0.02459
5	200	0	1323	33469	0.08717
6	225	0	1308	31955	0.18726
7	350	0	1344	34068	0.23597
8	615	0	1284	33115	0.31747
9	650	17108	1141	25863	0.47269
10	660	16609	1107	19193	0.63199
11	650	16700	1113	21214	0.82014
12	660	16778	1119	19942	0.93626
13	670	15477	1032	26343	0.83136
14	560	16065	1071	30328	0.77543
15	558	17555	1170	28813	0.57097
16	605	0	1287	35306	0.38143
17	820	0	1499	40354	0.21611
18	845	0	1860	44936	0.11105
19	785	0	1792	42623	0.02924
20	730	0	1794	45869	0.0
21	710	0	2000	43599	0.0
22	695	0	1941	46714	0.0
23	550	0	1835	46736	0.0

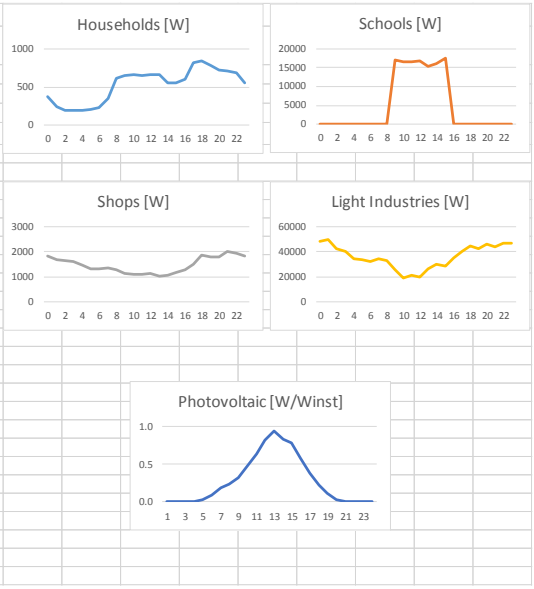

Fig. 2.1.2 ProfilesData Table

- *EVs settings* Inputs: in this area of GUI window (Fig. 2.1.1), user can set EVs parameters. Starting from the top, there is a drop down list with four different options.
  The first and of default one is "*No EVs*", where electric vehicles charging is not considered on the model.
  The second one is "*Dumb charging*", so the model considers dumb charging method to charge EVs that are on the grid (Sec. 2.2.1).
  The third one is "*Smart charging*", in this case the model considers smart charging strategy to charge EVs; therefore, it solves an optimization problem to define charging profiles (Sec. 2.2.1).
  The last available setting is "*V2G*", in which the model considers V2G technology to manage EVs. In this case, Matlab algorithm (Sec. 2.2.1) optimizes the charging/discharging profile of each EV. The power exchange between grid and EV is based on economic, electrotechnical and EV constraints.
  User can also set EVs efficiency expressed in kWh/mile, average daily trip in miles, percentage of the initial and final battery capacity of the EVs, charger efficiency and finally, the cell rating expressed in kWh.
  Initial and final battery capacity of the EVs means the battery capacity wanted at 12 a.m. and at 11 p.m. This is because, as said before, this model considers 24 points during the day, so hour by hour.
  Charger efficiency determines the amount of power provided by the charger to the EV during charging period, while it defines the amount of power provided by the charger to the grid during discharging session. For example, with a 3kW charger characterized by 90% of efficiency: during EV charging, it provides 2.7kW to the EV; while during EV discharging, it reduces the power coming from EV by 10%.
  Cell rating is necessary to evaluate battery degradation costs related to the charging/discharging profile; in fact, the latter is used during the optimization process as a variable.
  Finally, in this area of GUI panel, departure and arrival time of household EVs can be set. Sec. 2.2.1 explains the other EV schedules.

Home charging share input parameter defines the fraction of household EVs that charges their battery at home, therefore, considering their availability, during the evening or the morning. The remaining number of household EVs charge their battery during the day, in off-home charging infrastructure, which means along the streets, at charging station or at work, before getting home from work, exploiting solar generation and making V2G power exchange possible and profitable.
These off-home charges allow the EVs to achieve a battery capacity equal to the battery capacity after off-home charging input parameter.

- *Economic parameters* Inputs: last GUI input slot defines the specifications related to economic evaluations. *Data* button calls an Excel input table where user can insert the hourly electricity tariff in pence/kWh. The user can freely decide to impose two different prices during the day, one for peak hours and one for off-peak period, or different prices, one for each hour.
  For electricity generation a Feed-in Tariff is considered. In this way, the model applies two different tariffs, one for generation and one for export. The energy supplier pays the PV owner for each kWh of electricity generated (generation tariff) and it pays a further rate for each kWh exported back to the grid (export tariff). Normally, Feed-in Tariff supports more self-consumption than electricity injection into the distribution network. Therefore, PV export tariff consists of a lower price than the cost related to electricity purchase.
  Finally, the optimization process also needs other prices. Of course, it needs batteries price, in pence per kWh, to evaluate battery degradation costs and, in order to perform economic evaluation of off-home charging, the user has to set the related electricity price, in pence per kWh, and connection fee, in pence. In fact, public charging networks usually have a double pricing, one related to the amount of energy taken from charging point by the EV and the other one is just a fee paid to plug in the EV.

At the top right-hand side of GUI there are two slots called respectively *Visualization scale factors* and *Saving Settings*.
The first one is useful to modify grid scale factor of the model, we are going to create, and of the dimension of blocks in Simulink platform. This is required because this model has no width limit, thus to obtain a good representation of the grid a scaled visualization could be necessary. The default values are optimised for a network width of about 600 m.
The latter slot allows the user to select the save files format among comma-separated values tables and Excel tables. The results are printed in one of the aforementioned tables with clearly abbreviated headers. In the case of daily values array, the first table column reports the list of the daily 24 hours.

The *Evaluation* box contains the GUI main commands, *Build grid* and *Evaluate grid*.
The upper button calls the Matlab main script (Sec. 2.2.1), inside which there is the entire code needed to create the grid model on Simulink environment, considering all input parameters set in the Excel tables and in the GUI panels.
By pressing this button, the text area displays the notice "*Loading data…*", then once loaded, it shows "*Grid built*" and finally "*Ready for evaluation*" (First three lines of text area shown in Fig. 2.1.3). The tool creates the distribution network model, calling it ElectricityGrid.

After that, it enables the button called *Evaluate grid*. By pressing it, Simulink starts the evaluation of the ElectricityGrid model. Therefore, user can read "*Evaluating grid…*" in the text area.
Then, automatically, the program performs the electrotechnical computation calling another Matlab script (Sec. 2.2.2) and consequently it shows "*Electrotechnical computation…*".
Now, it saves the electrotechnical and economic results on tables, in according to the save files format set before and it displays "*Saving results…*" on the text area of GUI. The saving is performed calling another Matlab script (Sec. 2.2.3).
Finally, once all the aforementioned steps are completed, "*Completed*" will appear in the text area.

From now on, as Fig. 2.1.3 shows, GUI window enables all the output buttons inside the *Output data* panel.

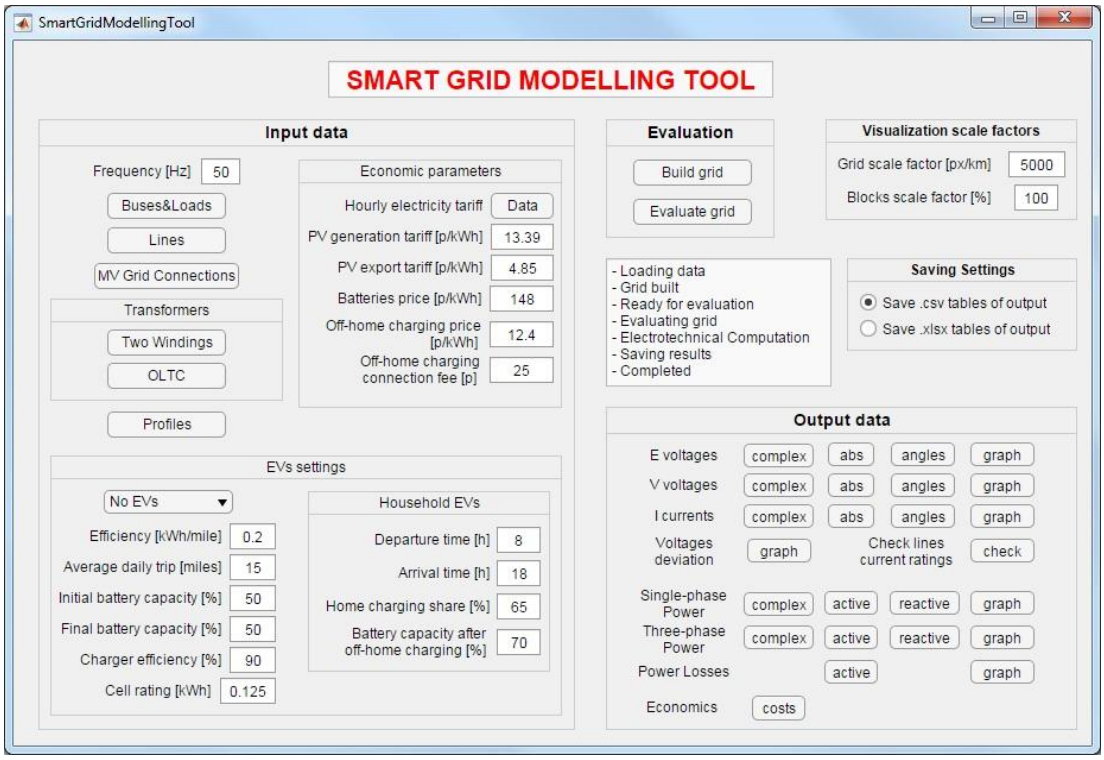

Fig. 2.1.3 GUI Final Window

All output tables, saved during "*Saving results…*" period, are now accessible through the *Output data* panel.
Voltage, single-phase power and power losses results are shown per each phase of each network bus, three-phase power results are evaluated per each bus, while current results are presented per each phase of each grid line.
In this panel user can find:

- *complex*, *abs*, *angles* Buttons: they refer to output voltages and currents tables with, respectively, complex values, complex magnitude values (modulus) and phase angle values;

- *graph* Button: it refers to voltage and current values, as well, but it calls a Matlab script in order to create graphical representations of the modulus of these quantities during the day. It shows a window for each voltage level (400V, 11kV and 33kV), if related buses exist on the electricity network. In each window, user can analyse three different charts one per each phase of the electricity grid. Currents graph displays pu current values, because the absolute results are compared to lines current ratings;

- *Voltage deviation graph* Button: it allows the user to view the trend of the difference between nominal and actual voltage during the 24 hours. Also in this case, it creates a window for each voltage level, if related buses exist on the electricity grid. In each window, three different figures are plotted, one for each phase, with the correspondent buses results.
  The graphs additionally show the voltage drop limits imposed by [32] for low voltage (LV) and medium voltage (MV) supplies. The user can easily verify if these bounds are complied or not by all the network feeder lines.
  The table below, Tab. 2.1.4, shows aforementioned voltage drop limits.

Tab. 2.1.4 Voltage drop specification [32]

Supply level	**Voltage drop**	
	Upper limit	Lower limit
Low Voltage (LV)	+ 10%	- 6%
Medium Voltage (MV)	+ 5%	- 5%

- *Check lines current ratings* Button: it refers to an output table where a comparison between nominal and maximum actual current for each line is printed.
  An example of output table can be Tab. 2.1.5:

Tab. 2.1.5 CheckIratings Output Table

Line_2-3	Current rating complied: 109.3035A vs 150A nominal
Line_3-4	Current rating complied: 99.5434A vs 150A nominal
Line_4-5	Current rating complied: 73.6941A vs 110A nominal
Line_5-6	Current rating complied: 52.4931A vs 110A nominal

- *complex*, *active*, *reactive* Buttons: they are related to output powers tables with, respectively, complex power values, active power values and reactive power values;
  Power losses results take account of the active power losses along each line of the electricity network.

- *graph* Buttons: it refers to powers values, as well, but it calls a Matlab script in order to create graphical representations of the active and apparent power during the 24 hours.
  In the case of single-phase power graph, it generates only one window with three different charts, where user can analyse the active power profile in each phase of each node of the electricity network.

By pressing three-phase power graph, it shows one chart with the three-phase apparent power profiles of all grid nodes.
The latter representation also takes into account the power rating of distribution transformer. In fact, the chart has a horizontal line corresponding to the value of transformer power rating. An example of a graphical representation of three-phase apparent power is shown in Fig. 2.1.4 below.

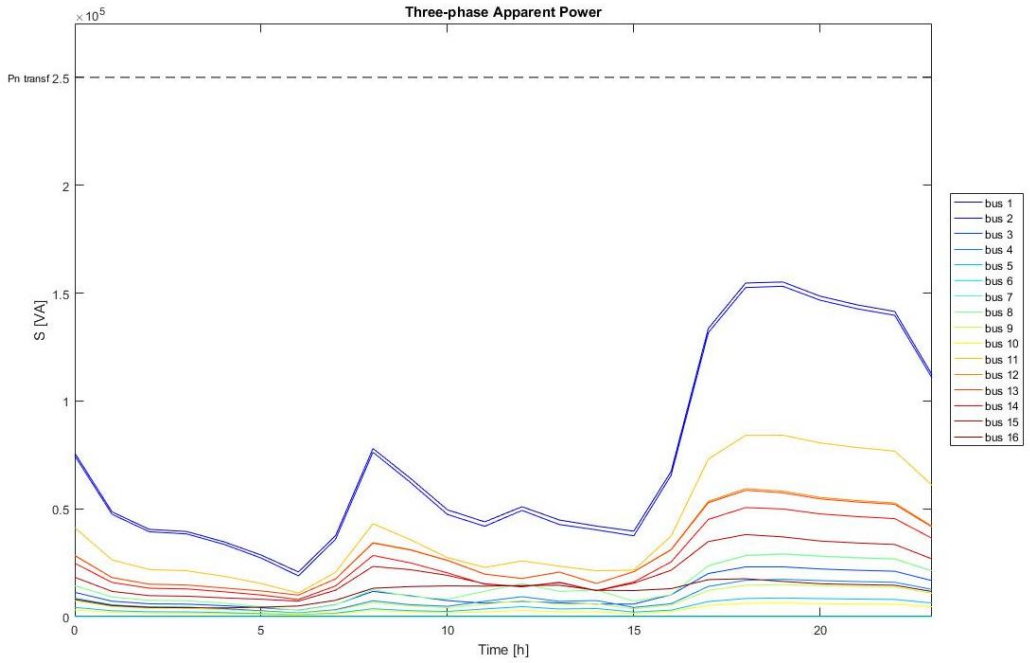

Fig. 2.1.4 Three-phase Apparent Power graph

- *costs* Button: it is linked to an output table where costs related to the operation of the electricity network, expressed in pound (£), are reported.
  The first rows (i.e. Tab. 2.1.6) show the operating costs of grid archetypes; each value can be positive or negative depending on the predominant typology of load, active or passive load. Printed archetypes costs are the sum of the costs related to the electricity absorbed by passive loads and the revenues from PV generation and export tariffs. In case of EVs implementation, the modelling tool takes account the electricity absorbed for EV charging, the electricity supplied by the EVs to the grid with V2G technology and finally it also considers battery degradation costs.
  If the cost of power absorbed by the archetype from the grid is higher than the revenues related to PV generation or V2G technology, the values will be positive; otherwise if revenues are higher than costs, it will be negative.
  The second group of rows report the costs of energy dissipated along each grid lines. Obviously, these values will be always positive and they are borne by the distribution system operator. They are evaluated, by the tool, in the same way of the other charges, which means through the hourly electricity tariff.
  Finally, at the bottom of the table, the user can find the overall operational cost of the entire grid.

Tab. 2.1.6 Costs Output Table

Archetype1	Archetype2	Archetype3	Archetype4	Archetype5	Archetype6	Archetype7
[£]	[£]	[£]	[£]	[£]	[£]	[£]
0.00	3.89	13.60	119.37	4.36	-6.45	26.42
ELoss23	ELoss34	ELoss45	ELoss26	ELoss67		
[£]	[£]	[£]	[£]	[£]		
1.05	1.10	0.06	0.04	0.39		
Total						
[£]						
163.83						

In this section, GUI has been presented; the user can set all parameters and find all results of the modelling tool directly from it, without any interaction with Matlab. This was a precondition; in fact, the intent was to create a Matlab tool that was also suitable for inexperienced users.

2.2. Description of main software routines

All the code needed for the modelling tool is on Matlab environment.
Three key scripts are presented below.

2.2.1. Main script

This code is the fundamental one, because it is responsible for all the model creation and characterization on Simulink. It has over 7300 lines of code.
It starts by loading all input parameters and settings provided in the GUI panels and in the input tables. Once it has raked all the values, it creates a Simulink model called *"ElectricityGrid"* and it sets the simulation parameters, such as simulation stop time and solver typology. Stop time is set equal to 82800 s (seconds), because the modelling tool is 24 hours based. The model simulates every second, but the results are saved at the beginning (t=0) and every 3600 s, therefore they result 24 values.
At the beginning, several solver typology were performed, but Ode23tb solver has been chosen as a compromise between processing time and solution accuracy.
To solve a phasor problem on Simulink, a *PowerGui* block is necessary. Thus, the script has some lines of code to set the parameters of this block, such as simulation type and frequency. As mentioned before, the simulation type must be set to "phasor" and the frequency depends on the GUI setting.
The modelling tool creates a geographical representation of the electricity grid, so it establishes, in an automatic way, a reference point on the model to link all the others to it.

The generated reference point (0 in Fig. 2.2.1.1) is located on the top-left side of the model because Simulink coordinate system has horizontal axis oriented to the right and the vertical one oriented downwards. Therefore, all other points have positive distances from it, as Fig. 2.2.1.1 shows.

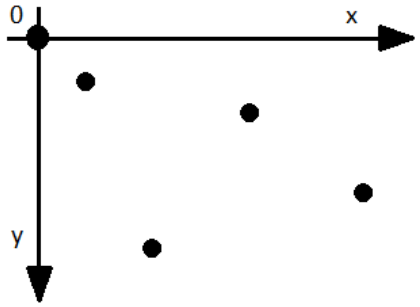

Fig. 2.2.1.1 Simulink Coordinate System

In the input table, buses position information are expressed in decimal degrees, so a unit conversion is needed.
As E. Heskey reports in [33], a recognised standard conversion from decimal degrees to linear distance, i.e. kilometres, is through the multiplication between the number of degrees and the factor 111.325.
In this way, a very simple characterization of the buses position is feasible because the program has already set the reference point, so by knowing its location, the tool can determine the relative distances between all grid nodes.

In according to [34], to add blocks into Simulink model, by using Matlab code, *add_block(source, dest)* function must be used. Where *"source"* slot needs the block path from Simulink library, while *"dest"* slot requires the specifications of destination model and block name. A position setting is necessary after destination path to insert the block in the desired area of the model. The instruction is like *[left, top, right, bottom]*, where the values of the block sides coordinates must be written in the related slots.
The program starts implementing grid buses in the model. Actually, they are not blocks directly available in Simulink library, but they are *subsystems* created ad hoc.
Inside them, there are several objects: currents and voltages measurements and a *To Workspace* block. The instruments measure complex values of the aforementioned quantities because they are essential for the network electrotechnical computation performed after Simulink evaluation. *To Workspace* block allows the measures saving, because otherwise all the results of model evaluation would remain on Simulink environment, while they are needed on Matlab workspace for further calculations.

The second implementation is about MV Grid Connections blocks. To add them in Simulink model, *Three-Phase Source* blocks must be considered.
Some lines of code are necessary to upload the input settings to the blocks using *set_param(Object, ParameterName, Value, ..., ParameterNameN, ValueN)*. In this function, *"Object"* is the allocation where the block path must be written, *"ParameterName"* is the name of the setting parameter and *"Value"* is the input value set.

At this point, depending on the last blocks positioning, a buses orientation adjustment is necessary to obtain correct results in terms of currents. Each grid node is characterized by input and output ports; therefore, to consider a proper currents evaluation along the network branches, they must be oriented in the right way. If the conventional current is flowing from

the left to the right side of the node, the related ports must be in the same order. Therefore, the input one must be on the left, while the output one must be on the right; otherwise, the currents evaluation determines opposite values.
For this purpose, the model considers the lines connections order and buses position information, written in the related input tables. For example, if there are two lines in the model, one 1-2 and the other 2-3, the first one starts at node 1 and finishes at node 2, while the other one is from bus 2 to bus 3. Therefore, depending on the relative position of the grid nodes, the input and output ports can be on the left or on the right side of the bus.

The third addition is about Transformers blocks, both OCTC and OLTC types. For this reason, *Three-Phase Transformer (Two Windings)* and *Three-Phase OLTC Regulating Transformer (Phasor Type)* blocks are implemented.
For OLTC transformer adding, the code firstly creates a subsystem block and then puts the transformer block inside it. This is necessary because the latter needs a voltage measure to control it through voltage regulator. Therefore, some other blocks are indispensable. The input measure is usually in terms of magnitude of positive-sequence voltage, expressed in pu.
As it will be explained in some paragraphs below, all the loads and PV generation blocks are modelled as current sources, so they need some initial conditions to correctly represent power profiles, like initial current phase. For this reason, the script presents some lines of code to determine initial conditions in according to transformers windings connections.

Now, the script implements lines blocks. It uploads *Three-phase Series RLC Branch* blocks into the model. They are positioned in a mean distance between the related grid nodes.
Since this model considers medium and low voltage systems, it can neglect cable capacitance, so the branch typology is set on RL type.

At this point, it is possible to connect all these objects through *add_line(sys, out, in)* command. Where *"sys"* is the allocation for model name, while *"out"* must be the output port name and *"in"* the input port name of the blocks which must be connected.

As mentioned before, the electricity network loads can be:

- Smart and traditional households (Fig. 2.2.1.2):

Fig. 2.2.1.2 Household blocks

- Smart and traditional schools (Fig. 2.2.1.3):

Fig. 2.2.1.3 School blocks

- Smart and traditional shops (Fig. 2.2.1.4):

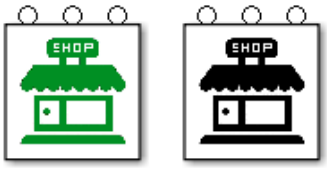

Fig. 2.2.1.4 Shop blocks

- Smart and traditional light industries (Fig. 2.2.1.5):

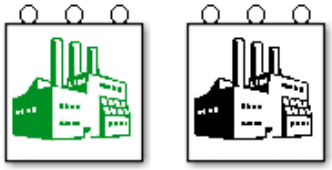

Fig. 2.2.1.5 Light Industry blocks

- Smart car parks (Fig. 2.2.1.6):

Fig. 2.2.1.6 Park block

The model groups all these loads into subsystems, called archetypes, one for each bus of the grid; this ensures a clearer view.
Now, the script considers every type of load, smart and traditional, one by one; for a pragmatic development convenience, it has many sections where each type of each category is considered systematically.

Before explaining how this part of the script works, it is important to focus on some hypothesis. In fact, some **preliminary assumptions** have been made about smart loads, in relation to EV charging and PV generation.
The first supposition is about EV fleet battery capacity: it has been considered that 80% of EVs has 30 kWh battery capacity and the remaining 20% has 85 kWh [35].
According to [35], it has been considered that charging infrastructures can absorb, from the electricity network, powers of 3, 7, 23 or 50 kW, depending on the voltage level and the number of phases of the power supply system. Moreover, charging points are characterized by a unitary power factor, as reported in [36].

Following Tab. 2.2.1.1 summarizes all other assumptions.

Tab. 2.2.1.1 Preliminary assumptions

	Electric Vehicle		**PV generation**
	Number of EV chargers	Power of charging points	Nominal Power PV power plant
Smart households	100% → 1	70% → 3 kW ˣ 30% → 7 kW ˣ	94% → 4 kW ˣ 4% → 6 kW ˣ 2% → 12 kW
Smart schools	50% → 0 30% → 3 20% → 5	70% → 3 kW ˣ 30% → 7 kW ˣ	70% → 10 kW 30% → 12 kW
Smart shops	50% → 0 40% → 1 10% → 2	100% → 7 kW ˣ	90% → 4 kW ˣ 7% → 6 kW ˣ 3% → 12 kW
Smart light industries	50% → 0 40% → 2 10% → 4	80% → 7 kW ˣ 20% → 23 kW	90% → 25 kW 10% → 60 kW
Smart car parks	10% → 20 30% → 8 60% → 2	50% → 7 kW ˣ 40% → 23 kW 10% → 50 kW	30% → 0 kW 60% → 8 kW ˣ 10% → 16 kW

Just to clarify the table above, smart schools, for example, are characterized by:

- 50% of the total number of smart schools at each node has no EV chargers, 30% has 3 EV chargers and 20% has 5 EV chargers;
- 70% of smart school EVs at each node has 3 kW chargers, 30% has 7kW chargers;
- 70% of the total number of smart schools at each node has 10 kW of PV generation and 30% has 12kW.

The ˣ symbol, shown in some power values, means they are single-phase active powers, so the script evaluates the total number of systems, for each category, at each node and it spreads them on the three-phase line to achieve a situation as balanced as possible.
This also happens for smart and traditional household loads, since they are single-phase loads as well.

The percentages and the nominal powers of PV power plants taken in Tab. 2.2.1.1 are based on the "Solar Photovoltaics Deployment in the UK" document [37], drafted by the Department for Business, Energy and Industrial Strategy of UK government. It has been considered how PV systems are spread in the UK, in terms of cumulative capacity and count, obtaining relevant percentages and nominal power sizes.

All load and generation blocks are based on the implementation of a *Controlled Current Sources* blocks. This means that, for each block, input power values govern the current generated by the source. The program uses *lookup tables* to impose currents values to the *Controlled Current Sources*. In this way, the user can directly see a representation of current profile inside each Simulink block.
Of course, three-phase loads and generation have three current sources blocks offset by 120 degrees.
Phase initial values, mentioned before, are now essential to create the right current phasor. To obtain it, some *Interpreted Matlab Fcn* blocks must be used inside each subsystem.
For the categories that have both single-phase and three-phase PV generation, to evaluate the number of plants of each size per phase, the script starts considering the total percentage of the cluster of single-phase PV plants and once found this, it allocates them to the related single-phase loads.

If user set EVs implementation in the model, the code considers EVs representation and characterization, after load and generation blocks creation.
Firstly, it assesses the total number of EVs for each category in each node, secondly it calculates the number of chargers in relation to the aforementioned assumptions, then it evaluates how many EVs have 30kWh battery capacity and vice versa how many have 85kWh battery capacity; finally, the script determines the daily-required energy by each EV.
In a for cycle, each EV is considered: the code generates random values of departure and arrival trip distances, which are normally distributed around half of the input value of average total daily mileage with variance equal to 1. This allows considering the existing EV users diversity.
Total daily mileage value obtained is necessary to evaluate the daily-required energy by each EV, taking into account the input value of EV efficiency.
Only household EVs schedule is editable in GUI window, providing to the code *t_arr* and *t_dep* parameters.
Following Tab. 2.2.1.2 groups all categories assumptions about availability time of EVs.

Tab. 2.2.1.2 EVs schedule assumptions

	EVs availability time			
	Lower limit [h]		Upper limit [h]	
Household EVs	*t_arr*		*t_dep*	
Schools EVs	8:00		14:00	
Shops EVs	10:00	18:00	12:00	20:00
Industries EVs	17:00		8:00	
Parks EVs	*t_dep* + 1		*t_arr* - 1	

With the values reported in Tab. 2.2.1.2, the script can build hourly EVs availability matrices per node and per phase for each load category. Starting from zero matrices, if the i-vehicle at x-hour is available at the charging point it sums 1, otherwise it sums 0. Therefore, the overall EVs availability matrix takes account of the total number of EVs, while an example of normalized results is shown in the following representations (Fig. 2.2.1.7).

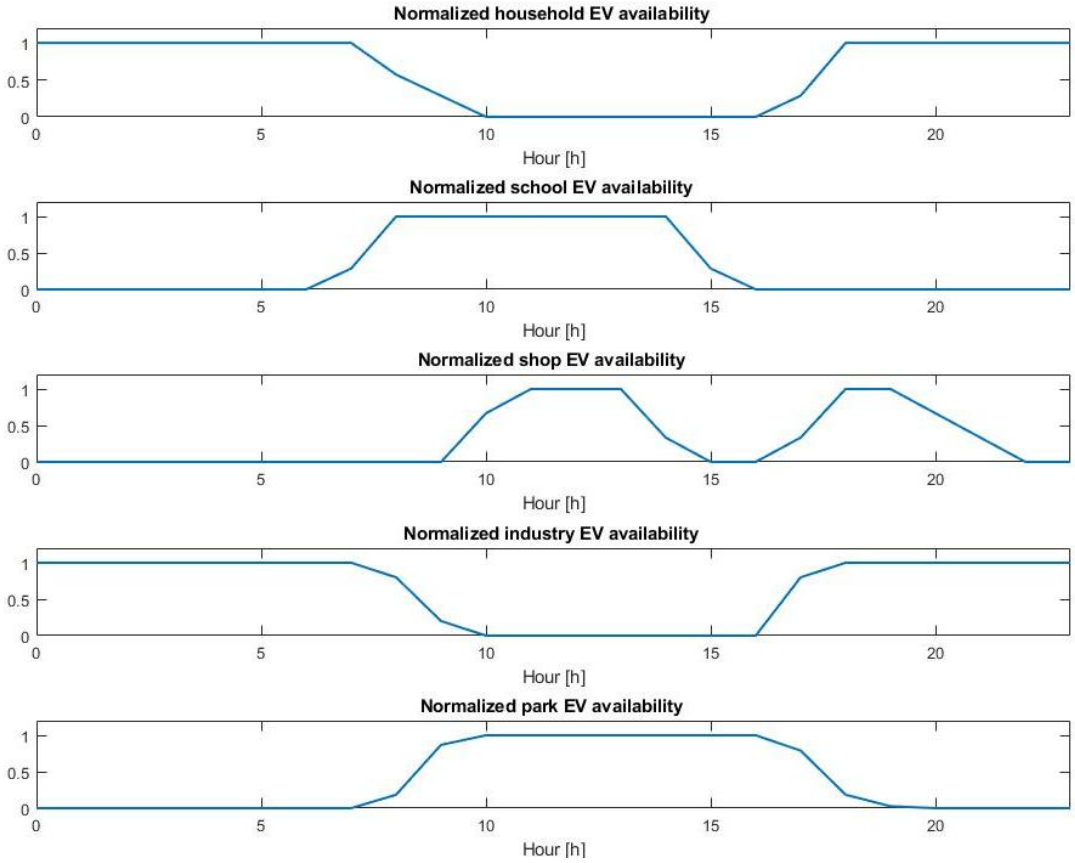

Fig. 2.2.1.7 Normalized EV availability

After this point, the EVs charging mode, set in input, is crucial as shown below:

- Dumb charging ("Uncontrolled charging"): in this case, the program evaluates the needed charging time by each EV related to its daily-required energy and builds the hourly chargers power matrix per node and per phase, starting from the EV arrival time. Therefore, EV owners charge their vehicles as soon as they arrive at the charging point. Finally, an external function is called to perform costs evaluation;
- Smart charging: under this circumstance, an optimization process is implemented to find the minimum of a cost function using *pattern search* solver, complying with some constraints (See sec. 2.2.1 to further details).
  With the optimization results, it is possible to define the hourly chargers power matrix per node and per phase and the charging cost. We will obtain a charging profile based on the economic profitability;
- V2G technology: this is the last event and, as for Smart charging mode, an optimization process is performed to find the minimum of a cost function using *pattern search* solver, complying with different constraints than the previous method (See 2.2.1 to further details). In this case, we can obtain positive and negative values, so both EV charging and discharging, depending on the economic viability.
  With the optimization results, it is possible to define the hourly chargers power matrix per node and per phase and the charging/discharging cost.

As aforementioned, a certain share of household EVs charges its battery at off-home infrastructures, which means their power profiles do not affect the household consumption, but only the economic results. In fact, the modelling tool evaluates the related off-home charging cost.

Following Fig. 2.2.1.8 reports a comparison of charging profiles, related to one household EV, obtained by the processing of the modelling tool in the three different charging strategies, considering the same boundary conditions.

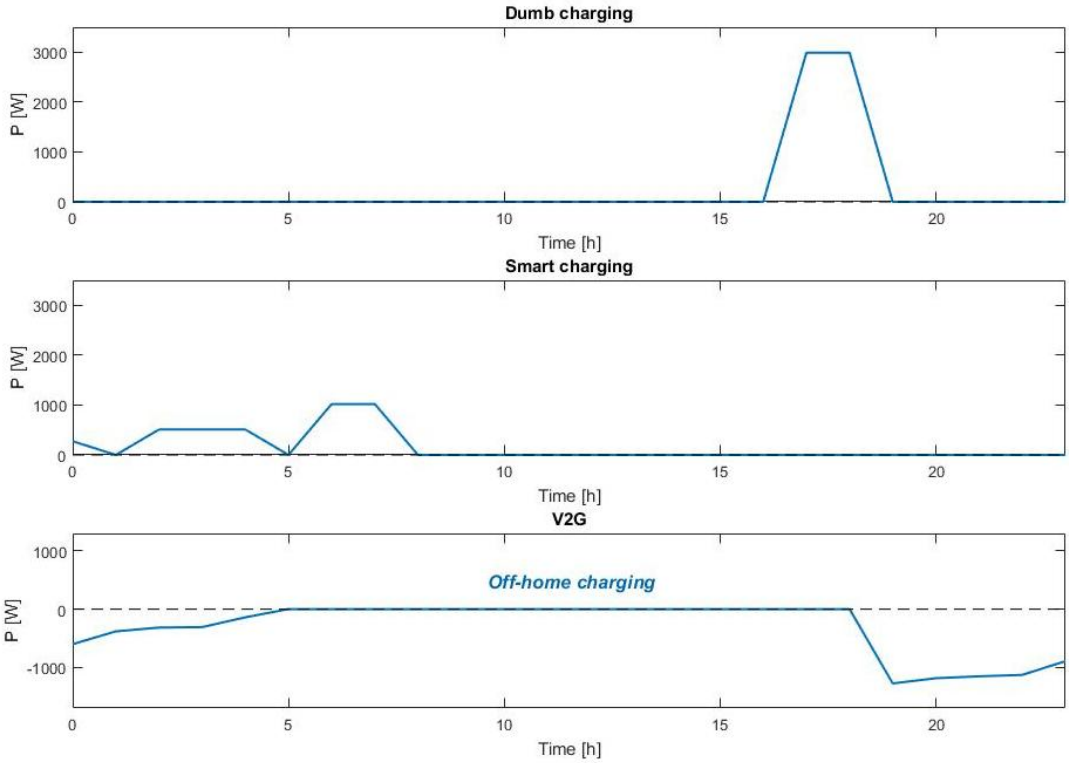

Fig. 2.2.1.8 EV charging profiles comparison

Optimization process

Smart charging and V2G technology need an optimization algorithm in order to obtain the chargers power profiles. As aforementioned, the Matlab solver used for the optimization process is *pattern search*. It is characterized by *x = patternsearch(fun, x0, A, b, Aeq, beq, lb, ub, nonlcon, options)*, where:

- *x*: is a vector of local minimums founded by the optimization;
- *fun*: is the function to minimize;
- *x0*: is a vector specifying the initial conditions for the algorithm;
- *A, b*: are useful to impose linear inequalities of the type A*x ≤ b;
- *Aeq, beq*: are useful to impose linear equalities of the type Aeq*x = beq;
- *lb, ub*: define a set of lower and upper bounds for the solution x, so *lb* ≤ x ≤ *ub*;
- *nonlcon*: subjects the minimization to the nonlinear inequalities, c(x) ≤ 0, or equalities, ceq(x) = 0, defined in *nonlcon*;
- *options*: permits to set optimization options.

The optimization process is the same for both smart charging and V2G technology, except the lower bound parameter. In fact, negative power values are not allowed for smart charging, while for V2G they are permitted.
The function to minimize is a cost function, where the variable x is the hourly active power vector absorbed for EV charging. The optimization process is performed for each load system that implements an electric vehicle, evaluating the net electric power absorbed from the grid, considering load consumption, PV generation and EV charging. The cost function takes into account also battery degradation. For this reason, another function is called during the optimization process, to evaluate the cost of battery degradation caused by the involved power exchange between grid and EV battery.

The optimization algorithm performs:

$$\min f(x)$$

$$f(x) = cost(x) \quad , \quad x = (x_1, x_2, \dots, x_{24})$$

$$cost(x) = c_{energy} \times P_{inport} - r_{gen} \times P_{solar} - r_{export} \times P_{export} + c_{deg} \times x$$

$$P_{net} = P_{baseload} - P_{solar} + x \quad , \quad \begin{cases} P_{export} = |P_{net}| & if \quad P_{net} < 0 \\ P_{inport} = P_{net} & if \quad P_{net} \geq 0 \end{cases}$$

Where:

- $cost(x)$ is the cost function to minimize;
- x is the hourly active power vector absorbed for EV charging;
- $P_{baseload}$ is the hourly active power vector of load consumption;
- P_{solar} is the hourly active power vector of PV generation;
- c_{energy} is the hourly electricity tariff vector;
- r_{gen} is the PV generation tariff;
- r_{export} is the PV export tariff;
- c_{deg} is the vector of battery degradation cost.

In each optimization step, the evaluated power exchange determines a consequently charging and discharging energy rate according to the maximum battery capacity. During all these considerations, we can easily translate power into energy because our data is defined hour by hour, so 1 kW results equal to 1 kWh.
Degradation cost function evaluates the entity of battery degradation related to the charging rate values. It applies some theories achieved by laboratory experiments performed at Northumbria University at Newcastle upon Tyne.
The obtained degradation data allows finding out the corresponding battery cycle life before the end of its life. The latter is defined as the moment in which maximum battery capacity reaches 80% of its original value, which corresponds 20% of battery degradation.
At this point, the function calculates the value of cell energy throughput scaled according to its rating. Finally, the cost of the cell is divided by the cell energy throughput before mentioned, to have the specific battery degradation cost.

Once, the cost function has received the specific battery degradation cost from the internal function, it can evaluate the consequently total energy cost of the overall load system, which means load consumption, PV generation and EV charging.

The solver performs some iterations to achieve an optimal solution of EV charging profile, according to all imposed constraints. Initially, a smart use of problem constrains was investigated in order to improve as much as possible the optimization efficiency and clarity in the definition of the problem.

In the following, these optimization problem constraints are systematically discussed.

- *x* boundary limitations: for both charging modes the upper one is related to the charger power rating. The lower one is equal to zero in the case of Smart charging, while, for V2G, *lb* is equal to the charger power rating, considered negative, if the load consumption of the related load category is higher than the charger rating, otherwise it is the opposite of the load power consumption, in the other case. In this way, the electric vehicle cannot inject power in to the grid, but it can at most feed the related load consumption requests on site, basically, it is a Vehicle-to-Home (V2H) implementation.
  Another clarification must be done. If there are more than one EV in the considered load system, each EV will be bound of a proportional share of the total load consumption.
- EVs availability constraints: they are imposed through *Aeq* and *beq* input parameters, so *x* has been forced to be equal to zero when EV is not available at the charging point;
- Linear inequalities and equalities related to EV battery capacity, EV daily-required energy, but also limitations in terms of positive and negative peak of net power absorbed from the grid, are considered by using *nonlcon* input parameter of the optimization algorithm. This is not a simple parameter, but it is a proper function called by the optimization process to set this type of constraints. Actually, there are two different functions, one related to off-home charging and the other one for all other charging typology. These functions evaluate the battery capacity at each time step considering the hourly power vector absorbed for EV charging optimized so far and it forces the following constraints, considering reported abbreviations. (Tab. 2.2.3.3)

Tab. 2.2.3.3 Constraints and abbreviations

cap(tinitial) = initial capacity + x(tinitial)*effch	(i)
cap(i) = cap(i-1) + x(i)*effch	(ii)
cap(tdep+1) = cap(tdep) – Etrip_dep	(iii)
cap(tarr) = cap(tarr-1) – Etrip_arr	(iv)
cap(tfinal) = final capacity	(v)
cap(tdep) ≥ 30% maxcap + Edailytrip	(vi)
cap(i) ≥ 30% maxcap	(vii)
cap(i) ≤ 80% maxcap	(viii)
Pnet(i) ≤ Positive Power peak without EVs	(ix)
Pnet(i) ≥ Negative Power peak without EVs	(x)
In case of off-home charging, (iv) and (vi) become:	
cap(tarr) = off-home charging capacity – Etrip_arr	
cap(tdep) ≥ 30% maxcap + Etrip_dep	

cap = battery capacity;
tinitial = hour 0;
effch = charger efficiency;
i = i-hour;
tdep = time of departure;
Etrip_dep = energy required by departure trip;
tarr = time of arrival;
Etrip_arr = energy required by arrival trip;
tfinal = hour 23.
Edailytrip = daily-required energy;
maxcap = max battery capacity;
Pnet = Net Power absorbed from the grid considering EVs charging;

Initial (i) and final (v) capacity restrictions allow the user to set the wanted EV battery conditions, as off-home charging capacity input parameter. They are directly read from the GUI panel.
It is important to stress, however, that the (vi) constraint already ensure the energy needed to perform the daily trip, so some different battery conditions could be set to find out different scenarios.
Equation (ii) takes into account the progress of energy stored in the battery in relation to hourly charging power, considering charger efficiency.
The consumptions related to departure and arrival trips are subtracted in the equations (iii) and (iv).
As mentioned in [2], it is not good practice to fully charge or discharge EV batteries, so (vii) and (viii) requirements are useful to maintain battery capacity, at each time step, between 30% and 80% of the maximum value, in order to ensure a longer battery life.
Finally, (ix) and (x) have been considered to avoid a worsening of power demand profile. Indeed, the hourly power vector absorbed for EV charging, obtained with the optimization process, must not create new peaks of power demand from the grid, so the algorithm evaluates charging profiles in order to achieve at most the same peak of the case without EV charging.
These last constraints have been implemented to guarantee a good network operation.
Of course, this can be a strong limitation for V2G provision, in fact, even if discharging towards the grid in those hours was economically profitable, the grid constraint would impede this option.

2.2.2. Electrotechnical computation

As mentioned before, inside each node block of the grid model there is a *To Workspace* block, with which is possible to export grid measurements from Simulink to Matlab platform.
This block saves on Matlab workspace a variable for each bus of the Electricity Grid. Each variable is a table with 24 rows, one value per hour, and 6 columns; the first three are the phase voltages values, the last three are the currents of each phase measured at the considered node.

To obtain magnitudes and phases results, *abs* and *angle* functions are implemented in the Matlab script.

For buses line-to-ground voltages evaluation, the script is very easy because all the data is already available from the workspace variables without any processing.
The code performs the standard following subtractions for each phase to evaluate line-to-line voltages. For example for a generic k-bus:

$$\bar{V}_{k-12} = \bar{E}_{k-ph1} - \bar{E}_{k-ph2}$$

$$\bar{V}_{k-23} = \bar{E}_{k-ph2} - \bar{E}_{k-ph3}$$

$$\bar{V}_{k-31} = \bar{E}_{k-ph3} - \bar{E}_{k-ph1}$$

For currents evaluation, line currents and bus currents must be distinguished.
Buses currents are directly derivable from the saved variables on the workspace; but the real currents flowing on the lines of the electricity grid, responsible of joule heating and so related to the lines current ratings, must be evaluated as well.

Buses currents are useful to calculate buses power.
The script considers single-phase apparent powers and three-phase apparent powers. In this way, results elaboration does not restrict the potential operating conditions of the grid. In fact, the script allows the user to implement also unbalanced loads on the electricity grid.
To evaluate single-phase apparent power, at j-phase of k-bus, the script performs the following formula:

$$\bar{S}_{k-phj} = \bar{E}_{k-phj} \times \check{I}_{k-phj}$$

To obtain single-phase active and reactive powers, the code applies *real* and *imag* functions to the single-phase apparent power.
Therefore, to achieve the three-phase active and reactive power values (P_k and Q_k), Matlab code executes the sum among the three single-phase power values, as shown below. For a generic k-node:

$$P_k = \sum_{j=1}^{3} P_j \quad ; \quad Q_k = \sum_{j=1}^{3} Q_j$$

Then, the electrotechnical computation script evaluates lines voltage drop starting from the line-to-ground voltage values, for example, if we want to calculate the voltage drop along phase 1 of line 1-2 (from bus 1 to bus 2), the formulation is:

$$\overline{dV}_{12-ph1} = \bar{E}_{1-ph1} - \bar{E}_{2-ph1}$$

Now, since the impedance $\dot{z} = R + jX_L$ of each branch is an input parameter of the model, lines current, in each phase, can be easily obtained from the voltage drop. For example, for a generic i-line, the current flowing along j-phase:

$$\bar{I}_{i-phj} = \frac{\overline{dV}_{i-phj}}{\dot{z}_i}$$

Another interesting physical quantity evaluated by the program is the active power loss in each phase of the network branches. It is found out from the voltage drop values, as well. For instance, the formulation to obtain active power loss along a j-phase of a general i-line is:

$$P_{loss_{i-phj}} = R_i \times \left| \left(\frac{\overline{dV}_{i-phj}}{\dot{z}_i} \right)^2 \right|$$

Lines current ratings are an input parameter, so this script checks the ratings compliance of all network lines. It builds a vector with the check results. To obtain this, it assesses the maximum current value detected on each phase of each line during the 24 hours; then, it checks the rating compliance for every three-phase feeder considering the highest value evaluated among the three phases.

Finally, it collects all the costs evaluated by the main program and sums them in different levels. It starts considering them from an archetype point of view, therefore it groups the costs of all categories within each archetype; then, it quantifies the costs related to the energy losses along network lines and finally it prints the overall cost of the electricity grid operation.

2.2.3. Saving Results

The third key script is responsible for results management and outputting.
Actually, there are two different scripts to perform this task, in relation to the *Saving Settings* selected in the GUI window.
At the beginning .txt files had been considered instead of .csv tables, but the printing of the output results inside text files, gave some range problems with large matrices. For this reason, .csv tables have been preferred. It has been chosen an alternative format than .xlsx because Matlab takes a long time to print the results in this kind of files; therefore, it has been necessary to find a quicker way to perform the whole process.

The first script is called when .csv tables are selected as output files.
This script exploits *cell2table(C, Name, Value)* and then *writetable(T, filename)* functions. Where *C* is the cell array we want to convert into table and in *Value* allocation must be entered the value of the parameter designated in *Name* argument, e.g. *'VariableNames'* that is useful to define the variable names in the table. *T* is the Matlab table that we want to save and *filename* is the slot where it is necessary to insert the name of .csv output table.
Each output table needs a customized code in order to obtain the wanted output features, like i.e. table headers.

The second script is called when .xlsx tables are selected as output files.
This script works mainly with *xlswrite(filename, A, sheet, xlRange)* function, where *filename* is the space for name of the .xlsx output table, *A* is the matrix we want to print in the .xlsx table, *sheet* is the allocation to specify the Excel worksheet number and *xlRange* is the Excel range where we want to write the table.
Also in this case, each output table needs a customized code in order to obtain the preferred output features, like i.e. table headers.

In addition, the user can have access to all the variables created and exploited by Matlab during the scripts/functions processing.
The modelling tool folder has been organized in some subfolders, in order to obtain a better clarity. In one of them, "Data" folder, all Matlab variables are saved.
If *workspace.mat* file is loaded on Matlab, the user can call them directly from Matlab workspace. Not all variables are useful because the scripts use some of them only for coding needs; these can be overwritten during the process.
The list, reported in Tab. A.1 (APPENDIX) shows the most interesting variables.

3. APPLICATION ON A REAL ELECTRICITY GRID

In the previous chapter, all the modelling tool sections have been inspected: from the GUI window appearance and utilization, to the internal Matlab functions.
It has been reported the logical procedure for input data implementation and the available choices for EVs implementation. Finally, it has shown a review of the obtainable output data.

This chapter aims to analyse a model of a real electricity grid, applying different scenarios in terms of PV generation and EV charging strategies.
In this way, we can easily make many comparisons in terms of voltage and current profiles, voltages deviations caused by network power flows and grid power losses.
The modelling tool allows also economic evaluations, so we can additionally deduce what are the most convenient scenarios in economic terms.

The scenarios will be inspected with the modelling tool are:

- Scenario 1: it implements only traditional loads in the electricity grid, so there are not PV generation and EV charging;
- Scenario 2: it considers traditional and smart loads, without EV implementation. The smart households share is 3.5% of the overall number. This is the amount of actual PV penetration in the UK;
- Scenario 3: it considers traditional and smart loads, without EV implementation, as Scenario 2, but with a different smart loads penetration. Its share is 15% compared to the overall number. This value is the PV penetration expected in the UK in the 2050;
- Scenario 4: it is based on the electricity network of Scenario 3, but it considers EV dumb charging;
- Scenario 5: it is based on the electricity network of Scenario 3, but it applies smart charging mode for EVs;
- Scenario 6: it is based on the electricity network of Scenario 3, but it implements V2G strategy.

3.1. Electricity network characterization

The real electricity grid studied in this thesis project has a traditional UK distribution scheme. This system includes an 11 kV connection, which represents the grid supply, with a maximum grid infeed of 60 MVA. The MV/LV substation has an 11/0.4 kV distribution transformer with Off-Circuit Tap Changer (OCTC) with 500 kVA of power rating.
The substation consists of four 400 V outgoing radial feeders, with an average length of 400m, which supply the network customers.

The information about the provided supply system are:

- MV connection:
  Three-phase short-circuit power: 60 MVA
  Voltage: 11 kV
- 11/0.4 kV transformer:
  Capacity: 500 kVA
  Impedance: 5% on rating X/R = 15 Winding: Delta-Star
  OCTC taps: (-5 ÷ 5) % with 2.5% steps

Following Fig. 3.1.1 shows a pictorial graph representation of the electricity network. As it can be seen, the grid has been split in some numerical nodes in order to allow a clear categorization of it. The detailed line diagram is reported in Fig. A.1 (APPENDIX).

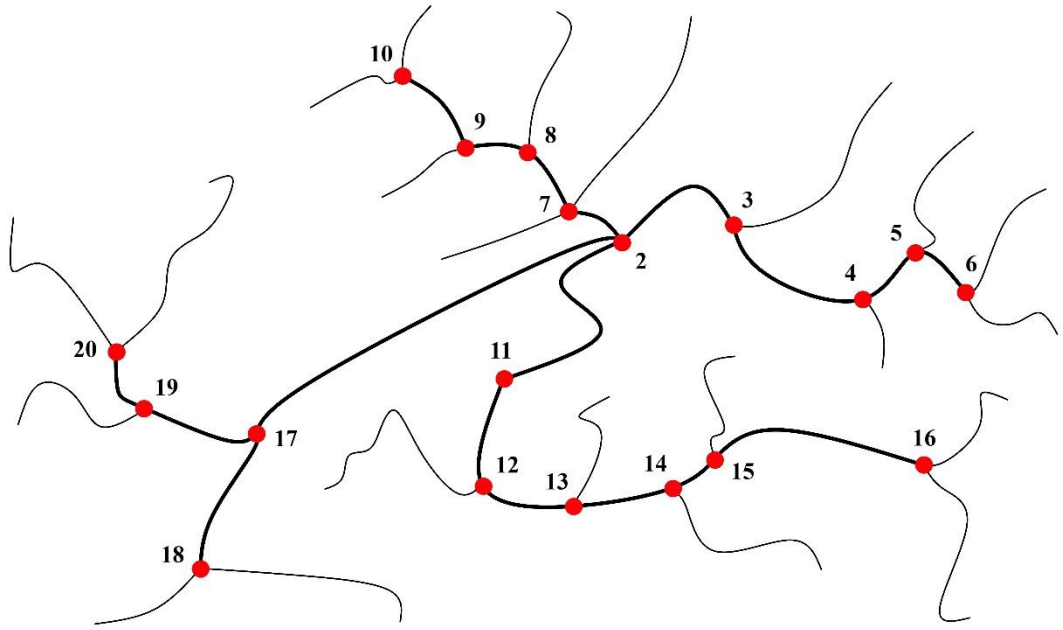

Fig. 3.1.1 Network graph

Moreover, the information about the typology and length of the existing distribution network feeders are summarized in Tab. 3.1.1 below:

Tab. 3.1.1 Network feeders information

Network buses		**Length [m]**	**Cable type**
from	to		
2	3	82	AL Consac 120 mm2
3	4	97	AL Consac 120 mm2
4	5	38	AL Consac 70 mm2
5	6	42	AL Consac 70 mm2
2	7	50	AL Consac 70 mm2
7	8	53	AL Consac 240 mm2
8	9	42	AL Consac 185 mm2
9	10	56	AL Consac 120 mm2
2	11	110	CU 240 mm2
11	12	65	CU 240 mm2
12	13	77	CU 185 mm2
13	14	45	CU 185 mm2
14	15	30	CU 185 mm2
15	16	130	CU 185 mm2
2	17	250	CU 185 mm2
17	18	100	CU 35 mm2
17	19	100	CU 185 mm2

The Simulink representation of the electricity grid, created by the Smart Grid Modelling Tool, is reported in Fig. A.1 (APPENDIX). It has minor differences compared to the graph shown in Fig. 3.1.1. It locates the grid buses in the right position on the resulting map, but it links them through straight branches, so eventual curves of feeder route are neglected.

3.2. Network loads characterization

The considered electricity grid is located in the UK, in a predominantly residential area. Indeed, the main customers are households.
At the beginning, to start the loads characterization, it has been performed a grid analysis in order to calculate the different types of load.
The results show that there are 295 houses, 3 shops and 1 school, connected to the grid.
To evaluate a more comprehensive and diverse case study some other types of load, i.e. light industries have been added.
Three light industries have been considered into the grid. Therefore, recapping, the loads taken into account in the case study are reported in the following Tab. 3.2.1.

Tab. 3.2.1 Load typologies

Load typology	**Number**
Households	295
Schools	1
Shops	3
Light industries	3

Each load category has a typical daily load profile, which are based on Distribution System Operators (DSOs) After Diversity Maximum Demand (ADMD) reports.
They have estimated Low Voltage (LV) network demands through the aforementioned procedure, considering a hundred nominal consumers and measuring their consumptions at the MV/LV substation [35].

Therefore, the following figures (Fig. 3.2.1 and Fig. 3.2.2) illustrate the load active power profiles considered for this case study.
While, Fig. 3.2.3 shows the specific active power considered for PV generation. To evaluate the actual power injected by the generating system, it is necessary to multiply these values by the nominal power of the PV power plant. These values, based on [35], are dependent on the geographic location and orientation and on the efficiency conditions of PVs.

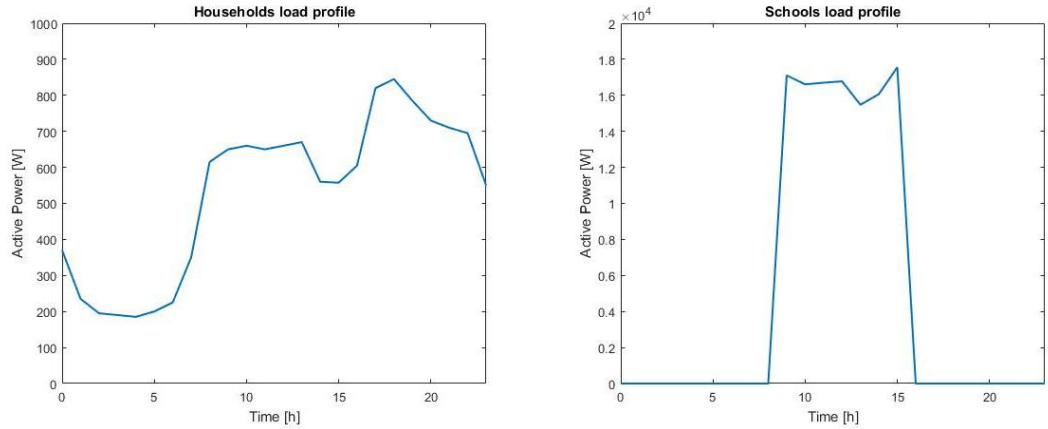

Fig. 3.2.1 Households and Schools profiles

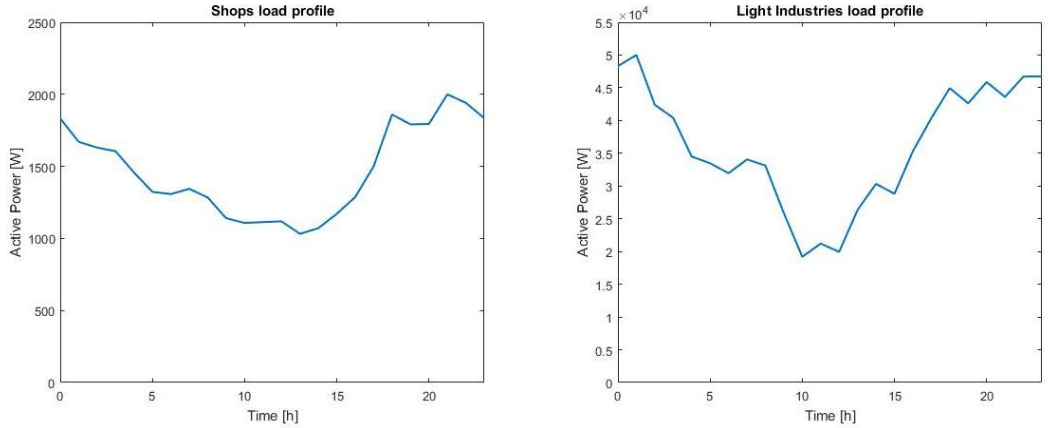

Fig. 3.2.2 Shops and Light Industries profiles

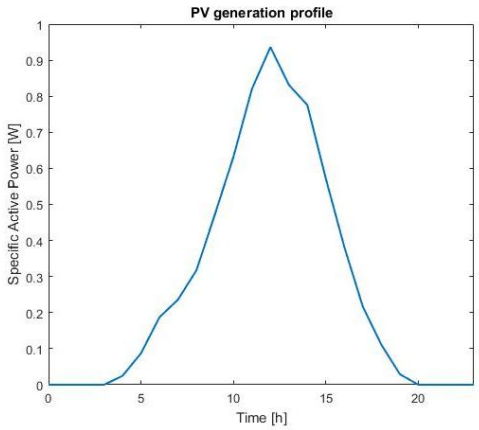

Fig. 3.2.3 PV generation profile

3.3. Economic parameters

To characterize all economic variables, four prices must be set. Firstly, it is necessary to fix hourly electricity tariff. In according to [38], it has been considered two different prices during the day: 16.64 p/kWh for peak hours; 5.73 p/kWh during off-peak time. So the input data for this parameter is shown in Tab. 3.3.1.

Tab. 3.3.1 Hourly electricity tariff

Time [h]	**Price** [p/kWh]
8 a.m. ≤ t ≤ 12 a.m.	16.64
1 a.m. ≤ t ≤ 7 a.m.	5.73

As aforementioned, for PV generation a Feed-in Tariff is considered. Therefore, two different values must be set, one for generation tariff and one for export tariff. The energy supplier pays PV owners for each kWh of electricity generated (generation tariff) and it pays them a further rate for each kWh exported back to the grid (export tariff). The considered values are 13.39 p/kWh for PV generation tariff and 4.85 p/kWh for PV export tariff [38].

Finally, in according to [38] the batteries price has been set equal to 148 p/kWh.

3.4. Electric Vehicles characterization

The parameters related to EVs, taken into account in this thesis project, result from a literature and state of art analysis.
The European Union has established a new procedure [39] to evaluate the official energy consumption and CO_2 emission for new cars starting from 1 September 2017. It is called WLTP (Worldwide Harmonised Light Vehicle Test Procedure) and it will replace the current unrealistic NEDC (New European Driving Cycle) procedure.
Anyway, the resulting average value of EVs efficiency is about 0.2 kWh/mile.
Comparisons, in terms of average daily trip, show up that a reliable value can be 24 km per day, which means about 15 miles per day [7].
Literature [40] indicates that charger efficiency is depending on the charging/discharging power, for example at 1 kW it is very low, about 80%, at 2.5 kW it moves up to 90%, finally above 6 kW it can be higher than 95%. Therefore, in this case study, it has been considered equal to 90% considering that the lowest EV charger power is 3kW.
To determine the battery cell rating value, some other comparisons has been realized. But, a relevant benchmark value is 0.125 kWh.
Once these parameters are set, the remaining two are initial and final capacity of EV batteries. To put real and reliable values it has been necessary a deep reasoning.
These values affect the charging and eventual discharging of EVs, so they have deserved close attention. The Matlab project needs these values, which are its initial conditions, because is based on 24-hours evaluations. It has been decided to set them with an equal value in order to support neither charging nor discharging. Hence, it has been put equal to 50%.
For the household EVs departure and arrival time, the default values have been maintained: 8 a.m. for the average departure time; 6 p.m. for the arrival one.
Overviews of EV market [41] report that about 65% of EV owners charge their vehicle at home between 4 p.m. and 10 p.m., which means as soon as they get home from work. Therefore, the input parameter related to home charging share has been set equal to 65%.
The remaining 35% charges its batteries in off-home charging points, along the streets, at charging stations or at work and it has been considered that these charges allow to achieve a battery capacity equal to 70% of their ratings.

From this point forward, it is possible to start studying the reference grid considering each scenario previously mentioned.

Anyway, first of all, each scenario will be explained to understand the reasons that led to making the relevant choices. For example about the share of smart load than traditional ones.

3.5. Scenario 1 (no PV, no EV charging)

In this first context, only traditional loads are implemented in the electricity grid. It means that neither PV generation, nor EV charging are considered.
It was reputed important to start from this framework for a first understanding of the network operation.
This scenario considers the loads reported in sec. 3.2 (Tab. 3.2.1). Their distribution on the electricity grid is shown in Tab. 3.5.1 below.

Tab. 3.5.1 Scenario 1 loads

Buses	Nominal voltage	LOADS CHARACTERIZATION								
		Households		Schools		Shops		Light Industries		Car Parks
N°	Vrms	N° Smart	N° Traditional	N° Smart	N° Traditional	N° Smart	N° Traditional	N° Smart	N° Traditional	N° Smart
1	11000	0	0	0	0	0	0	0	0	0
2	400	0	**12**	0	0	0	0	0	0	0
3	400	0	**12**	0	0	0	0	0	0	0
4	400	0	**8**	0	0	0	0	0	0	0
5	400	0	**12**	0	0	0	0	0	0	0
6	400	0	**12**	0	0	0	0	0	0	0
7	400	0	**17**	0	0	0	0	0	0	0
8	400	0	**18**	0	0	0	0	0	0	0
9	400	0	**11**	0	0	0	0	0	0	0
10	400	0	**8**	0	0	0	0	0	0	0
11	400	0	**12**	0	0	0	0	0	0	0
12	400	0	**26**	0	0	0	**1**	0	0	0
13	400	0	**9**	0	0	0	0	0	0	0
14	400	0	**17**	0	0	0	0	0	0	0
15	400	0	**25**	0	0	0	**1**	0	0	0
16	400	0	**21**	0	0	0	0	0	**1**	0
17	400	0	**17**	0	0	0	0	0	0	0
18	400	0	**5**	0	**1**	0	0	0	**1**	0
19	400	0	**23**	0	0	0	**1**	0	**1**	0
20	400	0	**30**	0	0	0	0	0	0	0

At this point, once all the network and loads parameters have been set on the modelling tool, all is ready for the creation and evaluation of the electricity grid.
The main results obtained by the network calculation are reported in the following.

Fig. 3.5.1 shows the hourly voltage deviation profile at the different 400V network nodes. It can be seen that, maintaining a transformer secondary voltage equal to 0.4 kV, which means an Off-Circuit Tap Changers (OCTC) value equal to 1 pu, the voltage curve at node 18 and 20 does not comply with the imposed limits [-6%, +10%].

The profile of bus 1, 11 kV, is not reported here because it is basically flat at the nominal voltage.

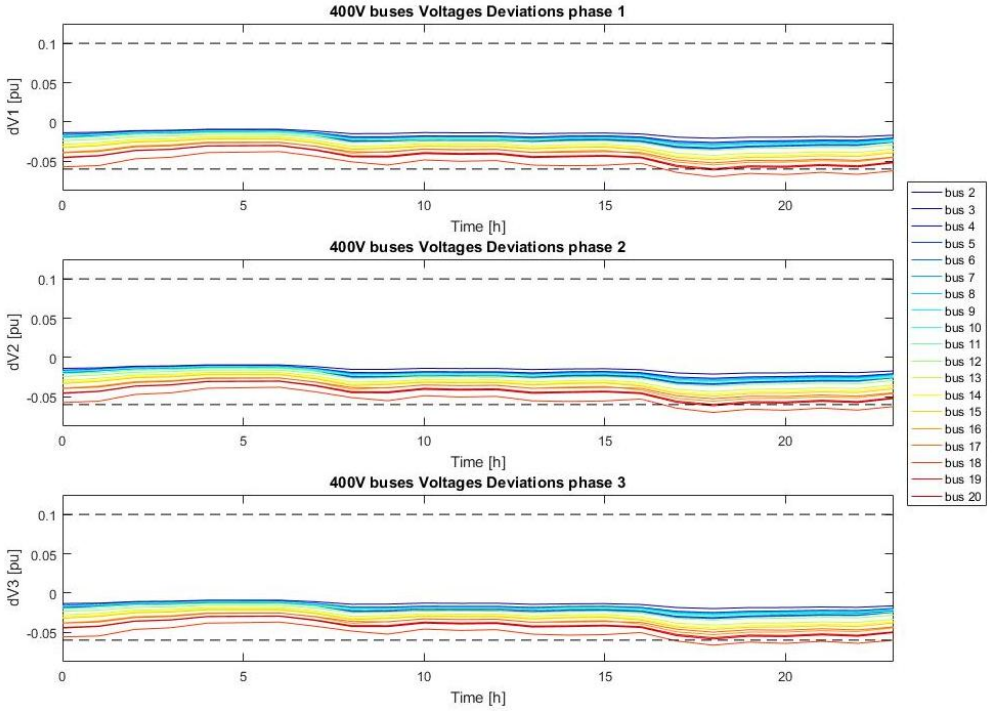

Fig. 3.5.1 S1 - Voltages deviations (tap=1)

For this reason, the calculation has been re-performed with a higher value of OCTC at the distribution transformer.

The necessary value in order to comply with the voltage constraints is 1.025 pu, which means +2.5% tap. The resulting voltage profiles at the different network nodes are shown in the following Fig. 3.5.2.

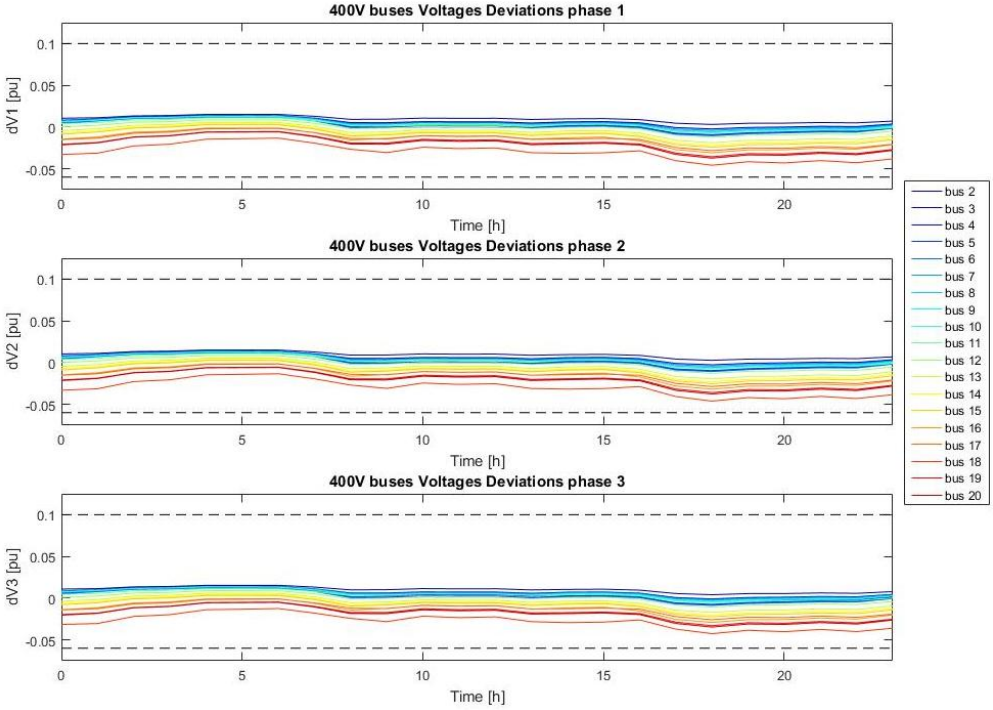

Fig. 3.5.2 S1 - Voltages deviations (tap=1.025)

In this case, all the voltage curves are within the limits; therefore, it makes sense to continue the network analysis considering this OCTC value.

Line currents can be inspected through two different outputs: graphical representation of branch currents (Fig. 3.5.3) and lines current ratings check table (Tab. 3.5.2).
It can be seen from them that there is no significant load in all the lines. The maximum line load is slightly greater than 70% and the mean value is around 40%. The most loaded branches are those at the beginning of the electricity network, nearby the distribution substation, and the line 17-18, which supplies both school and one light industry.

Fig. 3.5.3 allows us to realize how much the daily variation, in terms of lines utilization, is. In fact, if we consider the lines that supply industries, such as lines 2-17, 17-18 and 17-19, the load variation is very low during the day. While, for lines providing energy to residential areas this variation is very significant. For instance, for the line 2-11 the percentage ratio between daily minimum and maximum current value is more than 40%.

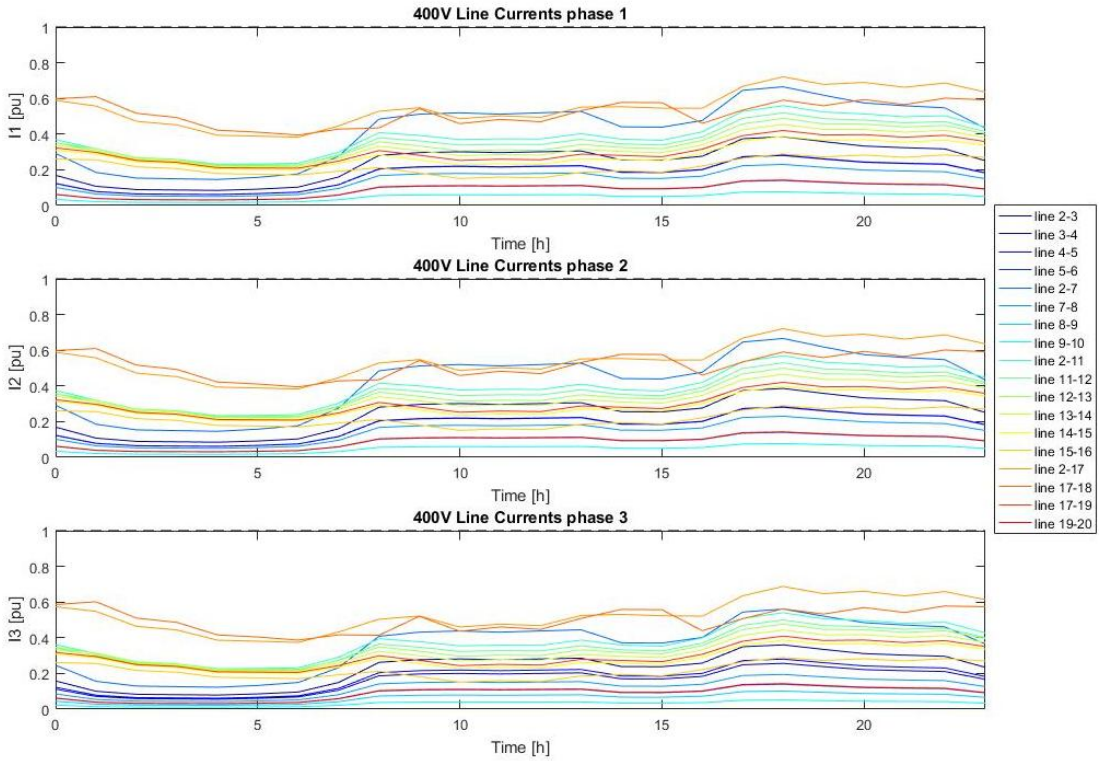

Fig. 3.5.3 S1 - Line Currents

Tab. 3.5.2 S1 - Lines current ratings

Line_2-3	Current rating complied: 57.8881A vs 150A nominal
Line_3-4	Current rating complied: 42.3285A vs 150A nominal
Line_4-5	Current rating complied: 30.8513A vs 110A nominal
Line_5-6	Current rating complied: 15.4067A vs 110A nominal
Line_2-7	Current rating complied: 73.2336A vs 110A nominal
Line_7-8	Current rating complied: 50.1581A vs 218A nominal
Line_8-9	Current rating complied: 26.9413A vs 190A nominal
Line_9-10	Current rating complied: 11.5503A vs 150A nominal
Line_2-11	Current rating complied: 223.7096A vs 393A nominal
Line_11-12	Current rating complied: 208.0792A vs 393A nominal
Line_12-13	Current rating complied: 170.7703A vs 342A nominal
Line_13-14	Current rating complied: 159.174A vs 342A nominal
Line_14-15	Current rating complied: 136.3357A vs 342A nominal
Line_15-16	Current rating complied: 98.8533A vs 342A nominal
Line_2-17	Current rating complied: 246.6463A vs 342A nominal
Line_17-18	Current rating complied: 82.2954A vs 135A nominal
Line_17-19	Current rating complied: 143.8072A vs 342A nominal
Line_19-20	Current rating complied: 38.5223A vs 270A nominal

In Fig. 3.5.3 above, the three graphs show the current profiles on each phase. If we compare them, we can see that the load is almost balanced.
The resulting output tables are huge, but if we consider the lines starting from the distribution substation, shown in the following Tab. 3.5.3, we can confirm what stated before.

Tab. 3.5.3 S1 - Phase currents comparison

Hour	Magnitude I23_ph1	Magnitude I23_ph2	Magnitude I23_ph3	Magnitude I27_ph1	Magnitude I27_ph2	Magnitude I27_ph3	Magnitude I211_ph1	Magnitude I211_ph2	Magnitude I211_ph3	Magnitude I217_ph1	Magnitude I217_ph2	Magnitude I217_ph3
[h]	[A]	[A]	[A]	[A]	[A]	[A]	[A]	[A]	[A]	[A]	[A]	[A]
0	25,354	25,381	23,683	32,061	32,085	27,025	145,193	146,899	141,888	201,335	201,357	196,298
1	16,126	16,143	15,054	20,377	20,391	17,169	124,696	125,774	122,591	190,583	190,598	187,372
2	13,383	13,396	12,492	16,909	16,920	14,247	105,659	106,553	103,911	161,408	161,420	158,743
3	13,038	13,051	12,171	16,475	16,486	13,881	101,569	102,441	99,867	154,431	154,444	151,835
4	12,689	12,702	11,848	16,038	16,049	13,515	90,802	91,651	89,146	134,651	134,662	132,126
5	13,714	13,728	12,806	17,336	17,348	14,610	91,264	92,184	89,476	132,909	132,921	130,182
6	15,421	15,437	14,403	19,498	19,513	16,434	92,994	94,031	90,985	130,977	130,991	127,913
7	23,969	23,995	22,395	30,319	30,343	25,561	117,513	119,130	114,391	152,546	152,567	147,787
8	42,086	42,132	39,334	53,256	53,301	44,907	160,418	163,269	154,940	180,683	180,718	172,328
9	44,471	44,522	41,569	56,280	56,330	47,462	154,290	157,310	148,507	187,309	187,345	178,475
10	45,147	45,198	42,204	57,141	57,192	48,190	145,224	148,292	139,353	166,350	166,386	157,380
11	44,466	44,516	41,566	56,276	56,327	47,461	146,784	149,805	141,001	171,778	171,814	162,944
12	45,148	45,199	42,204	57,141	57,192	48,191	146,454	149,521	140,582	169,018	169,055	160,048
13	45,839	45,891	42,848	58,011	58,063	48,922	158,096	161,209	152,135	188,572	188,610	179,467
14	38,323	38,367	35,819	48,493	48,536	40,893	146,053	148,652	141,069	189,268	189,301	181,657
15	38,150	38,194	35,658	48,276	48,319	40,710	143,512	146,101	138,551	186,532	186,565	178,955
16	41,405	41,450	38,696	52,392	52,436	44,178	162,244	165,048	156,855	186,526	186,560	178,306
17	56,110	56,172	52,443	71,005	71,065	59,875	207,167	210,969	199,864	228,420	228,466	217,281
18	57,824	57,888	54,044	73,172	73,234	61,701	219,793	223,710	212,266	246,599	246,646	235,119
19	53,720	53,779	50,207	67,977	68,034	57,320	205,785	209,423	198,792	231,997	232,041	221,333
20	49,963	50,018	46,693	63,219	63,272	53,306	201,720	205,102	195,217	235,906	235,947	225,987
21	48,593	48,646	45,413	61,486	61,537	51,845	195,348	198,637	189,023	226,583	226,623	216,936
22	47,572	47,623	44,456	60,190	60,240	50,751	197,625	200,843	191,432	234,703	234,742	225,259
23	37,658	37,699	35,188	47,640	47,678	40,165	172,931	175,475	168,028	217,498	217,530	210,021

From a voltage unbalances point of view, we can evaluate the hourly percentage value with the following formula:

$$Voltage\ Unbalance\ [\%] = 100 \times \frac{Maximum\ Voltage\ Deviation}{Average\ Voltage} \qquad (3.5.1)$$

If we consider upstream and downstream nodes of the transformer, so bus number 1 and 2, the average value of voltage unbalance, as shown in Tab. 3.5.4, is 0.009 % in the MV bus, while is 0.048 % in the LV node.

Tab. 3.5.4 S1 - Phase voltages comparison

Hour	Magnitude E1_ph1	Magnitude E1_ph2	Magnitude E1_ph3	Voltage unbalance	Magnitude E2_ph1	Magnitude E2_ph2	Magnitude E2_ph3	Voltage unbalance
[h]	[V]	[V]	[V]		[V]	[V]	[V]	
0	6339,25	6339,04	6339,72	0,006%	233,378	233,343	233,459	0,028%
1	6339,63	6339,53	6339,95	0,004%	233,512	233,489	233,573	0,021%
2	6341,43	6341,34	6341,69	0,003%	234,015	233,997	234,066	0,017%
3	6341,84	6341,75	6342,09	0,003%	234,129	234,111	234,178	0,017%
4	6342,92	6342,84	6343,17	0,003%	234,435	234,417	234,482	0,016%
5	6342,95	6342,85	6343,22	0,003%	234,441	234,421	234,492	0,017%
6	6342,93	6342,82	6343,23	0,004%	234,432	234,410	234,489	0,020%
7	6341,12	6340,96	6341,59	0,006%	233,917	233,883	234,008	0,031%
8	6338,12	6337,85	6338,96	0,010%	233,074	233,014	233,237	0,055%
9	6338,27	6337,99	6339,16	0,011%	233,108	233,044	233,282	0,059%
10	6339,36	6339,07	6340,27	0,011%	233,408	233,344	233,584	0,059%
11	6339,12	6338,84	6340,01	0,011%	233,343	233,279	233,516	0,058%
12	6339,22	6338,93	6340,13	0,011%	233,370	233,306	233,546	0,059%
13	6338,02	6337,73	6338,94	0,011%	233,040	232,975	233,220	0,061%
14	6338,61	6338,37	6339,38	0,009%	233,208	233,154	233,358	0,051%
15	6338,85	6338,60	6339,61	0,009%	233,271	233,217	233,419	0,050%
16	6337,83	6337,57	6338,66	0,010%	232,995	232,937	233,157	0,055%
17	6334,18	6333,85	6335,33	0,014%	231,996	231,915	232,220	0,076%
18	6332,93	6332,60	6334,11	0,014%	231,658	231,575	231,891	0,079%
19	6334,14	6333,83	6335,23	0,013%	231,985	231,908	232,200	0,073%
20	6334,25	6333,96	6335,27	0,012%	232,016	231,944	232,216	0,068%
21	6334,90	6334,61	6335,88	0,012%	232,192	232,122	232,385	0,066%
22	6334,53	6334,24	6335,49	0,012%	232,091	232,023	232,281	0,064%
23	6336,36	6336,13	6337,12	0,009%	232,594	232,540	232,742	0,050%
				0,009%				0,048%

The grid modelling tool provides also power graphs. Fig. 3.5.4 shows the single-phase active power at each phase of network nodes.
Through the results printed on the output tables of power, it is possible to obtain the hourly values of utilization factor of the distribution transformer.
As aforementioned, it has a power rating of 500 kVA and the graphical representation of hourly three-phase apparent power at each grid node is reported in Fig. 3.5.5, while the values of power flowing towards the distribution network are reported in Tab. 3.5.5 below. It demonstrates that the transformer utilization factor is, naturally, very low in the morning, while it reaches the highest values during the evening.
The daily average value is around 60%, so it means that this residential area can be extended, in terms of number of houses or, more in general, number of loads, without overloading the distribution transformer. It will be very interesting to study this area in the next scenarios to understand how much future trends can change this values.

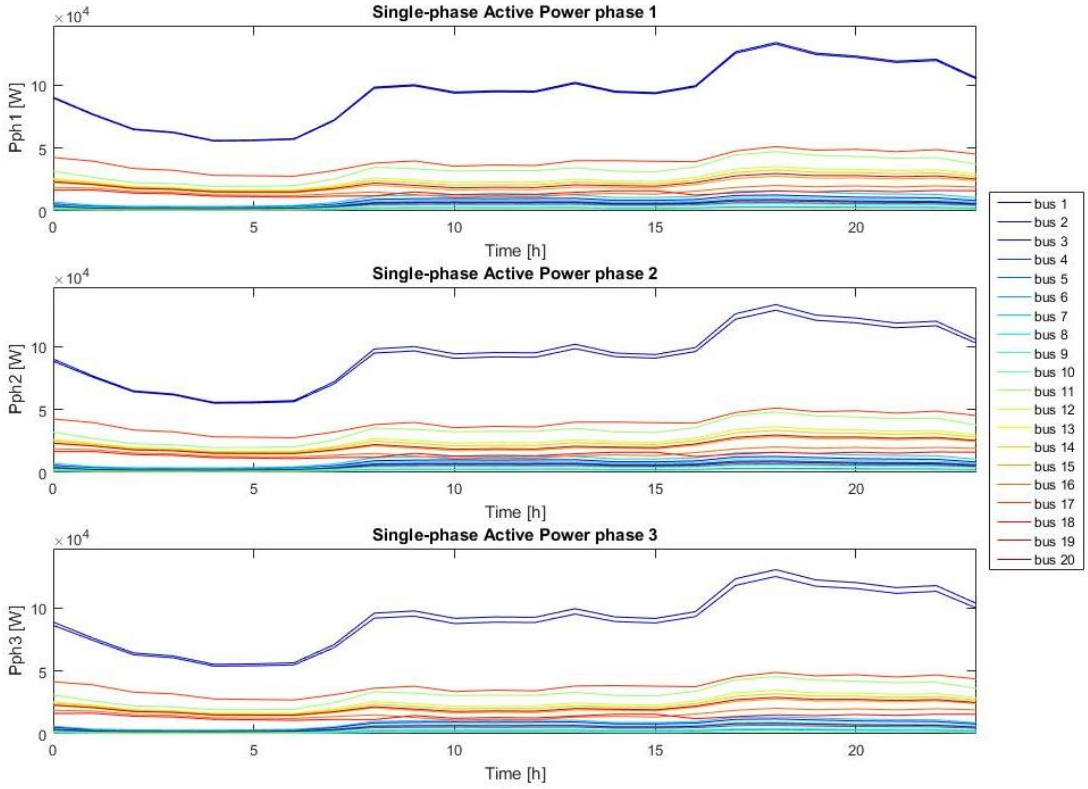

Fig. 3.5.4 S1 - Single-phase Active Power

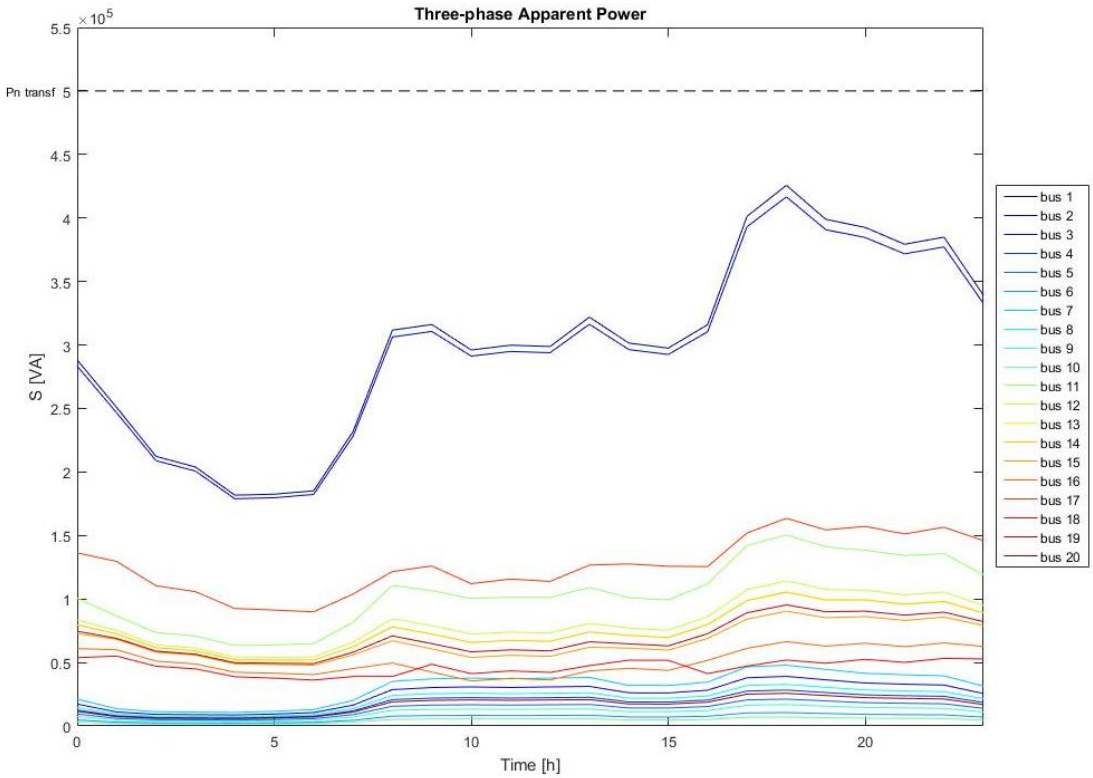

Fig. 3.5.5 S1 - Three-phase Apparent Power

Tab. 3.5.5 S1 - Transformer utilization factor

Hour	P + jQ	A	Transformer Utilization factor
[h]	[W + jVAr]	[VA]	
0	265658.82 + 98449.71i	283314,24	57%
1	226613.64 + 97229.80i	246591,52	49%
2	191965.83 + 82365.18i	208889,69	42%
3	184500.16 + 78930.91i	200674,86	40%
4	164814.36 + 69643.95i	178924,71	36%
5	165780.04 + 69338.48i	179696,54	36%
6	168611.52 + 69386.19i	182330,17	36%
7	212117.52 + 83907.73i	228110,39	46%
8	287148.57 + 106539.28i	306275,89	61%
9	292458.32 + 104767.22i	310657,43	62%
10	275028.22 + 95763.15i	291223,46	58%
11	278209.16 + 97805.45i	294900,40	59%
12	277464.96 + 96891.55i	293895,86	59%
13	297809.07 + 106609.12i	316315,90	63%
14	278002.76 + 102747.27i	296382,41	59%
15	274575.58 + 100854.97i	292512,35	59%
16	290642.73 + 108976.65i	310401,52	62%
17	368870.92 + 135888.40i	393104,84	79%
18	390461.57+ 145335.22i	416632,41	83%
19	366074.41 + 136608.53i	390733,11	78%
20	359624.27 + 136303.95i	384588,59	77%
21	347770.93 + 131409.18i	371770,08	74%
22	352374.89 + 134480.90i	377164,66	75%
23	309834.70 + 121364.98i	332756,67	67%
			59%

At this point, it is possible to focus on the power losses in the network lines. They depend on the characteristics of the cable and on the magnitude of the current that is flowing in them. The most critical line in terms of power loss is the 2-17 (Fig. 3.5.6), because it supplies energy to two light industries and one school, so the flowing current is very high.

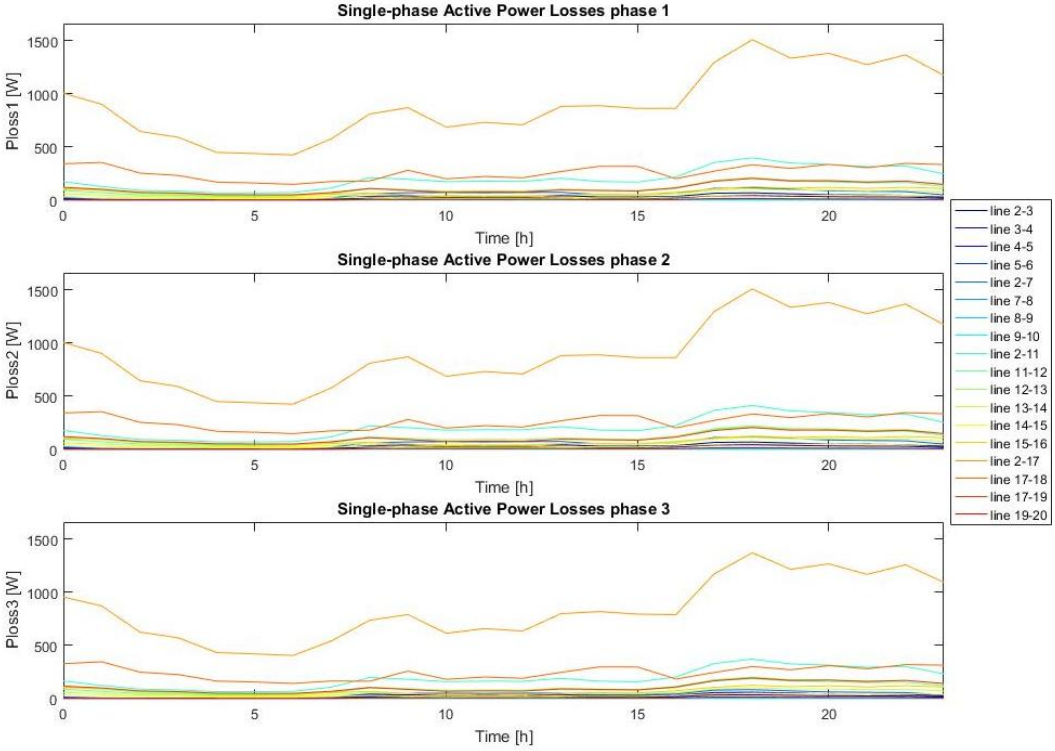

Fig. 3.5.6 S1 - Power losses

Finally, we can investigate the economic results of the electricity network operation. The modelling tool calculates them in terms of operational costs, so it evaluates the costs related to the energy flowing in the grid. The results are presented in an output table where the operational costs of the archetypes are systematically printed, then it shows the costs related to the energy loss in each lines and, in conclusion, it indicates the total cost.
The economic results are as follows in Tab. 3.5.6.

Tab. 3.5.6 S1 - Economic results

Archetype1	Archetype2	Archetype3	Archetype4	Archetype5	Archetype6	Archetype7	Archetype8	Archetype9	Archetype10
[£]	[£]	[£]	[£]	[£]	[£]	[£]	[£]	[£]	[£]
0	23.32	23.32	15.54	23.32	23.32	33.03	34.97	21.37	15.54
Archetype11	Archetype12	Archetype13	Archetype14	Archetype15	Archetype16	Archetype17	Archetype18	Archetype19	Archetype20
[£]	[£]	[£]	[£]	[£]	[£]	[£]	[£]	[£]	[£]
23.32	55.25	17.49	33.03	53.31	155.81	33.03	144.07	164.43	58.29

ELoss23	ELoss34	ELoss45	ELoss56	ELoss27	ELoss78	ELoss89	ELoss910	ELoss211
[£]	[£]	[£]	[£]	[£]	[£]	[£]	[£]	[£]
0.35	0.22	0.09	0.02	0.57	0.08	0.02	0.01	2.18
ELoss1112	ELoss1213	ELoss1314	ELoss1415	ELoss1516	ELoss217	ELoss1718	ELoss1719	ELoss1920
[£]	[£]	[£]	[£]	[£]	[£]	[£]	[£]	[£]
1.12	1.2	0.61	0.31	0.76	9.23	2.57	1.15	0.07

Total
[£]
972.31

As could be expected, the higher costs are related to the Archetypes number 16, 18 and 19, where are located industries and school.
Through a comparison between the costs of energy consumed and those of energy losses, we can observe that the firsts are about 98% of the overall cost, £ 951.74 compared to a total cost of £ 972.31. Therefore, we can state that this electricity network with the data considered by Scenario 1 is operating in an efficient way.

3.6. Scenario 2 (3.5% of household PV, no EV charging)

The second scenario investigates the operating conditions of the considered electricity network with a 3.5% of smart households share compared to the overall number, without considering EVs on the grid.
This value has been evaluated considering the actual PV penetration level in the UK, through National Statistics reports.
The first document analysed is Solar Photovoltaics Deployment in the UK: December 2017 [37], which is provided by the Department for Business, Energy & Industrial Strategy of the UK government. Table 1 of the report shows the amount of the total capacity and the cumulative count of PVs subdivided by power rating.
The second information investigated is about the actual number of houses in the UK. This information is provided by the ONS (Office for National Statistics) of UK government [42].
At this point, some calculations have been made to evaluate the share as follows.

- Number of household PV plants in the UK [37]: 933065;
- Number of houses in the UK [42]: 26994000.

Therefore, finally it is possible to evaluate the actual share by dividing the values shown above, obtaining about 3.5%.

The total number of electricity customers is maintained equal to the Scenario 1, so, as aforementioned, the total number of households is 295. While, the houses that actually have PV generation, called smart households, are now 10.
Their location on the electricity network is established by a statistical approach. The most populated nodes of the grid have been evaluated in order to draw up an ordered list. Thus, the 10 smart houses have been spread in relation to this sequence.

From the provided data of the electricity grid, we can state that:

- The school, at node 18, has a 10kW rooftop photovoltaic generation;
- All the shops do not have PV installations;
- Only the light industry at node 19 has a 25kW rooftop photovoltaic generation, while the others do not have generation.

In conclusion, the distribution of the customers on the electricity network is reported in Tab. 3.6.1 below.

Tab. 3.6.1 Scenario 2 loads

Buses	Nominal voltage	LOADS CHARACTERIZATION								
		Households		Schools		Shops		Light Industries		Car Parks
N°	Vrms	N° Smart	N° Traditional	N° Smart	N° Traditional	N° Smart	N° Traditional	N° Smart	N° Traditional	N° Smart
1	11000	0	0	0	0	0	0	0	0	0
2	400	0	**12**	0	0	0	0	0	0	0
3	400	0	**12**	0	0	0	0	0	0	0
4	400	0	**8**	0	0	0	0	0	0	0
5	400	0	**12**	0	0	0	0	0	0	0
6	400	0	**12**	0	0	0	0	0	0	0
7	400	**1**	**16**	0	0	0	0	0	0	0
8	400	**1**	**17**	0	0	0	0	0	0	0
9	400	0	**11**	0	0	0	0	0	0	0
10	400	0	**8**	0	0	0	0	0	0	0
11	400	0	**12**	0	0	0	0	0	0	0
12	400	**1**	**25**	0	0	0	**1**	0	0	0
13	400	0	**9**	0	0	0	0	0	0	0
14	400	**1**	**16**	0	0	0	0	0	0	0
15	400	**1**	**24**	0	0	0	**1**	0	0	0
16	400	**1**	**20**	0	0	0	0	0	**1**	0
17	400	**1**	**16**	0	0	0	0	0	0	0
18	400	0	**5**	**1**	0	0	0	0	**1**	0
19	400	**1**	**22**	0	0	0	**1**	**1**	0	0
20	400	**2**	**28**	0	0	0	0	0	0	0

To evaluate this new scenario, it is necessary to change the information inside Buses&Loads input table and then click on the relevant GUI buttons.

The resulting grid representation, from a macroscopic point of view, is the same as before, but if we look under the Archetype blocks, we can find the different loads. Now we have smart household blocks, smart school block and smart light industry block.

The first analysis of the electricity grid is in terms of voltage deviation.
Fig. 3.6.1 shows that, by setting an OCTC value of the transformer equal to 1.025 pu, the voltage is within the imposed limits, while with 1 pu they are not complied (this last situation is not graphically reported on these pages).
The profile of bus 1, 11 kV, is not shown because it is basically flat at the nominal voltage.

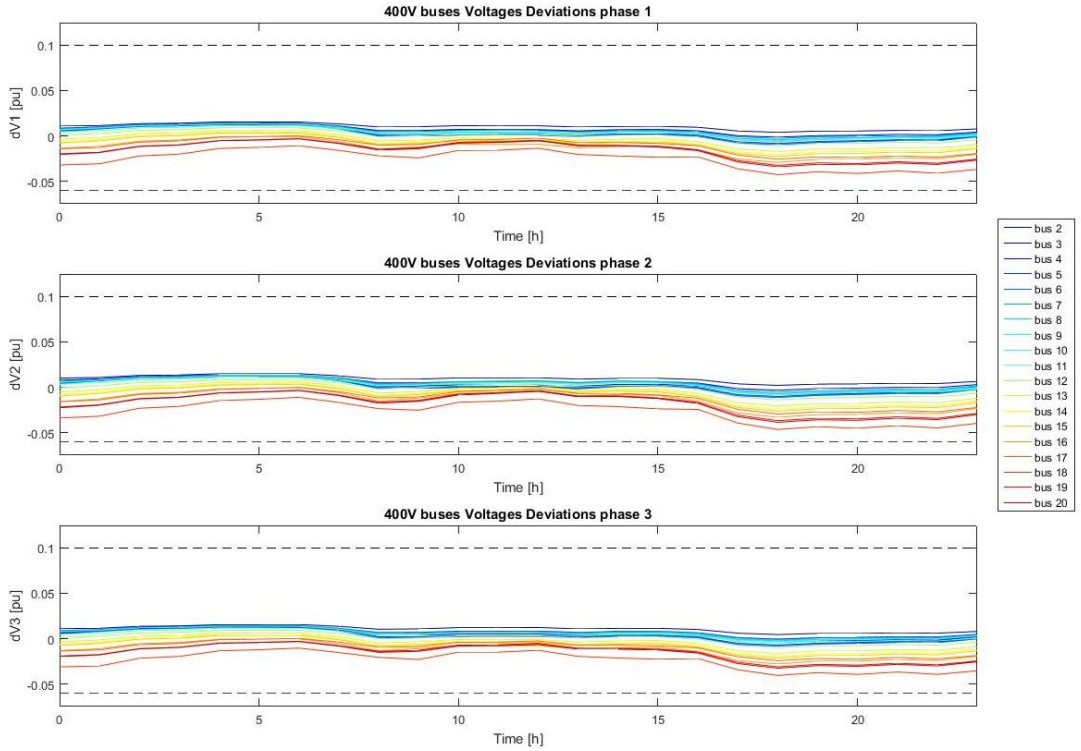

Fig. 3.6.1 S2 - Voltages deviations

If we compare the voltages deviations of Scenario 1 and Scenario 2 (Fig. 3.5.2 and Fig. 3.6.1) we can observe different profile shapes during the central hours of the day, when PV generation reduces the amount of power absorbed from the electricity grid.
There are not major discrepancies because the share of prosumers in the network is very low, therefore, much energy is still provided by the grid.

These slight differences can be easily observed in the graphical representation of branch currents. In Fig. 3.6.2 the profiles of lines 2-17, 17-18 and 17-19 stay lower than Fig. 3.5.3, relative to Scenario 1, because the related archetypes directly consume the power produced by the installed PV plants.
There are no differences in terms of maximum line load, as shown in Tab. 3.6.2, because PV generation operates in the central hours of the day, while the peak of power demand, detectable in Fig. 3.6.2, is during the late afternoon/evening.

If we compare the actual maximum current values of Scenario 1 and 2 (Tab. 3.5.2 and Tab. 3.6.2) we can observe minor differences. They are not caused by errors, but since there are different values of voltage on the electricity grid, there are also different values of flowing current.

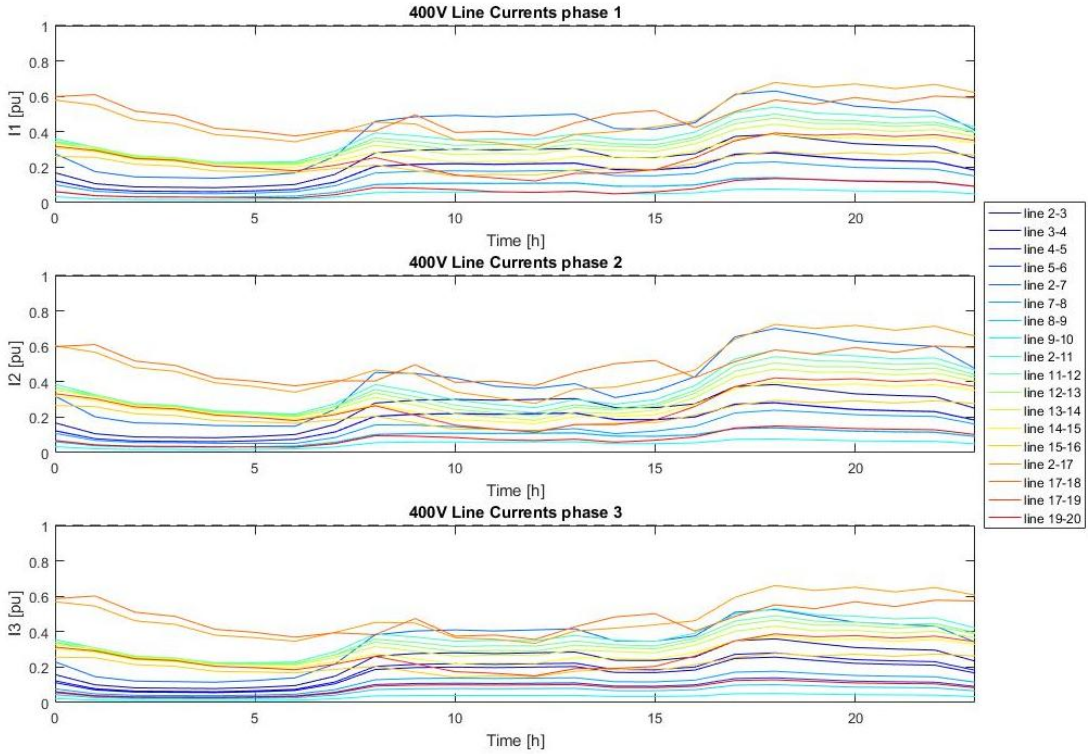

Fig. 3.6.2 S2 - Line Currents

Tab. 3.6.2 S2 - Lines current ratings

Line_2-3	Current rating complied: 57.8196A vs 150A nominal
Line_3-4	Current rating complied: 42.3493A vs 150A nominal
Line_4-5	Current rating complied: 30.8804A vs 110A nominal
Line_5-6	Current rating complied: 15.3978A vs 110A nominal
Line_2-7	Current rating complied: 77.1032A vs 110A nominal
Line_7-8	Current rating complied: 52.1933A vs 218A nominal
Line_8-9	Current rating complied: 26.9681A vs 190A nominal
Line_9-10	Current rating complied: 11.5427A vs 150A nominal
Line_2-11	Current rating complied: 227.6817A vs 393A nominal
Line_11-12	Current rating complied: 212.7926A vs 393A nominal
Line_12-13	Current rating complied: 173.1024A vs 342A nominal
Line_13-14	Current rating complied: 161.5523A vs 342A nominal
Line_14-15	Current rating complied: 136.4983A vs 342A nominal
Line_15-16	Current rating complied: 100.9337A vs 342A nominal
Line_2-17	Current rating complied: 247.5479A vs 342A nominal
Line_17-18	Current rating complied: 82.3155A vs 135A nominal
Line_17-19	Current rating complied: 144.3187A vs 342A nominal
Line_19-20	Current rating complied: 40.5478A vs 270A nominal

In the following Tab. 3.6.3, it is possible to compare the values of current flowing in each phase of the three-phase lines starting from the distribution substation.
The household PV generation, implemented in this scenario, is represented by single-phase systems, therefore their low penetration and consequent uneven distribution leads to current imbalances; while vice versa if the penetration was higher, the total would result almost balanced.
This is evident if we consider Tab. 3.6.3 below. Line 2-3 is not subject to smart households, so its phase currents are nearly balanced. Line 2-7 and 2-11 have some PV systems, in fact, we can observe important imbalances mostly during the central hours of the day, when the generation is not negligible. While line 2-17, having predominant three-phase PV systems of light industry and school, shows an almost balanced condition.

Tab. 3.6.3 S2 - Phase currents comparison

Hour	Magnitude I23_ph1	Magnitude I23_ph2	Magnitude I23_ph3	Magnitude I27_ph1	Magnitude I27_ph2	Magnitude I27_ph3	Magnitude I211_ph1	Magnitude I211_ph2	Magnitude I211_ph3	Magnitude I217_ph1	Magnitude I217_ph2	Magnitude I217_ph3
[h]	[A]	[A]	[A]	[A]	[A]	[A]	[A]	[A]	[A]	[A]	[A]	[A]
0	25,329	25,204	23,641	30,363	35,091	25,306	141,815	151,638	140,113	197,967	206,263	194,585
1	16,095	15,980	15,025	19,287	22,242	16,075	122,536	128,688	121,455	188,434	193,667	186,278
2	13,356	13,259	12,468	16,004	18,455	13,339	103,865	108,967	102,969	159,624	163,965	157,835
3	13,013	12,920	12,148	15,593	17,984	12,997	99,822	104,797	98,949	152,694	156,924	150,951
4	12,669	12,587	11,826	15,182	16,831	12,654	89,105	92,403	88,254	131,446	134,798	130,138
5	13,694	13,614	12,782	16,413	16,559	13,680	89,433	89,167	88,512	125,725	127,463	125,260
6	15,404	15,325	14,377	18,464	16,377	15,389	90,939	85,046	89,903	117,462	116,704	118,315
7	23,955	23,862	22,357	28,721	26,875	23,937	114,328	108,654	112,715	134,870	135,408	135,355
8	42,082	41,966	39,272	50,463	49,772	42,057	154,842	151,021	152,005	155,479	159,435	154,850
9	44,471	44,368	41,504	53,332	49,145	44,452	148,401	135,686	145,403	152,070	152,075	153,553
10	45,153	45,062	42,138	54,152	46,260	45,135	139,249	116,835	136,203	121,353	117,109	125,107
11	44,469	44,379	41,501	53,332	41,253	44,451	140,899	106,800	137,897	115,824	106,532	122,316
12	45,153	45,065	42,138	54,152	39,878	45,134	140,479	99,728	137,431	106,306	94,748	114,233
13	45,839	45,738	42,779	54,974	42,813	45,819	152,027	117,731	148,933	131,756	122,380	138,273
14	38,317	38,218	35,760	45,949	34,189	38,297	140,974	107,460	138,389	136,926	126,649	143,601
15	38,145	38,046	35,600	45,743	38,211	38,127	138,456	117,268	135,885	146,295	141,438	150,059
16	41,399	41,281	38,634	49,643	47,188	41,373	156,757	148,631	153,965	157,537	159,343	157,972
17	56,108	55,958	52,361	67,284	71,877	56,076	199,734	207,869	195,953	207,530	219,203	203,476
18	57,820	57,657	53,960	69,336	77,103	57,786	212,131	227,682	208,236	232,003	247,548	226,062
19	53,714	53,561	50,129	64,413	73,672	53,683	198,666	217,876	195,049	223,043	239,838	216,349
20	49,953	49,799	46,620	59,900	69,259	49,922	195,096	214,689	191,733	229,276	245,749	222,616
21	48,584	48,436	45,342	58,259	67,364	48,555	188,905	207,967	185,635	220,134	236,159	213,657
22	47,560	47,407	44,386	57,029	65,934	47,529	191,315	209,955	188,114	228,390	244,066	222,049
23	37,641	37,502	35,130	45,132	52,166	37,614	167,931	182,638	165,399	212,499	224,882	207,479

In the same way as Scenario 1, it is possible to evaluate the voltage unbalances in the electricity network. It can be expected, from the above, that the results will be worse than before.

If we just look at upstream and downstream nodes of the transformer, bus 1 and 2, we can calculate the hourly values considering the above equation 3.5.1.

Tab. 3.6.4 shows that the average value of voltage unbalance is 0.017% in the MV bus and 0.082% in the LV node. However, while in Scenario 1 the average values were very close to the peaks, in this case the upper values are 0.035% and 0.140%, respectively.

Tab. 3.6.4 S2 - Phase voltages comparison

Hour	Magnitude E1_ph1	Magnitude E1_ph2	Magnitude E1_ph3	Voltage unbalance	Magnitude E2_ph1	Magnitude E2_ph2	Magnitude E2_ph3	Voltage unbalance
[h]	[V]	[V]	[V]		[V]	[V]	[V]	
0	6339,68	6338,59	6339,81	0,012%	233,445	233,275	233,474	0,053%
1	6339,89	6339,24	6340,02	0,008%	233,560	233,436	233,586	0,039%
2	6341,65	6341,10	6341,75	0,006%	234,055	233,953	234,076	0,032%
3	6342,05	6341,51	6342,15	0,006%	234,168	234,069	234,188	0,031%
4	6343,06	6342,69	6343,22	0,005%	234,472	234,381	234,497	0,029%
5	6342,93	6342,90	6343,26	0,004%	234,480	234,393	234,519	0,030%
6	6342,65	6343,17	6343,26	0,006%	234,475	234,394	234,537	0,032%
7	6340,87	6341,34	6341,67	0,007%	233,988	233,853	234,074	0,051%
8	6338,00	6338,24	6339,16	0,011%	233,206	232,953	233,338	0,091%
9	6337,79	6338,88	6339,36	0,014%	233,250	233,011	233,418	0,092%
10	6338,45	6340,50	6340,44	0,021%	233,551	233,337	233,751	0,089%
11	6337,69	6340,92	6340,17	0,030%	233,484	233,312	233,721	0,092%
12	6337,48	6341,40	6340,27	0,035%	233,513	233,357	233,774	0,097%
13	6336,63	6339,87	6339,13	0,030%	233,191	233,015	233,432	0,094%
14	6337,22	6340,42	6339,52	0,029%	233,333	233,200	233,551	0,081%
15	6337,99	6339,95	6339,76	0,020%	233,394	233,223	233,570	0,075%
16	6337,55	6338,21	6338,86	0,010%	233,129	232,896	233,273	0,087%
17	6334,59	6333,66	6335,63	0,016%	232,178	231,795	232,317	0,130%
18	6333,60	6331,98	6334,43	0,021%	231,844	231,418	231,968	0,140%
19	6334,92	6332,96	6335,52	0,024%	232,154	231,740	232,254	0,133%
20	6335,04	6333,05	6335,53	0,024%	232,171	231,779	232,259	0,125%
21	6335,67	6333,73	6336,13	0,023%	232,342	231,962	232,427	0,121%
22	6335,28	6333,38	6335,74	0,022%	232,239	231,866	232,322	0,119%
23	6336,96	6335,44	6337,30	0,018%	232,709	232,417	232,774	0,093%
				0,017%				0,082%

From an electric power point of view, Fig. 3.6.3 shows the single-phase active power at each phase of network nodes.

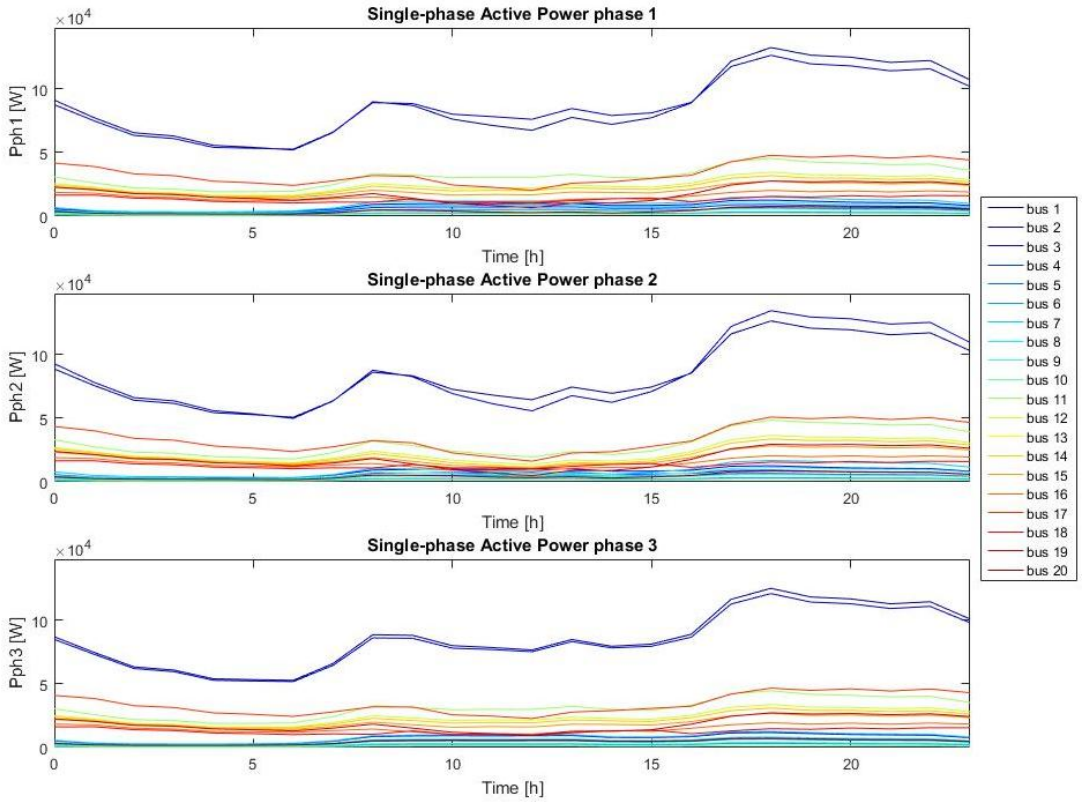

Fig. 3.6.3 S2 - Single-phase Active Power

If we make a comparison with Fig. 3.5.4, it is possible to notice a bigger difference among the power profiles of bus 1 and 2. This is because of the actual load unbalance conditions.

The peak of power consumption is experienced during the evening, when PV generation is not producing; therefore, it is not different from the case of Scenario 1. Indeed, also analysing Fig. 3.6.4, which shows the hourly profiles of apparent power at each node of the electricity grid, we can state that the power supplied to the loads by the transformer is lower than its nominal power. If we compare the following figure with Fig. 3.5.5 of Scenario 1, we can observe a significant decrease in the power absorbed from the MV connection by the distribution network during the daytime, thanks to the electricity supplied by PV generation.

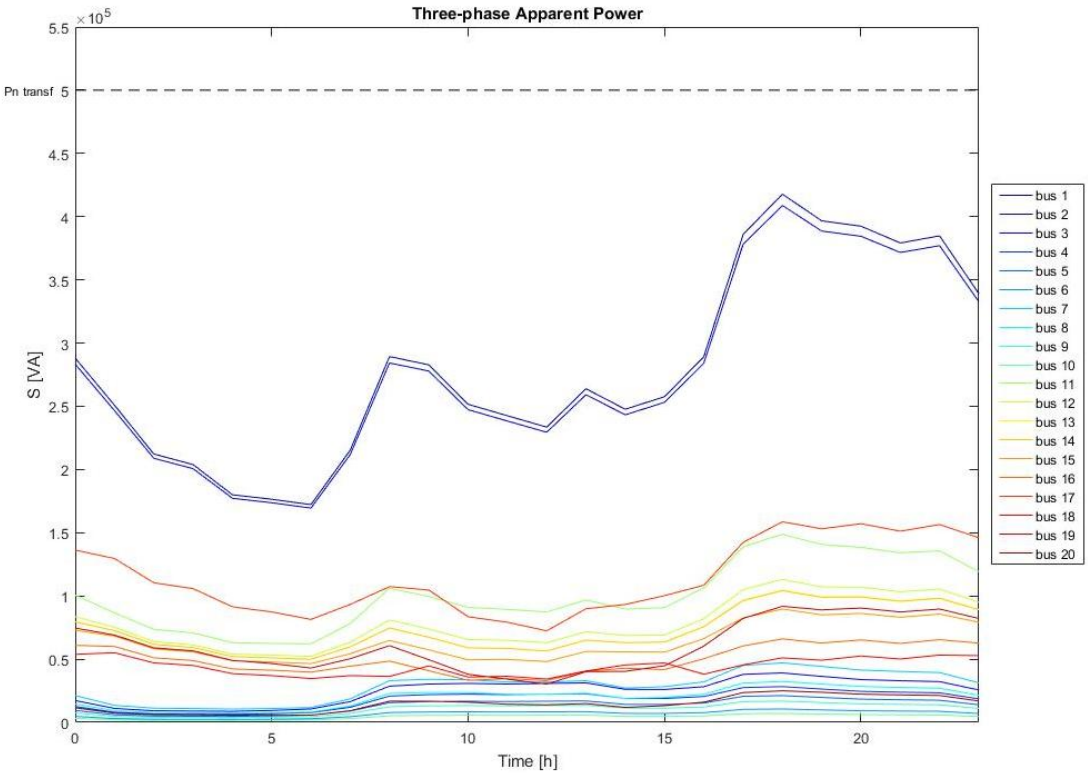

Fig. 3.6.4 S2 - Three-phase Apparent Power

What stated before is confirmed by Tab. 3.6.5. It is based on the power output tables and it shows the hourly values of the utilization factor of the distribution transformer.
The resulting average value is 55%, with lower values during the morning (minimum equal to 34%) and higher values in the evening (maximum equal to 82%).
As mentioned before, in the central hours of the day, the utilization factor of the transformer results lower than the case of Scenario 1, because PV generation supplies electric energy to the loads. Therefore, the overall average value goes down from 59% to 55%.

Tab. 3.6.5 S2 - Transformer utilization factor

Hour	P + jQ	A	Transformer Utilization factor
[h]	[W + jVAr]	[VA]	
0	265668.09 + 98239.35i	283249,89	57%
1	226622.78 + 97089.52i	246544,63	49%
2	191973.27 + 82249.89i	208851,09	42%
3	184507.25 + 78818.78i	200637,30	40%
4	162971.25 + 69573.73i	177200,83	35%
5	159230.20 + 69356.46i	173679,52	35%
6	154533.79 + 69545.70i	169461,78	34%
7	194445.30 + 84044.60i	211831,23	42%
8	263507.93 + 106610.21i	284257,22	57%
9	257229.32 + 105027.97i	277844,91	56%
10	227806.10 + 96301.54i	247324,90	49%
11	216935.92 + 98644.52i	238310,58	48%
12	207495.34 + 97915.37i	229437,86	46%
13	235858.11 + 107350.91i	259139,47	52%
14	220159.80 + 103453.90i	243255,11	49%
15	231998.10 + 101247.00i	253128,58	51%
16	262274.41 + 109070.03i	284049,54	57%
17	352946.55 + 135577.36i	378090,59	76%
18	382322.58 + 144884.18i	408854,47	82%
19	363956.03 + 136123.03i	388578,78	78%
20	359658.68 + 135837.79i	384455,82	77%
21	347800.98 + 130964.32i	371641,19	74%
22	352404.57 + 134045.36i	377037,32	75%
23	309857.73 + 121025.73i	332654,54	67%
			55%

Considering now the power losses in the network lines, we can expect lower values in the central part of the day than Scenario 1, because PV generation directly supplies the loads located at the same grid node, without affecting the network branches.
This is an advantage of local consumption of the electricity generated by PV systems. In fact, from an electricity grid point of view, this energy does not affect the grid, or at least it affects very few parts of the grid.
Fig. 3.6.5 below shows the profiles of active power losses in the network lines.
As aforementioned, it can be observed that the power losses in the electricity grid are lower during the day, while in the morning and in the evening they remain equal.
The most critical line is still the 2-17, because it supplies energy to two light industries and one school, so the flowing current is very high.

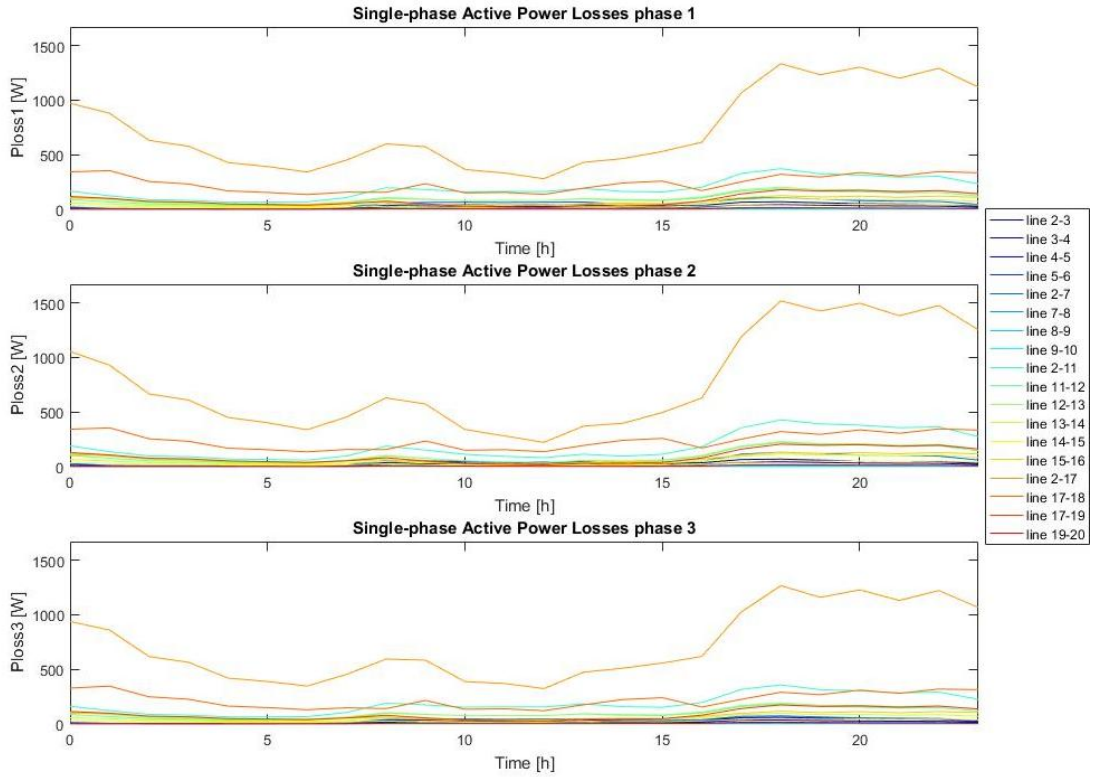

Fig. 3.6.5 S2 - Power losses

In conclusion, we can investigate the economic results of the electricity network operation, through the output table provided by the modelling tool, reported in Tab. 3.6.6.
Comparing it with the economic results of Scenario 1 shown in Tab. 3.5.6, it is evident that the nodes, where there is PV generation, have a lower operational cost than the previous scenario. The overall cost results equal to £ 847.08 (in the Scenario 1 was £ 972.31).
The cost of energy consumed is now £ 829.13£ (£ 951.74), while the cost of energy losses is £ 17.96 (£ 20.56). The first cost typology cover about 98% of the total cost.
The saving related to the lower cost of energy losses confirms what previously stated, which is that PV generation, if locally consumed, reduces line currents and consequently the losses.

Tab. 3.6.6 S2 - Economic results

Archetype1	Archetype2	Archetype3	Archetype4	Archetype5	Archetype6	Archetype7	Archetype8	Archetype9	Archetype10
[£]	[£]	[£]	[£]	[£]	[£]	[£]	[£]	[£]	[£]
0.00	23.32	23.32	15.54	23.32	23.32	27.36	29.30	21.37	15.54
Archetype11	Archetype12	Archetype13	Archetype14	Archetype15	Archetype16	Archetype17	Archetype18	Archetype19	Archetype20
[£]	[£]	[£]	[£]	[£]	[£]	[£]	[£]	[£]	[£]
23.32	49.58	17.49	27.36	47.64	150.14	27.36	126.04	110.86	46.95

ELoss23	ELoss34	ELoss45	ELoss56	ELoss27	ELoss78	ELoss89	ELoss910	ELoss211
[£]	[£]	[£]	[£]	[£]	[£]	[£]	[£]	[£]
0.35	0.22	0.09	0.02	0.51	0.07	0.02	0.01	2.03
ELoss1112	ELoss1213	ELoss1314	ELoss1415	ELoss1516	ELoss217	ELoss1718	ELoss1719	ELoss1920
[£]	[£]	[£]	[£]	[£]	[£]	[£]	[£]	[£]
1.04	1.12	0.57	0.29	0.73	7.61	2.30	0.92	0.06

Total
[£]
847.08

3.7. Scenario 3 (15% of household PV, no EV charging)

This scenario inspects the operating conditions of the considered electricity network with a view to the year 2050, without considering EVs on the grid. Therefore, it considers a 15% of smart households share compared to the overall number, which is increased by 17% than the actual one.
Some National Statistics reports and forecasts have been analysed to find out the information related to the year 2050.
National Grid in [43] investigates the UK Future Energy Scenarios. It expects a rapid growth from the mid-2020s of wind and solar generation capacity. It forecasts that the actual 12.7 GW of solar generation capacity [37] will become 63 GW in 2050.
Nowadays, the total number of PV systems in the UK is 937421 [37], so if we perform a ratio between the actual generation capacity and the overall number of PV, we can obtain an average value of power of each plant. It results equal to 13.55 kW. Assuming that, this value will remain constant also in the 2050, we can evaluate the total number of PV plants in the UK in 2050 by dividing the expected power capacity by the average power per plant.
It results equal to 4650199 units. Nowadays in the UK, the ratio between the total number of PV and the number of household PV, evaluated considering [37], is 99.5%. Assuming that this percentage will remain valid also in 2050, the number of household PV systems in the year 2050 will be equal to 4628590.
To evaluate the share of smart households compared to the overall number, another value is necessary. This is the total number of houses in the UK in 2050. It has been evaluated starting from the population increase.
The current UK population is around 65.64 million [44], while the number of houses, as aforementioned, is 26994000 [42]. Therefore, the resulting average number of people in each house is 2.43. Population forecasts expects [44] 77 million people in the UK in 2050.
Assuming that the number of people per house will remain constant, we can evaluate the number of houses in the UK in the year 2050. It results equal to 31665722.
Hence, we can state the following:

- The penetration level of household PV in 2050 will be around 15%;
- The number of houses in the UK by 2050 will increase by around 17%.

To proceed with the evaluation of the electricity grid is firstly needed to redefine the number of electricity customers.
Nowadays, in the considered electricity network, the number of households is 295, but considering the increase mentioned above, the houses will be 345 in 2050, of which 52 (15%) will have PV generation.

Since the location of the electricity grid in the UK is known, the 50 new houses (345-295) will be considered in nodes where new buildings can be potentially built, in according to the available land space. These nodes are 6, 10, 16 and 19 with respectively 16, 8, 16 and 10 new houses. It has been considered that most of the new buildings has PV generation, so this has been taken into account to allocate the 52 households with solar panels. The resulting distribution of them on the grid is shown below.

With a view to the year 2050, one new car park at node 6 and one new shop at node 4 are added to the grid. The new shop is considered “smart”, so it implements a PV generation system. The modelling tool applies a 4 kW PV power plant on the smart shop, while an 8 kW system on the car park.

In conclusion, the distribution of the customers on the electricity network is reported in the following Tab. 3.7.1.

Tab. 3.7.1 Scenario 3 loads

Buses	Nominal voltage	LOADS CHARACTERIZATION								
		Households		Schools		Shops		Light Industries		Car Parks
N°	Vrms	N° Smart	N° Traditional	N° Smart	N° Traditional	N° Smart	N° Traditional	N° Smart	N° Traditional	N° Smart
1	11000	0	0	0	0	0	0	0	0	0
2	400	**1**	**11**	0	0	0	0	0	0	0
3	400	**1**	**11**	0	0	0	0	0	0	0
4	400	0	**8**	0	0	**1**	0	0	0	0
5	400	**1**	**11**	0	0	0	0	0	0	0
6	400	**10**	**18**	0	0	0	0	0	0	**1**
7	400	**2**	**15**	0	0	0	0	0	0	0
8	400	**2**	**16**	0	0	0	0	0	0	0
9	400	**1**	**10**	0	0	0	0	0	0	0
10	400	**6**	**10**	0	0	0	0	0	0	0
11	400	0	**12**	0	0	0	0	0	0	0
12	400	**2**	**24**	0	0	0	**1**	0	0	0
13	400	0	**9**	0	0	0	0	0	0	0
14	400	**2**	**15**	0	0	0	0	0	0	0
15	400	**2**	**23**	0	0	0	**1**	0	0	0
16	400	**10**	**27**	0	0	0	0	0	**1**	0
17	400	**1**	**16**	0	0	0	0	0	0	0
18	400	0	**5**	**1**	0	0	0	0	**1**	0
19	400	**8**	**25**	0	0	0	**1**	**1**	0	0
20	400	**3**	**27**	0	0	0	0	0	0	0

To evaluate this new scenario, the new information must be loaded inside Buses&Loads input table and then click on the relevant GUI buttons.

Also in this case, the resulting grid representation, from a macroscopic point of view, is the same as before, because new network nodes have not been added to the grid; but inside the Archetype blocks, we can find all different typologies of load.

This scenario considers a higher PV penetration, but at the same time also a higher power consumption because the number of loads is greater. Therefore, we can expect higher shapes in the morning and evening compared to Scenario 2, while the opposite during the daytime.

To follow a standard scheme, the first analysis of the electricity grid is in terms of voltage deviation.
Here again, it has been set an OCTC value of the distribution transformer equal to 1.025 pu and, as can be seen in the following Fig. 3.7.1, the voltage deviations comply with the voltage constraints.

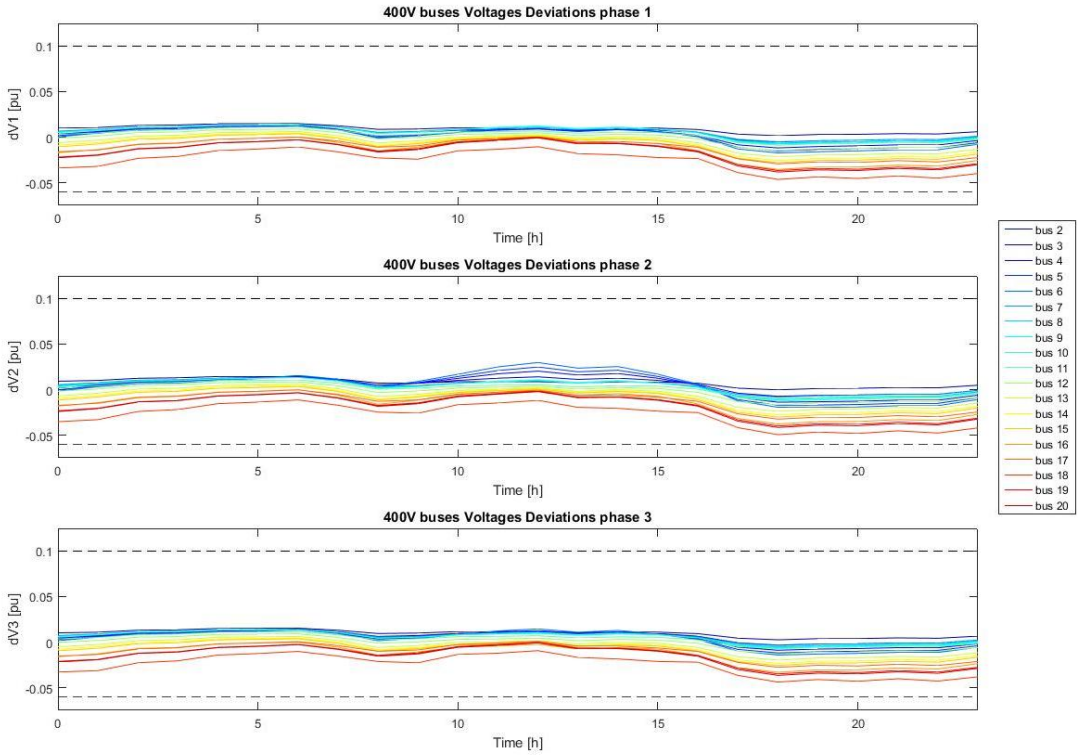

Fig. 3.7.1 S3 - Voltages deviations

Analysing these diagrams, we can notice a rise of the profiles during the central hours of the day, because of solar generation. Moreover, in the second diagram, concerning the second phase of the distribution lines, there is a greater voltage increase. This phenomenon can be explained taking into account the random distribution of the single-phase systems. In fact, the modelling tool performs a random splitting inside each archetype, so could be possible to obtain a more loaded phase, from an overall point of view, if uneven single-phase systems are considered on the grid.

If we perform a line currents analysis, as shown in the Fig. 3.7.2 below, it is evident that some branches are more loaded in the daytime, compared to Fig. 3.6.2 of Scenario 2. These lines are, for instance, those relative to the branch 2-3-4-5-6. This phenomenon can be explained considering the high PV penetration at node 6, in fact, during these hours, generation is much higher than consumption in this part of the network, so we have a reverse power flow.
As aforementioned, this can be a big issue for PV generation deployment, if local consumption is not guarantee.
Hence, if we consider the results reported in Tab. 3.7.2, but also the complete currents output tables, network lines are more loaded than Scenario 2 (Tab. 3.6.2).
Since Fig. 3.7.2 and Tab. 3.7.2 show only results in terms of pu or modules, we cannot state that this higher load causes an overall worsening in economic terms, because we need more information. Of course, we will have higher costs related to energy losses, but we could have savings by consuming renewable electricity, rather than electricity from power system.

In the following, through the transformer analysis, power profiles and economic results, it will be easier to investigate on this point.

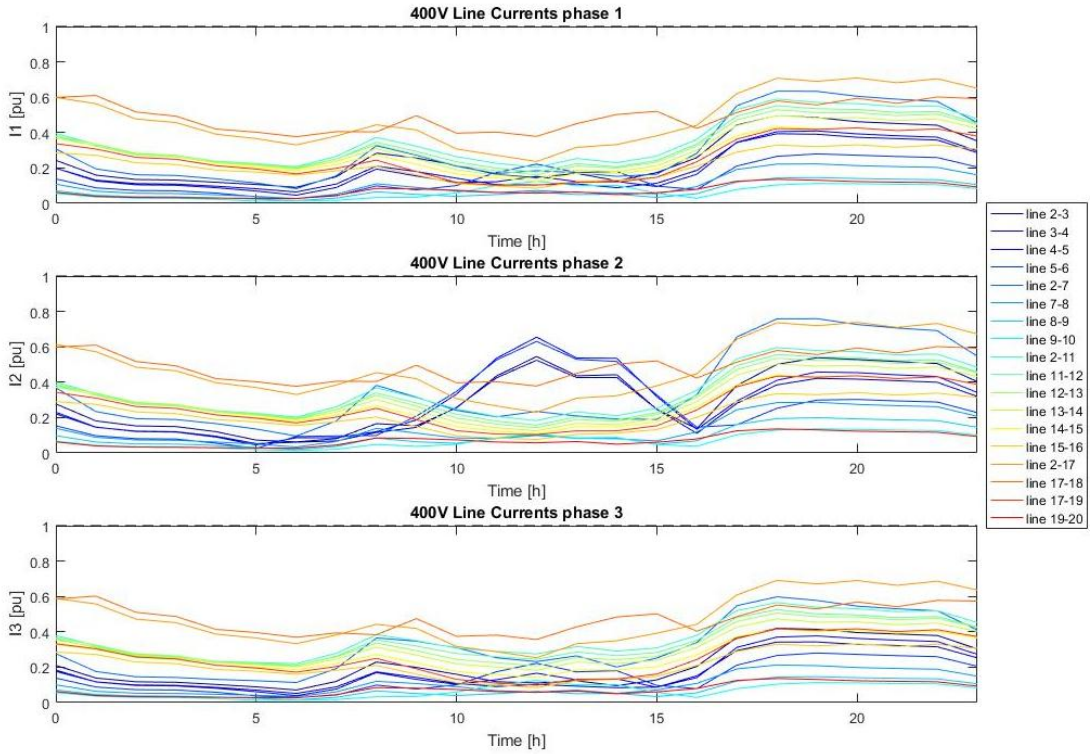

Fig. 3.7.2 S3 - Line Currents

Tab. 3.7.2 S3 - Lines current ratings

Line_2-3	Current rating complied: 85.7761A vs 150A nominal
Line_3-4	Current rating complied: 81.5819A vs 150A nominal
Line_4-5	Current rating complied: 72.8923A vs 110A nominal
Line_5-6	Current rating complied: 69.3132A vs 110A nominal
Line_2-7	Current rating complied: 83.4999A vs 110A nominal
Line_7-8	Current rating complied: 62.4773A vs 218A nominal
Line_8-9	Current rating complied: 37.8997A vs 190A nominal
Line_9-10	Current rating complied: 20.5157A vs 150A nominal
Line_2-11	Current rating complied: 234.1801A vs 393A nominal
Line_11-12	Current rating complied: 218.8523A vs 393A nominal
Line_12-13	Current rating complied: 183.0237A vs 342A nominal
Line_13-14	Current rating complied: 171.7519A vs 342A nominal
Line_14-15	Current rating complied: 150.3624A vs 342A nominal
Line_15-16	Current rating complied: 116.5622A vs 342A nominal
Line_2-17	Current rating complied: 252.4726A vs 342A nominal
Line_17-18	Current rating complied: 82.317A vs 135A nominal
Line_17-19	Current rating complied: 149.1494A vs 342A nominal
Line_19-20	Current rating complied: 36.7007A vs 270A nominal

In the Tab. 3.7.3 below, it is possible to compare the values of current flowing in each phase of the three-phase lines starting from the distribution substation.
The worst unbalanced conditions are in the line 2-3. In fact, for example at 12 and 2 p.m., it has very high differences among the three currents values.
As explained above, in this branch we have an even PV generation at node 6, but uneven PV distribution at nodes 2, 3 and 5.
Line 2-17 is almost balanced; in fact, we can observe very slightly differences in phase current values.
While, lines 2-7 and 2-11 are in a middle operational condition, in fact we can notice higher imbalances during the central hours of the day.

Tab. 3.7.3 S3 - Phase currents comparison

Hour	Magnitude I23_ph1	Magnitude I23_ph2	Magnitude I23_ph3	Magnitude I27_ph1	Magnitude I27_ph2	Magnitude I27_ph3	Magnitude I211_ph1	Magnitude I211_ph2	Magnitude I211_ph3	Magnitude I217_ph1	Magnitude I217_ph2	Magnitude I217_ph3
[h]	[A]	[A]	[A]	[A]	[A]	[A]	[A]	[A]	[A]	[A]	[A]	[A]
0	36,526	41,597	31,519	33,786	40,497	30,412	155,239	156,945	148,665	204,657	209,694	201,355
1	23,968	27,195	20,789	21,468	25,726	19,319	131,033	132,127	126,897	192,669	195,871	190,585
2	20,259	22,937	17,622	17,814	21,347	16,030	110,915	111,826	107,486	163,137	165,795	161,409
3	19,765	22,374	17,195	17,356	20,799	15,619	106,693	107,579	103,350	156,117	158,707	154,433
4	17,875	18,444	15,372	15,287	18,239	14,399	93,447	93,917	91,359	133,619	135,750	132,363
5	16,007	13,011	13,311	12,665	14,904	13,600	88,370	87,928	88,969	125,242	126,598	124,824
6	13,602	13,422	10,652	9,159	10,516	12,489	81,398	79,563	86,170	112,866	113,048	113,731
7	22,634	18,452	17,976	17,188	19,933	21,146	104,605	102,558	109,481	130,257	131,370	130,756
8	42,673	33,342	34,412	35,889	42,056	40,230	146,777	144,605	150,850	151,813	155,228	151,207
9	38,443	34,600	29,857	29,991	34,675	38,186	127,040	122,768	137,568	141,992	143,583	143,371
10	32,338	47,021	24,018	23,102	26,497	34,103	103,787	97,557	120,977	105,096	104,840	108,383
11	24,430	70,521	17,714	18,553	22,558	27,837	89,108	81,165	113,676	92,900	90,761	98,162
12	21,839	85,776	16,649	20,351	25,882	25,477	79,848	71,546	108,058	80,787	78,426	86,524
13	25,496	70,920	18,436	19,123	23,097	29,086	99,691	91,443	124,659	108,198	105,895	113,678
14	19,144	70,041	14,339	16,813	21,202	22,118	90,338	82,587	114,429	113,554	110,455	119,351
15	26,128	43,720	19,248	18,149	20,886	27,698	105,179	99,363	121,376	130,551	129,647	134,030
16	38,792	31,083	30,722	31,213	36,312	37,382	142,358	139,203	149,537	150,849	153,193	151,266
17	66,480	61,726	55,388	60,792	72,180	60,316	208,684	208,967	204,378	212,144	219,863	208,190
18	74,424	77,227	62,984	69,857	83,381	65,799	232,113	234,180	222,334	242,032	251,754	236,207
19	72,868	81,224	62,240	69,731	83,500	63,554	224,389	227,499	211,736	235,898	246,117	229,308
20	69,299	79,287	59,416	66,637	79,886	59,997	221,649	224,983	208,576	242,532	252,473	235,973
21	67,787	77,503	58,175	64,810	77,697	58,353	214,733	217,977	202,018	233,028	242,697	226,649
22	66,330	75,841	56,922	63,443	76,057	57,121	216,590	219,767	204,152	241,007	250,470	234,765
23	52,945	60,475	45,500	50,211	60,191	45,205	187,918	190,437	178,095	222,472	229,960	217,542

To evaluate the network imbalances, we can assess a calculation of voltage unbalances in the electricity grid. Because of the uneven distribution, we can expect worse values than the previous scenarios.

Tab. 3.7.4 reports the measured voltage values at upstream and downstream nodes of the distribution transformer, so at bus 1 and 2, and the hourly results of the voltage unbalances evaluation, calculated through the above equation 3.5.1.

The average values are 0.022% and 0.106% at MV and LV sides respectively.
As it can be seen in Tab. 3.7.4, the maximum values are 0.055% and 0.171% much higher than the previous scenarios and they occur at 1 p.m. when PV production is about at its maximum.

Tab. 3.7.4 S3 - Phase voltages comparison

Hour	Magnitude E1_ph1	Magnitude E1_ph2	Magnitude E1_ph3	Voltage unbalance	Magnitude E2_ph1	Magnitude E2_ph2	Magnitude E2_ph3	Voltage unbalance
[h]	[V]	[V]	[V]		[V]	[V]	[V]	
0	6338,84	6337,78	6339,24	0,013%	233,220	233,063	233,284	0,054%
1	6339,25	6338,62	6339,56	0,008%	233,384	233,272	233,439	0,040%
2	6341,12	6340,59	6341,36	0,007%	233,908	233,816	233,953	0,033%
3	6341,53	6341,02	6341,77	0,007%	234,026	233,936	234,069	0,032%
4	6342,55	6342,27	6342,84	0,004%	234,344	234,254	234,390	0,032%
5	6342,34	6342,60	6342,79	0,004%	234,365	234,262	234,426	0,038%
6	6341,92	6343,02	6342,63	0,009%	234,377	234,251	234,463	0,048%
7	6339,84	6341,04	6340,81	0,011%	233,830	233,641	233,951	0,071%
8	6336,36	6337,57	6337,82	0,014%	232,914	232,594	233,107	0,119%
9	6335,98	6338,51	6337,83	0,023%	232,995	232,642	233,224	0,134%
10	6336,44	6340,40	6338,69	0,033%	233,337	232,957	233,601	0,146%
11	6335,47	6341,17	6338,20	0,046%	233,331	232,925	233,633	0,159%
12	6335,05	6341,80	6338,11	0,055%	233,382	232,949	233,714	0,171%
13	6334,43	6340,16	6337,18	0,046%	233,041	232,626	233,347	0,163%
14	6335,27	6340,80	6337,77	0,045%	233,228	232,870	233,501	0,141%
15	6336,29	6339,96	6338,27	0,030%	233,230	232,906	233,458	0,125%
16	6335,91	6337,73	6337,49	0,018%	232,871	232,551	233,072	0,120%
17	6332,48	6332,26	6334,01	0,017%	231,709	231,301	231,936	0,150%
18	6331,34	6330,16	6332,74	0,021%	231,296	230,877	231,518	0,153%
19	6332,79	6331,03	6333,96	0,025%	231,606	231,219	231,803	0,140%
20	6333,03	6331,16	6334,08	0,025%	231,645	231,287	231,826	0,129%
21	6333,71	6331,89	6334,72	0,025%	231,829	231,481	232,004	0,125%
22	6333,36	6331,58	6334,35	0,024%	231,736	231,395	231,908	0,123%
23	6335,46	6334,03	6336,23	0,019%	232,313	232,045	232,446	0,096%
				0,022%				0,106%

At this point, we can focus on the electric power analysis. Fig. 3.7.3 shows the single-phase active power at each phase of network nodes, while Fig. 3.7.4 illustrates the profiles of three-phase apparent power.
If we compare this figure with Fig. 3.6.3, related to Scenario 2, we can notice two main things. The first one is about the evening load, it is higher than before due to the greater number of loads on the grid; while the second thing concerns the profile shapes during the daytime, they decresed because of the higher penetration of PV generation.

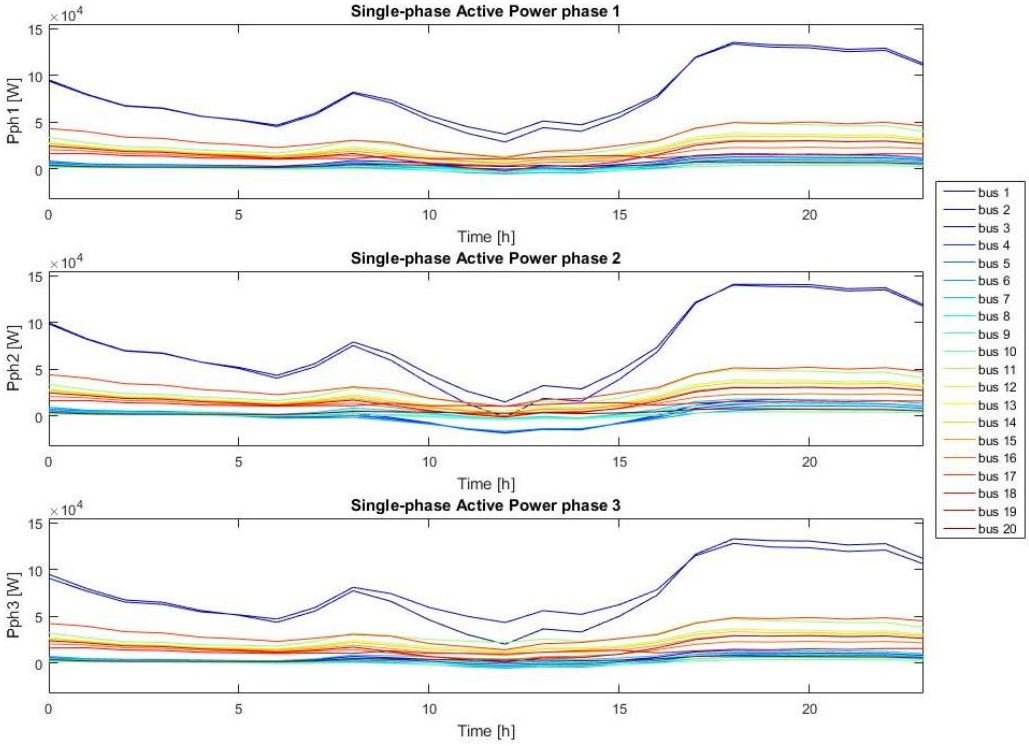

Fig. 3.7.3 S3 - Single-phase Active Power

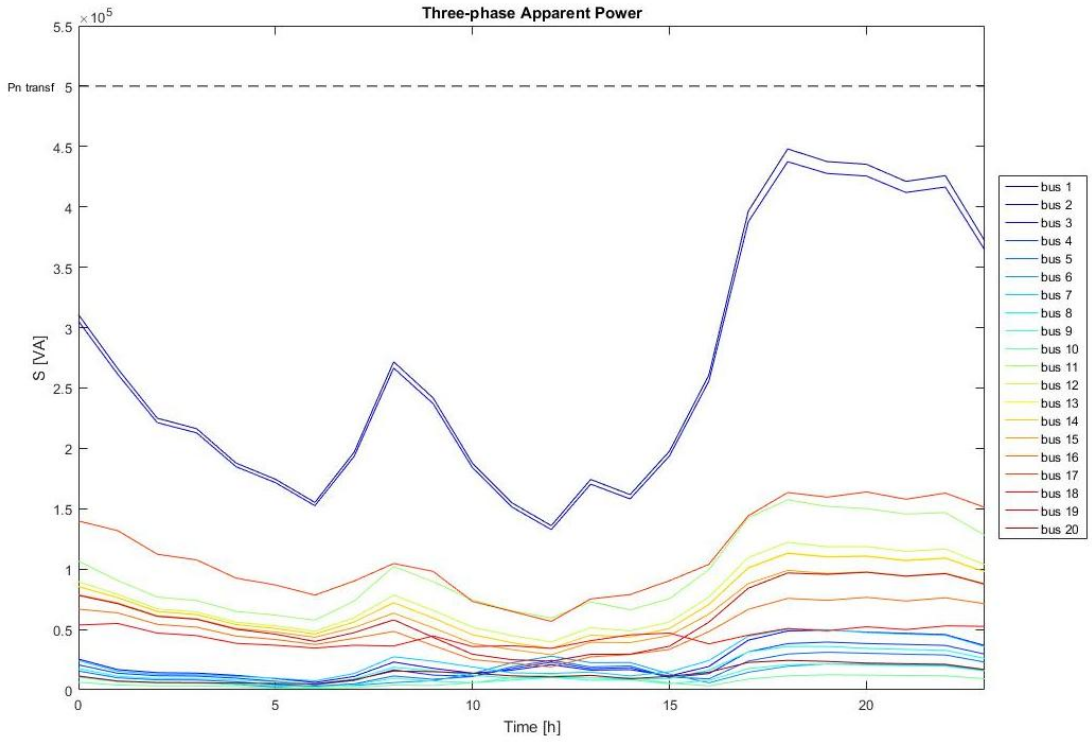

Fig. 3.7.4 S3 - Three-phase Apparent Power

In Fig. 3.7.4, we can also notice that, even though the peak of load consumption is increased, the power rating of the distribution transformer is big enough to manage the overall power demand.

What was mentioned above is confirmed by the following Tab. 3.7.5, which shows the hourly values of the transformer utilization factor. In fact, if we compare it with Tab. 3.6.5, we can notice that the electricity provided by the MV grid is lower, compared to Scenario 2, between 6 a.m. and 5 p.m., while it is higher in the rest of the time. In these results, the effects of PV generation are very evident. The resulting average value is 53%, so two percentage points less than Scenario 2, but the range between minimum and maximum values is wider, therefore the transformer works in very different conditions during the day.

Another important thing must be noticed in the following figure. PV systems generate only active power because their power factor is set equal to 1. Therefore, during the central hours of the day, some active power consumptions of the electric loads are covered by solar generation, while reactive power must be supplied by the power system. It means that, in the event of high PV penetration, in the MV grid connection can flow more reactive power than active power.
This happen at 1 p.m., when the transformer sees a very unnatural power flow.

Tab. 3.7.5 S3 - Transformer utilization factor

Hour	P + jQ	A	Transformer Utilization factor
[h]	[W + jVAr]	[VA]	
1	286266,37 + 106180,57i	305324,00	61%
2	239843,11 + 103357,59i	261165,67	52%
3	203249,54 + 87522,01i	221292,74	44%
4	195526,04 + 83954,79i	212788,25	43%
5	169137,43 + 74467,18i	184804,85	37%
6	154585,90 + 74382,30i	171550,37	34%
7	132843,20 + 74893,35i	152500,26	31%
8	170175,14 + 92225,90i	193559,28	39%
9	237506,26 + 120815,09i	266468,59	53%
10	204663,36 + 119636,57i	237065,39	47%
11	146727,61 + 110822,55i	183876,67	37%
12	101208,16 + 112631,68i	151423,21	30%
13	71157,82 + 112022,42i	132711,93	27%
14	119243,33 + 121669,73i	170359,90	34%
15	108165,42 + 115291,46i	158088,20	32%
16	157115,66 + 113386,47i	193757,12	39%
17	224270,30 + 122754,79i	255667,57	51%
18	355358,01 + 154902,72i	387652,12	78%
19	404948,93 + 165415,64i	437431,10	87%
20	398342,99 + 155598,53i	427654,11	86%
21	396637,47 + 154145,57i	425537,47	85%
22	384083,11 + 148865,05i	411923,10	82%
23	387873,36 + 151560,36i	416432,81	83%
24	338391,98 + 135009,06i	364330,31	73%
			53%

Considering now power losses in the network lines, we can expect higher values than Scenario 2, during almost all the day; because more energy flows in the daytime due to solar generation, while there is more load consumption during the night, than the previous scenario.
The first cause is due to the low presence of local consumption of the power generated by PV systems, so this energy must flow in the network lines to reach load points.
Fig. 3.7.5 below shows the profiles of active power losses in the network lines.

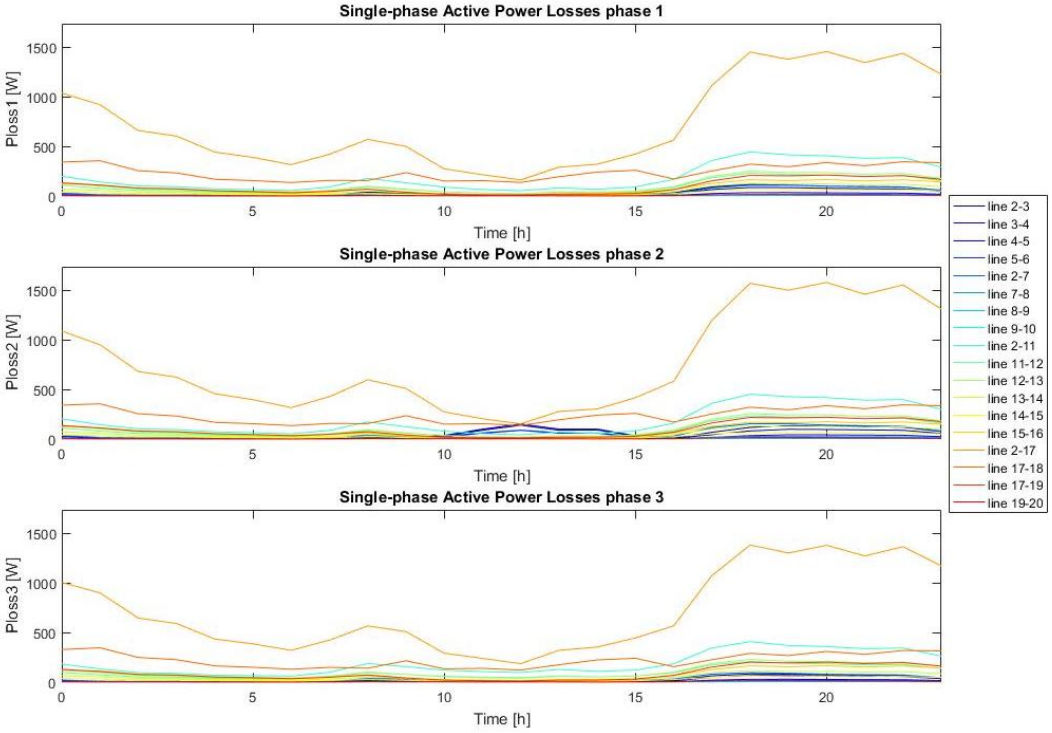

Fig. 3.7.5 S3 - Power losses

Comparing it with Fig. 3.6.5, we can notice what was explained above. For example, graph of phase 2 shows a considerable increase between 10 a.m. and 3 p.m., in the network branch 2-6, while all the graphs demonstrate a decrease of the power losses in the line 2-17, during the same period, thanks to a local consumption of solar electricity by school and industries.

In conclusion, to understand if the overall operating conditions of the electricity network are more cost-effective than the previous Scenario 2, it is necessary to consider the available output table of economic results.
Following Tab. 3.7.6 shows that the overall operating cost results equal to £ 696.27.

Tab. 3.7.6 S3 - Economic results

Archetype1	Archetype2	Archetype3	Archetype4	Archetype5	Archetype6	Archetype7	Archetype8	Archetype9	Archetype10
[£]	[£]	[£]	[£]	[£]	[£]	[£]	[£]	[£]	[£]
0,00	17,65	17,65	14,90	17,65	-11,98	21,69	23,63	15,70	-2,94
Archetype11	Archetype12	Archetype13	Archetype14	Archetype15	Archetype16	Archetype17	Archetype18	Archetype19	Archetype20
[£]	[£]	[£]	[£]	[£]	[£]	[£]	[£]	[£]	[£]
23,32	43,91	17,49	21,69	41,97	130,19	27,36	126,04	90,59	41,28

ELoss23	ELoss34	ELoss45	ELoss56	ELoss27	ELoss78	ELoss89	ELoss910	ELoss211
[£]	[£]	[£]	[£]	[£]	[£]	[£]	[£]	[£]
0,47	0,38	0,17	0,13	0,45	0,07	0,03	0,02	2,00
ELoss1112	ELoss1213	ELoss1314	ELoss1415	ELoss1516	ELoss217	ELoss1718	ELoss1719	ELoss1920
[£]	[£]	[£]	[£]	[£]	[£]	[£]	[£]	[£]
1,03	1,14	0,58	0,31	0,82	7,60	2,30	0,96	0,05

Total
[£]
696,27

In Scenario 2 the total cost resulted equal to £ 847.08, so even if network loads have increased in Scenario 3, for instance household loads have increased by 17%, the overall cost is lower thanks to the higher PV penetration. Therefore, from a macroscopic point of view, the amount of energy supplied by the MV network is lower.
The cost of energy consumed is now £ 677.77 (in the Scenario 2 was £ 829.13) and it covers about 97% of the total, while the cost of energy losses is £ 18.50 (£ 17.96).
As reported, the amount related to the losses has increased, but it is worth because we have a huge saving in terms of energy consumed.
Finally, we can state that, if this grid will operate as forecast without considering EV implementation, it will be much more affordable than the present.

3.8. Scenario 4 (15% of household PV, EV uncontrolled charging)

This scenario investigates the operating conditions of the inspected electricity distribution network considering the same load configuration as in Scenario 3 (Tab. 3.7.1), but, in addition, it also implements electric vehicles on the grid.
Therefore, it considers the operating conditions expected for the year 2050, if all the EV owners will apply dumb charging mode to charge their vehicles. It means that all the household EV owners will charge their vehicles as soon as they get home from work and more generally, all EV owners will charge as soon as they arrive at the recharging station.
As explained in section 2.2.1, the modelling tool implements one EV per each smart household, while for smart schools, smart shops, smart industries and smart car parks it considers different numbers of EVs in relation to the percentages reported in Tab. 2.2.1.1.

The total number of EVs in the electricity grid is 54. 52 related to smart houses and 2 to the smart park.
As aforementioned, not all the EVs, related to the smart household loads, are charged at home, in fact, their percentage is an input variable of the modelling tool and it has been set equal to 65%. The remaining 35% charges its batteries in off-home charging infrastructures, along the streets, at charging stations or at work. It has been considered that these charges allow the vehicles to achieve a battery capacity equal to 70% of their ratings.

Once all the parameters have been uploaded on the modelling tool, we can proceed with the grid analysis.
In this scenario, we can find new blocks inside the archetype blocks, those related to the EV chargers. In fact, they take into account the power consumed to charge the aggregated EVs.

What we can expect from the analysis of the operating conditions of Scenario 4 is an increase of daily power peak, because power demand related to EV charging occurs in the same hours of the peak of power consumed by household loads. This is the main problem of an uncontrolled charging of electric vehicles. They can lead to very dangerous consequences on the electricity network.

To follow the same scheme as before, the first analysis of the grid is in terms of voltage deviation.
Scenario 4 considers the same distribution transformer as Scenario 3, with same settings and ratings. This because we want to compare the consequences, on the electricity network, caused by different EVs charging strategies.

Following Fig. 3.8.1 shows the voltage deviations for each phase of each grid node.
The profiles of node 1, MV bus, are not reported because they do not add useful information since they are basically flat at the nominal voltage. In the figure below, the profiles of phases 1 and 3 are within the imposed limits, while phase 2 of bus 18 slightly exceeds the lower limit. This is caused by the high power demand in that part of the electricity grid.
Comparing Fig. 3.8.1 with Fig. 3.7.1 of Scenario 3, many differences can be notice during the evening: all shapes have an important decrease.
From a voltage deviation point of view, an higher OCTC value of the distribution transformer would be necessary to ensure that the voltage constraints are actually complied.

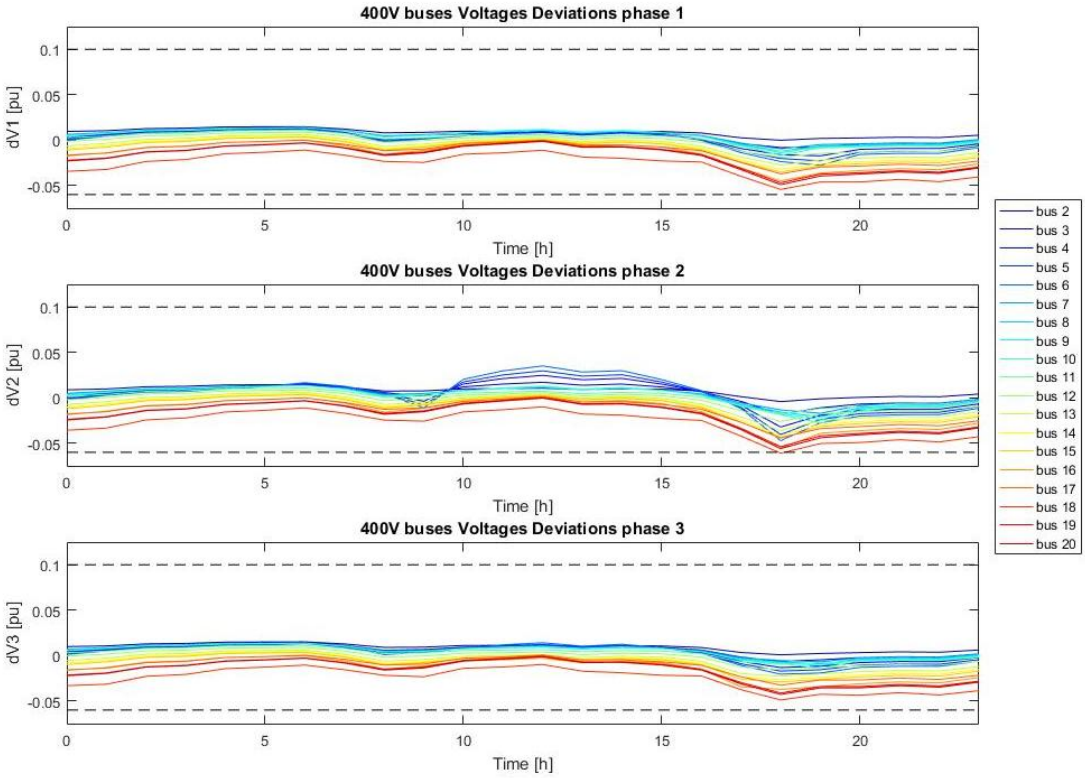

Fig. 3.8.1 S4 - Voltages deviations

Considering now line current profiles and lines current ratings, shown in Fig. 3.8.2 and Tab. 3.8.1 respectively, we can observe that branches 2-3, 4-5 and 2-7 are overloaded. As it can be seen in Fig. 3.8.2, the worsening of operational conditions is limited to the evening, when all EV charging is performed.

This means that uncontrolled charging will need significant grid upgrades, therefore huge investments should be planned by the distribution system operators.

Fig. 3.8.2 shows worse results in phase number 2 compared against the others. This is due to the random distribution of single-phase loads and therefore EV chargers on the electricity grid. As aforementioned, this kind of load demand causes a higher daily peak, hence, enhanced power infrastructures would be only needed to satisfy the greater power demand during the evening, while it would result very oversized in the other hours of the day. In fact, for instance, comparing the maximum value of current flowing in the branch 2-7 with its average value, thanks to the available results in the output tables, we can state the following. The rating of this line is exploited only about 30% during the day, while it reaches about 148% at 6 p.m.

Comparing Fig. 3.8.2 with Fig. 3.7.2, related to Scenario 3, we can also observe some differences, between 7 and 11 a.m., in the phase 2 of lines correlated to node 6 because of the charging of the EVs at the car park located in that node.

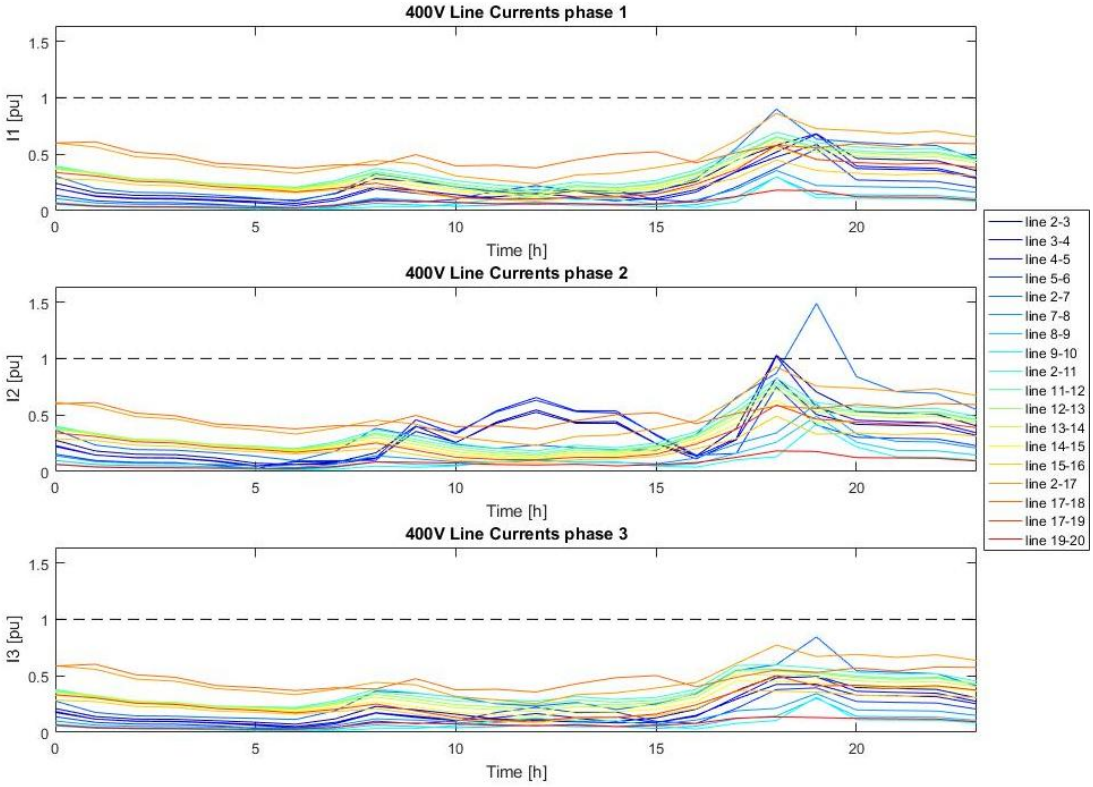

Fig. 3.8.2 S4 - Line Currents

Tab. 3.8.1 S4 - Lines current ratings

Line_2-3	Current rating exceeded: 154.4774A vs 150A nominal
Line_3-4	Current rating complied: 124.4772A vs 150A nominal
Line_4-5	Current rating exceeded: 112.156A vs 110A nominal
Line_5-6	Current rating complied: 82.2426A vs 110A nominal
Line_2-7	Current rating exceeded: 163.5479A vs 110A nominal
Line_7-8	Current rating complied: 130.0176A vs 218A nominal
Line_8-9	Current rating complied: 92.9636A vs 190A nominal
Line_9-10	Current rating complied: 63.0425A vs 150A nominal
Line_2-11	Current rating complied: 324.5024A vs 393A nominal
Line_11-12	Current rating complied: 309.6A vs 393A nominal
Line_12-13	Current rating complied: 261.0846A vs 342A nominal
Line_13-14	Current rating complied: 249.5088A vs 342A nominal
Line_14-15	Current rating complied: 215.8556A vs 342A nominal
Line_15-16	Current rating complied: 167.7657A vs 342A nominal
Line_2-17	Current rating complied: 316.5061A vs 342A nominal
Line_17-18	Current rating complied: 82.3145A vs 135A nominal
Line_17-19	Current rating complied: 201.3989A vs 342A nominal
Line_19-20	Current rating complied: 49.1466A vs 270A nominal

Following Tab. 3.8.2 shows the values of current flowing in each phase of the three-phase branches starting from the distribution substation.

The worst unbalanced conditions in terms of currents are experienced in the line 2-3 as in the Scenario 3 at 12 and 2 p.m.
Considering the values reported in Tab. 3.7.3, related to Scenario 3, we can notice the significant increase of current absorbed by loads for EV charging during the charging period. In addition to what has been said in the previous scenario analysis, we can see an increase of imbalances during the EV charging period.

Tab. 3.8.2 S4 - Phase currents comparison

Hour	Magnitude I23_ph1	Magnitude I23_ph2	Magnitude I23_ph3	Magnitude I27_ph1	Magnitude I27_ph2	Magnitude I27_ph3	Magnitude I211_ph1	Magnitude I211_ph2	Magnitude I211_ph3	Magnitude I217_ph1	Magnitude I217_ph2	Magnitude I217_ph3
[h]	[A]	[A]	[A]	[A]	[A]	[A]	[A]	[A]	[A]	[A]	[A]	[A]
0	36,58	41,58	31,53	33,78	40,48	30,39	155,27	156,83	148,53	204,68	209,69	201,30
1	24,02	27,18	20,81	21,46	25,71	19,31	131,06	132,03	126,80	192,69	195,87	190,54
2	20,30	22,92	17,64	17,81	21,33	16,03	110,94	111,74	107,40	163,16	165,79	161,37
3	19,81	22,36	17,21	17,35	20,78	15,61	106,72	107,50	103,27	156,14	158,70	154,40
4	17,91	18,01	15,38	15,28	18,23	14,39	93,47	93,84	91,28	133,63	135,75	132,33
5	16,04	10,93	13,32	12,67	14,89	13,59	88,40	87,85	88,89	125,26	126,60	124,79
6	13,64	9,37	10,66	9,16	10,51	12,48	81,44	79,49	86,09	112,89	113,06	113,70
7	22,68	12,11	17,97	17,19	19,92	21,13	104,66	102,46	109,38	130,28	131,38	130,72
8	42,74	24,84	34,39	35,89	42,05	40,19	146,85	144,48	150,69	151,85	155,26	151,17
9	38,51	60,29	29,83	30,00	34,66	38,15	127,14	122,69	137,42	142,04	143,63	143,35
10	32,41	38,28	23,99	23,11	26,47	34,07	103,92	97,48	120,84	105,17	104,92	108,39
11	24,51	65,30	17,71	18,54	22,49	27,82	89,29	81,14	113,56	93,03	90,91	98,22
12	21,92	81,70	16,65	20,33	25,79	25,47	80,08	71,58	107,95	80,96	78,63	86,63
13	25,58	65,39	18,43	19,12	23,02	29,07	99,87	91,40	124,53	108,33	106,04	113,74
14	19,22	66,32	14,34	16,80	21,13	22,11	90,50	82,55	114,32	113,66	110,57	119,40
15	26,20	36,97	19,24	18,16	20,86	27,68	105,29	99,27	121,25	130,61	129,71	134,03
16	38,86	20,62	30,71	31,22	36,30	37,35	142,43	139,08	149,38	150,90	153,23	151,23
17	66,56	57,23	55,37	60,78	72,16	60,27	208,76	220,85	232,65	212,18	219,89	208,12
18	86,87	154,48	75,31	98,86	95,65	65,75	272,98	324,50	234,29	294,54	316,51	264,19
19	102,14	105,60	74,69	69,72	163,55	92,77	236,69	239,55	223,76	247,97	258,17	229,24
20	69,37	79,27	59,40	66,62	92,29	59,95	221,72	224,86	208,38	242,56	252,48	235,90
21	67,86	77,48	58,16	64,79	77,67	58,30	214,81	217,85	201,83	233,05	242,70	226,57
22	66,40	75,82	56,91	63,42	76,03	57,07	216,66	219,64	203,97	241,03	250,47	234,69
23	53,01	60,46	45,49	50,20	60,17	45,17	187,98	190,32	177,94	222,50	229,96	217,48

As performed for previous scenarios, to evaluate the network imbalances, we can perform an evaluation of voltage unbalances in the distribution grid.

Tab. 3.8.3 shows the measured voltage values at upstream and downstream nodes of the distribution transformer, so at bus 1 and 2, and the hourly values of voltage unbalances evaluation, calculated through the aforementioned equation 3.5.1.

The average values are 0.027% and 0.091% at 11 kV and 400 V sides, respectively.
The maximum values of voltage unbalance occur at 6 p.m., when the power consumed for EV charging is the highest, and they result equal to 0.087% and 0.298%.
These results are greater than the values assessed in Scenario 3, once again because of the uneven distribution of single-phase EV chargers on the three-phase distribution system related to the low number of EV chargers on some nodes of the electricity network.

Tab. 3.8.3 S4 - Phase voltages comparison

Hour	Magnitude E1_ph1	Magnitude E1_ph2	Magnitude E1_ph3	Voltage unbalance	Magnitude E2_ph1	Magnitude E2_ph2	Magnitude E2_ph3	Voltage unbalance
[h]	[V]	[V]	[V]		[V]	[V]	[V]	
0	6339,01	6338,54	6337,52	0,013%	233,15	232,98	233,23	0,061%
1	6339,40	6339,04	6338,44	0,008%	233,34	233,21	233,40	0,045%
2	6341,23	6340,95	6340,44	0,007%	233,87	233,77	233,92	0,036%
3	6341,65	6341,37	6340,88	0,007%	233,99	233,89	234,04	0,035%
4	6342,72	6342,43	6342,18	0,004%	234,31	234,23	234,36	0,031%
5	6342,66	6342,28	6342,58	0,004%	234,33	234,27	234,40	0,028%
6	6342,48	6341,95	6343,14	0,010%	234,34	234,32	234,43	0,029%
7	6340,58	6339,82	6341,15	0,011%	233,77	233,72	233,90	0,046%
8	6337,41	6336,20	6337,61	0,014%	232,80	232,66	233,02	0,083%
9	6337,40	6337,24	6337,30	0,001%	232,92	232,71	233,08	0,083%
10	6338,26	6336,60	6340,87	0,036%	233,22	233,22	233,52	0,085%
11	6337,77	6335,83	6341,92	0,054%	233,21	233,31	233,55	0,083%
12	6337,67	6335,52	6342,69	0,064%	233,26	233,40	233,63	0,086%
13	6336,73	6334,78	6340,90	0,054%	232,92	233,01	233,26	0,085%
14	6337,40	6335,65	6341,54	0,053%	233,13	233,25	233,43	0,070%
15	6337,90	6336,47	6340,41	0,034%	233,13	233,15	233,39	0,070%
16	6337,09	6335,84	6337,87	0,017%	232,76	232,66	232,99	0,079%
17	6332,69	6332,24	6332,17	0,005%	231,53	231,24	231,73	0,112%
18	6333,08	6331,26	6323,87	0,087%	230,91	229,99	231,13	0,298%
19	6332,95	6333,17	6327,71	0,056%	231,37	230,69	231,47	0,211%
20	6333,55	6332,58	6330,25	0,030%	231,50	231,07	231,69	0,153%
21	6334,23	6333,08	6331,33	0,024%	231,68	231,30	231,89	0,140%
22	6333,87	6332,74	6331,04	0,024%	231,59	231,22	231,80	0,137%
23	6335,85	6334,98	6333,61	0,019%	232,20	231,91	232,36	0,107%
				0,027%				0,091%

From the point of view of electric power analysis, following Fig. 3.8.3 shows the graphical representation of the single-phase active power profiles at each phase of network nodes.
New power peaks, due to EV charging, can be easily observed between 5 and 8 p.m. and their values are much higher than Scenario 3, while in the other hours of the day the shapes are basically the same, since there are minor load differences.

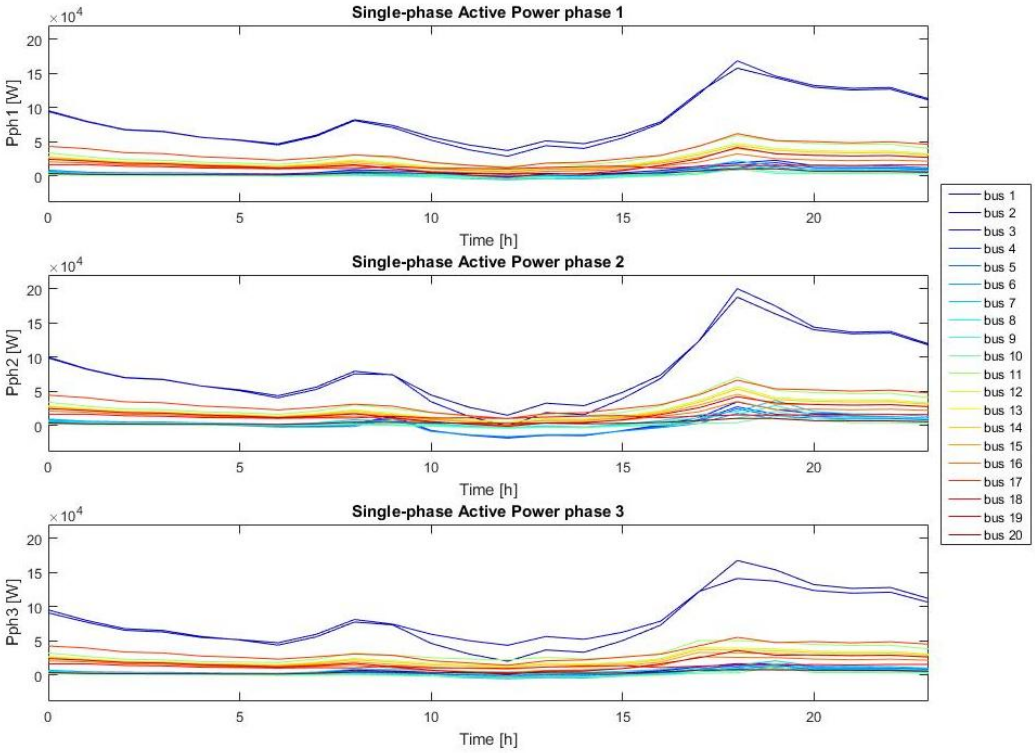

Fig. 3.8.3 S4 - Single-phase Active Power

Fig. 3.8.4 shows the profiles of three-phase apparent power at each grid node compared to the nominal power rating of the distribution transformer, which is equal to 500 kVA. It is evident that dumb charging lead to significant overload for the transformer. Therefore, as aforementioned, this charging method would need significant grid upgrades in order to satisfy the increased peak of power demand.
Comparing the graphs of three-phase apparent power of Scenario 4 and Scenario 3, so the effects of dumb charging implementation on the baseline scenario, we can observe significant increases of power demand in many network nodes during the evening.

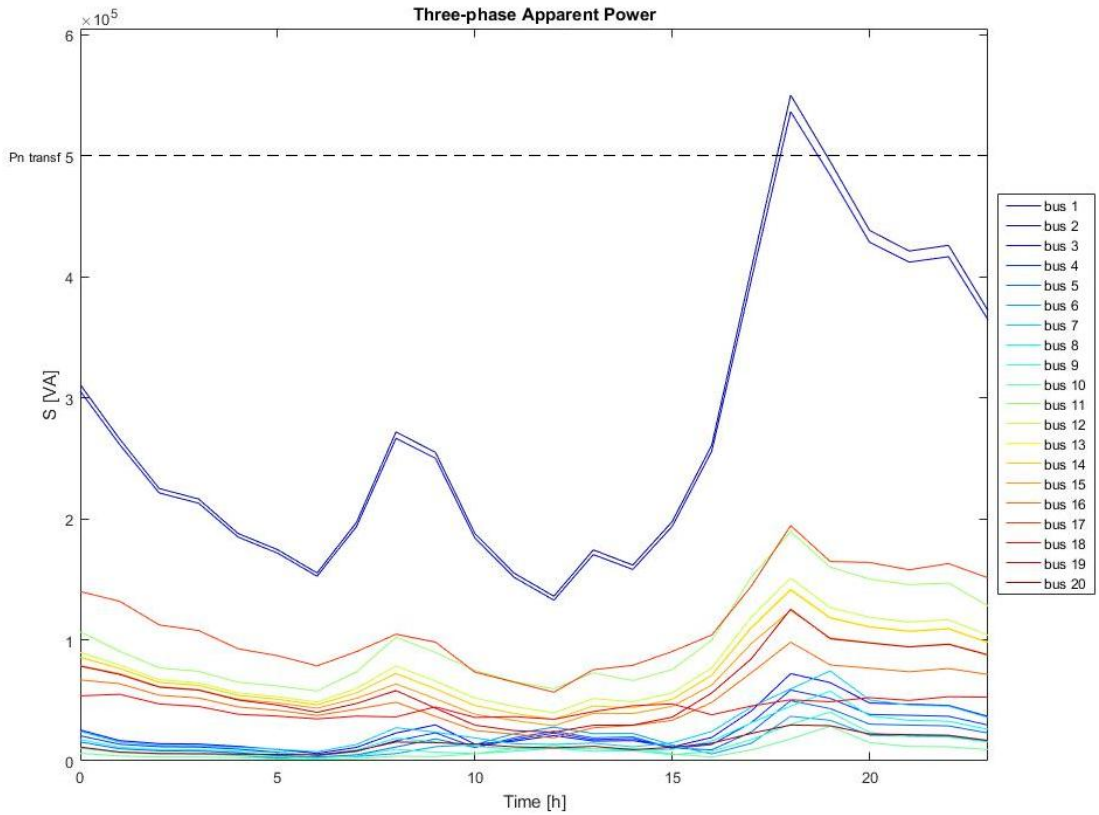

Fig. 3.8.4 S4 - Three-phase Apparent Power

What was stated above is confirmed by the hourly values of utilization factor of the distribution transformer, shown in the following Tab. 3.8.4. We can observe significant increases between 5 and 8 p.m. when EV charging is performed. Comparing Tab. 3.8.4 with Tab. 3.7.5 of Scenario 3, we can confirm another point. The average values of utilization factor in the two different scenarios are very close, the first one is 54% and the second one was 53%. Therefore, related huge investments to enhance power infrastructures would be only needed to satisfy the greater power demand during the evening, leading to significant oversizing in the other hours of the day.
As can be seen in following Tab. 3.8.4, the maximum value, experienced at 6 p.m., is about 536 kVA, 7% more than the nominal power rating of the distribution transformer.

Tab. 3.8.4 S4 - Transformer utilization factor

Hour	P + jQ	A	Transformer Utilization factor
[h]	[W + jVAr]	[VA]	
0	286266,65 + 106180,58i	305324,28	61%
1	239843,25 + 103357,60i	261165,81	52%
2	203249,64 + 87522,02i	221292,84	44%
3	195526,14 + 83954,80i	212788,34	43%
4	169137,51 + 74467,18i	184804,92	37%
5	154585,99 + 74382,32i	171550,45	34%
6	132843,29 + 74893,37i	152500,34	31%
7	170175,31 + 92225,94i	193559,45	39%
8	237506,69 + 120815,18i	266469,01	53%
9	219414,31 + 119559,20i	249874,05	50%
10	146711,94 + 110831,62i	183869,63	37%
11	101208,41 + 112631,83i	151423,48	30%
12	71158,02 + 112022,58i	132712,18	27%
13	119243,62 + 121669,89i	170360,21	34%
14	108165,63 + 115291,59i	158088,44	32%
15	157115,95 + 113386,58i	193757,41	39%
16	224270,70 + 122754,89i	255667,97	51%
17	365269,80 + 155129,22i	396846,45	79%
18	509442,35 + 167302,17i	536210,34	107%
19	457754,14 + 156290,03i	483699,72	97%
20	399541,08 + 154330,61i	428311,82	86%
21	384080,02 + 148874,10i	411923,48	82%
22	387874,11 + 151560,45i	416433,55	83%
23	338392,49 + 135009,12i	364330,82	73%
			54%

Another interesting analysis is about the evaluation of power losses along the network lines. We can expect greater losses during the evening, given the higher power flows due to EV charging, while only minor differences in the rest of the day.
Fig. 3.8.5 below shows the profiles of active power losses in the network lines.

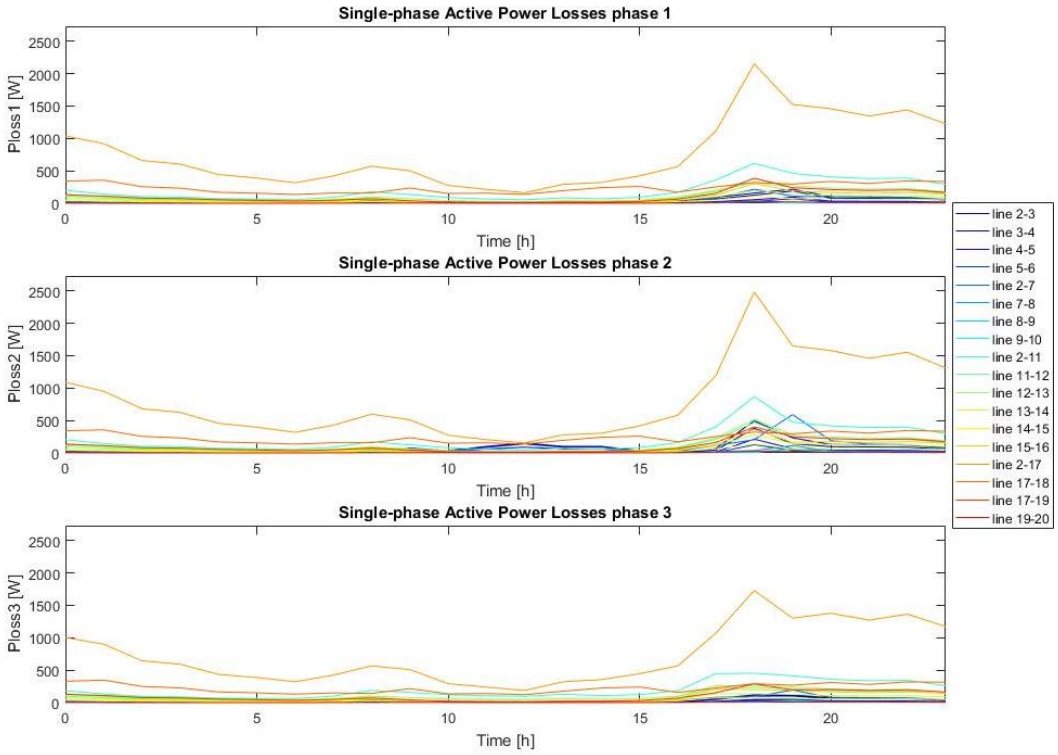

Fig. 3.8.5 S4 - Power losses

Fig. 3.8.5 shows very high values in the line 2-17, indeed 316.5 A flow on it at 6 p.m., causing about 2500 W of power loss.

To conclude the analysis of Scenario 4, the economic results, shown in Tab. 3.8.5, must be investigated.
The overall operating cost results now equal to £ 767.37, while in Scenario 3 it was equal to £ 696.27. We can assess the overall cost of EV charging comparing the sums of the archetype costs of two scenarios. Concerning Scenario 4, it results equal to £ 747.37, while about Scenario 3, it was equal to £ 677.76. Therefore, the overall cost, related to 54 EVs applied on the electricity grid, is £ 69.61, which means, on average, about £ 1.30 per each electric vehicle. The cost of energy consumed, as already presented, is now £ 747.37 and covers about 97% of the total cost. Power losses and therefore the related cost have increased by 7.5% than previous Scenario 3.

Tab. 3.8.5 S4 - Economic results

Archetype1	Archetype2	Archetype3	Archetype4	Archetype5	Archetype6	Archetype7	Archetype8	Archetype9	Archetype10
[£]	[£]	[£]	[£]	[£]	[£]	[£]	[£]	[£]	[£]
0,00	18,31	18,97	14,90	18,31	7,86	23,53	25,49	17,03	5,59
Archetype11	Archetype12	Archetype13	Archetype14	Archetype15	Archetype16	Archetype17	Archetype18	Archetype19	Archetype20
[£]	[£]	[£]	[£]	[£]	[£]	[£]	[£]	[£]	[£]
23,32	45,77	17,49	24,23	44,52	142,56	28,02	126,04	100,33	45,12

ELoss23	ELoss34	ELoss45	ELoss56	ELoss27	ELoss78	ELoss89	ELoss910	ELoss211
[£]	[£]	[£]	[£]	[£]	[£]	[£]	[£]	[£]
0,60	0,48	0,23	0,17	0,57	0,09	0,04	0,04	2,16
ELoss1112	ELoss1213	ELoss1314	ELoss1415	ELoss1516	ELoss217	ELoss1718	ELoss1719	ELoss1920
[£]	[£]	[£]	[£]	[£]	[£]	[£]	[£]	[£]
1,11	1,24	0,64	0,34	0,91	7,97	2,30	1,04	0,06

Total
[£]
767,37

3.9. Scenario 5 (15% of household PV, EV smart charging)

The fifth scenario analyses the operating conditions of the reference electricity distribution network considering the same load configuration as in Scenario 3 (Tab. 3.7.1), but, in this case, to perform EV charging, it applies smart charging mode.
Therefore, it considers the operating conditions expected for the year 2050, if all EV owners will apply smart charging mode to charge their vehicles. It means that all the electric vehicles will be charged in an optimized way in order to minimize charging costs (Sec. 2.2.1).
As explained in section 2.2.1, the modelling tool implements one EV per each smart household, while for smart schools, smart shops, smart industries and smart car parks it considers different numbers of EVs in relation to the percentages reported in Tab. 2.2.1.1. In conclusion, the number of EVs applied on the electricity network is the same of Scenario 4, but with different charging profiles, because now they are optimized.
The total number of EVs is 54. 52 related to smart houses and 2 to the smart park.
As aforementioned, not all the EVs related to the smart household loads, are charged at home, in fact, their percentage is an input variable of the modelling tool and it has been set equal to 65%. The remaining 35% charges its batteries in off-home charging infrastructures, along the

streets, at charging stations or at work. It has been considered that these charges allow the vehicles to achieve a battery capacity equal to 70% of their ratings.

Once all the parameters have been uploaded on the modelling tool, we can proceed with the grid analysis. Also in this scenario, we can find EV chargers blocks, which take into account the power consumed to charge the aggregated EVs, inside archetype blocks.

The optimization of EV charging, applied in Scenario 5, should be able to lead to money savings, because the minimization algorithm is based on a cost function, complying with some constraints. Therefore, power demand related to EV charging will occur when it causes the lowest costs. Considering the electricity tariff (Tab. 3.3.1) and the generation tariff (Sec. 3.3) taken into account in this case study, they will be placed during the morning if the EVs are not available during PV generation hours, otherwise they will exploit the PV generation if they are available in the central hours of the day.

To follow the same scheme as before, the first analysis of the grid is in terms of voltage deviation.
Scenario 5 considers the same distribution transformer as Scenario 3, with same settings and ratings. This because we want to compare the consequences, on the electricity network, caused by different EVs charging strategies.

Fig. 3.9.1 shows the graphical representation of voltage deviations for each phase of each grid node. The results at bus 1, MV node, are not reported because they are basically flat at the value of nominal voltage. In this scenario, as can be seen in figure below, all the profiles are within the imposed limits, contrary to what happened in Scenario 4.
Comparing Fig. 3.9.1 with Fig. 3.7.1, related to the voltage deviations of Scenario 3 (without EV charging), we can observe that they have only minor differences.

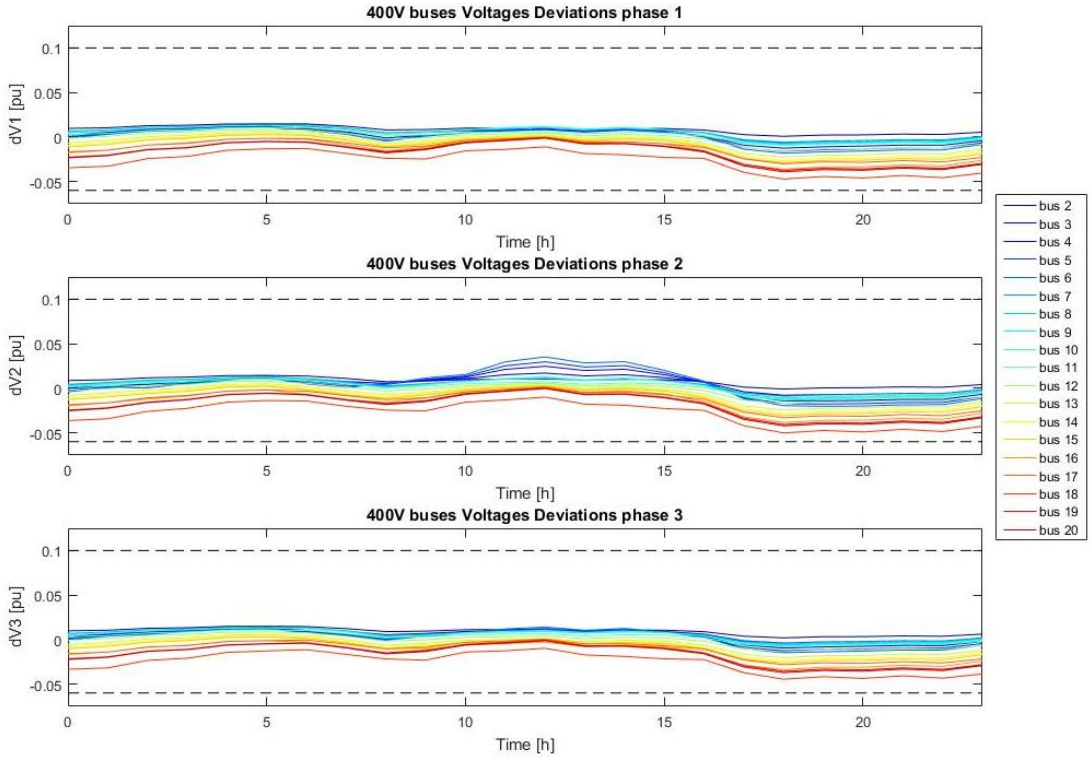

Fig. 3.9.1 S5 - Voltages deviations

Indeed, the optimization process, performed by the modelling tool, avoids the creation of new peaks in the profile of power demand; therefore, as will be shown below, the resulting shapes will be very close to those of Scenario 3, with the exception of absolute values.

From a line currents point of view, Fig. 3.9.2 shows their hourly profiles, while Tab. 3.9.1 reports the results compared to the lines current rating.

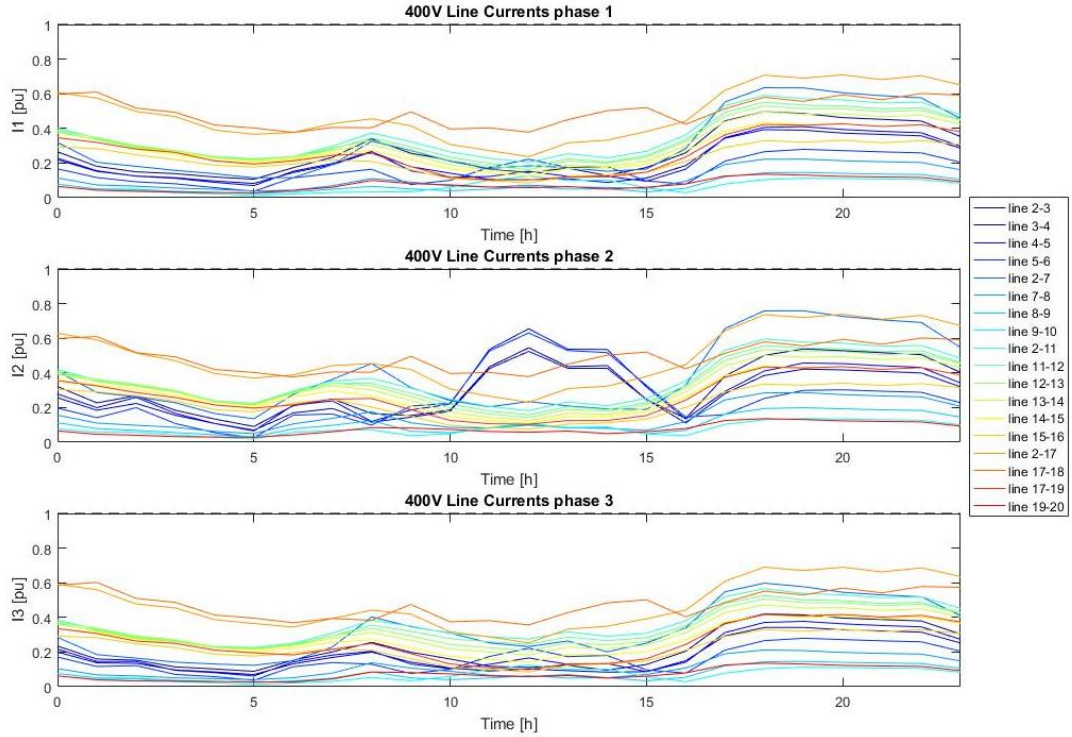

Fig. 3.9.2 S5 - Line Currents

Tab. 3.9.1 S5 - Lines current ratings

Line_2-3	Current rating complied: 81.7031A vs 150A nominal
Line_3-4	Current rating complied: 78.6454A vs 150A nominal
Line_4-5	Current rating complied: 72.036A vs 110A nominal
Line_5-6	Current rating complied: 69.3645A vs 110A nominal
Line_2-7	Current rating complied: 83.4754A vs 110A nominal
Line_7-8	Current rating complied: 62.502A vs 218A nominal
Line_8-9	Current rating complied: 37.902A vs 190A nominal
Line_9-10	Current rating complied: 20.508A vs 150A nominal
Line_2-11	Current rating complied: 234.0262A vs 393A nominal
Line_11-12	Current rating complied: 219.0903A vs 393A nominal
Line_12-13	Current rating complied: 183.0707A vs 342A nominal
Line_13-14	Current rating complied: 171.6393A vs 342A nominal
Line_14-15	Current rating complied: 150.3795A vs 342A nominal
Line_15-16	Current rating complied: 116.5816A vs 342A nominal
Line_2-17	Current rating complied: 252.4761A vs 342A nominal
Line_17-18	Current rating complied: 82.3145A vs 135A nominal
Line_17-19	Current rating complied: 149.1602A vs 342A nominal
Line_19-20	Current rating complied: 36.7036A vs 270A nominal

In this scenario, as shown before, all current ratings of network branches are complied. This means that EV charging will not negatively affect the overall distribution system, if it is properly managed. Therefore, in this scenario, contrary to what happened in Scenario 4, where uncontrolled charging has been implemented, the distribution network does not need lines upgrades in order to satisfy power request. The existing grid is already able to respond to the power demand of the loads.
Analysing Fig. 3.9.2 and Fig. 3.7.2 of Scenario 3, we can recognize some differences throughout the morning until midday, because there is a global increase of current flowing along the lines due to the power absorbed to charge the EVs.
Focusing on the second chart of Fig. 3.9.2, the currents flowing from bus 2 to bus 6 and vice versa are lower thanks to the power consumed by car park, located inside archetype 6, to charge the EVs during the daytime. This consumption increase the local exploitation of electricity generated by PV systems.

Following Tab. 3.9.2 shows the values of current of each phase of the three-phase branches starting from the distribution substation.
The worst unbalanced conditions in terms of currents are experienced in the line 2-3 as in the Scenario 3 at 12 and 2 p.m.
Considering the values reported in Tab. 3.7.3, related to Scenario 3, we can notice the increases of current absorbed by loads for EV charging during the charging periods and the aforementioned current decrease in phase 2 of line 2-3.

Tab. 3.9.2 S5 - Phase currents comparison

Hour	Magnitude I23_ph1	Magnitude I23_ph2	Magnitude I23_ph3	Magnitude I27_ph1	Magnitude I27_ph2	Magnitude I27_ph3	Magnitude I211_ph1	Magnitude I211_ph2	Magnitude I211_ph3	Magnitude I217_ph1	Magnitude I217_ph2	Magnitude I217_ph3
[h]	[A]	[A]	[A]	[A]	[A]	[A]	[A]	[A]	[A]	[A]	[A]	[A]
0	39,72	48,15	35,15	35,06	44,91	31,34	157,96	164,52	150,77	207,63	214,96	202,08
1	27,20	34,10	23,99	22,52	31,56	20,37	135,16	141,27	130,90	196,74	201,95	191,55
2	22,42	40,16	22,97	19,93	28,80	18,15	117,10	130,35	113,56	170,25	175,95	163,39
3	20,86	27,68	17,21	17,35	25,04	15,61	106,72	116,75	105,31	160,18	160,73	155,40
4	17,91	20,08	15,38	15,28	18,23	14,39	93,47	93,84	91,28	133,63	135,75	132,33
5	16,04	13,62	13,32	12,67	14,89	13,59	88,40	87,85	88,89	125,26	126,60	124,79
6	25,97	31,61	22,89	12,72	30,32	16,55	93,47	116,17	98,35	128,74	132,86	117,64
7	35,00	37,49	30,21	20,97	39,94	25,22	116,74	139,12	121,66	146,13	151,17	134,67
8	50,90	24,84	38,41	35,89	49,92	44,31	146,86	144,48	150,70	155,78	155,26	151,17
9	38,51	23,05	29,83	30,00	34,66	38,15	127,14	122,66	137,42	142,04	143,63	143,35
10	32,41	27,97	23,99	23,11	26,47	34,07	103,92	97,49	120,84	105,17	104,92	108,39
11	24,51	65,30	17,71	18,54	22,49	27,82	89,29	81,14	113,56	93,03	90,91	98,22
12	21,92	81,70	16,65	20,33	25,79	25,47	80,08	71,58	107,95	80,96	78,63	86,63
13	25,58	65,39	18,43	19,12	23,02	29,07	99,87	91,40	124,53	108,33	106,04	113,74
14	19,22	66,32	14,34	16,80	21,13	22,11	90,50	82,55	114,32	113,66	110,57	119,40
15	26,20	36,97	19,24	18,16	20,86	27,68	105,29	99,27	121,25	130,61	129,71	134,03
16	38,86	20,62	30,71	31,22	36,30	37,35	142,43	139,08	149,38	150,90	153,23	151,23
17	66,56	57,23	55,36	60,78	72,16	60,26	208,76	208,81	204,17	212,18	219,88	208,12
18	74,50	75,17	62,96	69,84	83,36	65,74	232,19	234,03	222,12	242,06	251,77	236,13
19	72,94	80,71	62,21	69,71	83,48	63,50	224,47	227,37	211,54	235,92	246,12	229,23
20	69,37	79,27	59,40	66,62	79,86	59,95	221,72	224,85	208,38	242,56	252,48	235,90
21	67,86	77,48	58,16	64,79	77,67	58,30	214,81	217,85	201,83	233,05	242,70	226,57
22	66,40	75,82	56,91	63,42	76,03	57,07	216,66	219,64	203,97	241,03	250,47	234,69
23	53,01	60,46	45,49	50,20	60,17	45,17	187,98	190,32	177,94	222,50	229,96	217,48

To analyse the network imbalances, we can evaluate the voltage unbalances in the electricity grid. Tab. 3.9.3 reports the measured values of voltage at upstream and downstream nodes of the distribution transformer, bus 1 and bus 2, and the hourly values of voltage unbalances evaluated through the equation 3.5.1 described above.
The average values are 0.026% and 0.087% at 11 kV and 400 V sides, respectively. They are slightly lower than those of Scenario 4 because the charging profiles are optimized vehicle by

vehicle, so the overall power consumption is better spread during the hours of the day, while in Scenario 4 all EV charging was at the same time.
The maximum values of voltage unbalance are lower as well and they result equal to 0.064% and 0.150%.

Tab. 3.9.3 S5 - Phase voltages comparison

Hour	Magnitude E1_ph1	Magnitude E1_ph2	Magnitude E1_ph3	Voltage unbalance	Magnitude E2_ph1	Magnitude E2_ph2	Magnitude E2_ph3	Voltage unbalance
[h]	[V]	[V]	[V]		[V]	[V]	[V]	
0	6339,07	6338,89	6337,12	0,020%	233,16	232,96	233,21	0,064%
1	6339,41	6339,29	6337,92	0,015%	233,33	233,15	233,37	0,055%
2	6341,20	6341,63	6339,38	0,021%	233,87	233,66	233,86	0,058%
3	6341,67	6341,71	6340,37	0,014%	233,99	233,84	234,02	0,046%
4	6342,72	6342,51	6342,07	0,006%	234,31	234,22	234,36	0,033%
5	6342,66	6342,34	6342,51	0,003%	234,33	234,27	234,40	0,027%
6	6342,64	6343,31	6341,00	0,021%	234,33	234,12	234,31	0,058%
7	6340,70	6341,11	6338,95	0,021%	233,75	233,50	233,78	0,077%
8	6337,45	6336,05	6337,56	0,015%	232,77	232,64	233,01	0,086%
9	6337,40	6335,97	6338,75	0,022%	232,87	232,81	233,14	0,085%
10	6338,26	6336,90	6340,56	0,031%	233,23	233,21	233,50	0,082%
11	6337,77	6335,83	6341,92	0,054%	233,21	233,31	233,55	0,083%
12	6337,67	6335,52	6342,69	0,064%	233,26	233,40	233,63	0,086%
13	6336,73	6334,78	6340,90	0,054%	232,92	233,01	233,26	0,085%
14	6337,40	6335,65	6341,54	0,053%	233,13	233,25	233,43	0,070%
15	6337,90	6336,47	6340,41	0,034%	233,13	233,15	233,39	0,070%
16	6337,09	6335,84	6337,87	0,017%	232,76	232,66	232,99	0,079%
17	6333,45	6332,02	6331,97	0,015%	231,55	231,25	231,81	0,124%
18	6332,16	6330,73	6329,68	0,021%	231,12	230,74	231,39	0,148%
19	6333,41	6332,12	6330,47	0,024%	231,44	231,04	231,68	0,150%
20	6333,57	6332,38	6330,59	0,025%	231,49	231,10	231,71	0,144%
21	6334,23	6333,08	6331,34	0,024%	231,68	231,30	231,89	0,140%
22	6333,87	6332,74	6331,04	0,024%	231,59	231,22	231,80	0,137%
23	6335,85	6334,98	6333,61	0,019%	232,20	231,91	232,36	0,107%
				0,026%				0,087%

From an electric power point of view, following Fig. 3.9.3 shows the profiles of single-phase active power at each phase of each grid node.

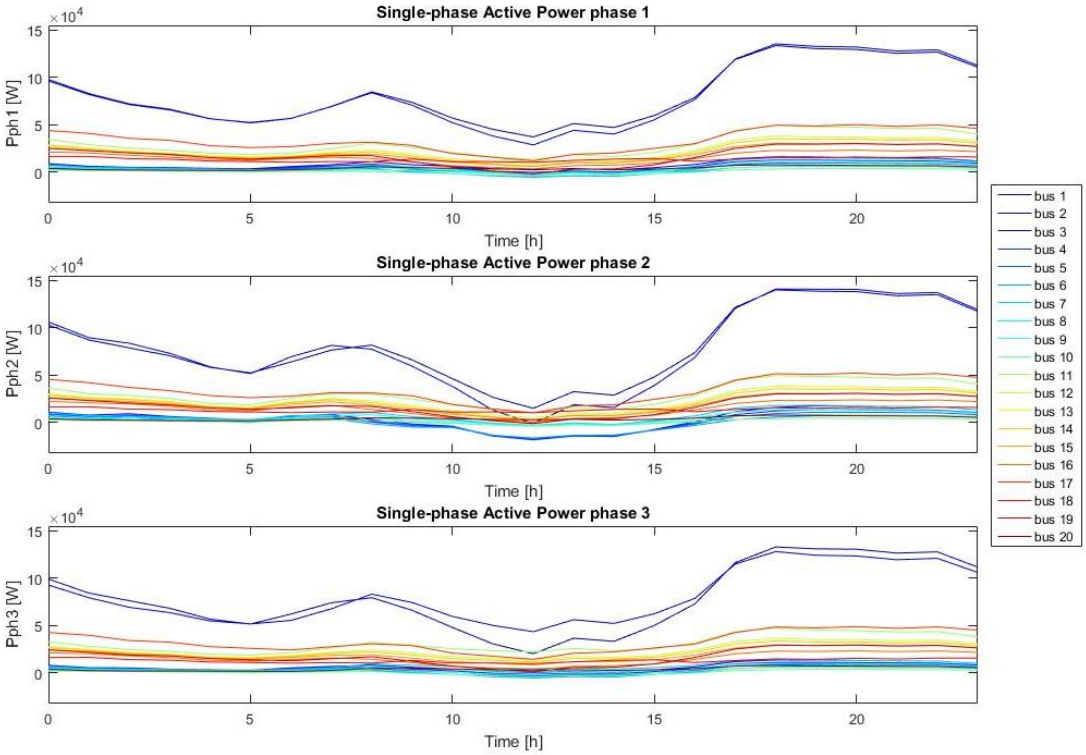

Fig. 3.9.3 S5 - Single-phase Active Power

It has been stated in the previous pages that car park, located at node 6, increased local power consumption of PV generation by limiting reverse power flows. It can be seen also in Fig. 3.9.3. Indeed, comparing it with Fig. 3.7.3 of Scenario 3, we can observe a decrease of negative power around 10 a.m.

In general, the magnitude of power flows is slightly increased throughout the morning until midday, increasing the power consumed during the valley hours, while it is the same in the other part of the day.
Consequently, as shown in Fig. 3.9.4, the peak of the daily power demand is the same as in Scenario 3 and, therefore, the power rating of the distribution transformer is suitable to respond to the load demand of the distribution network.

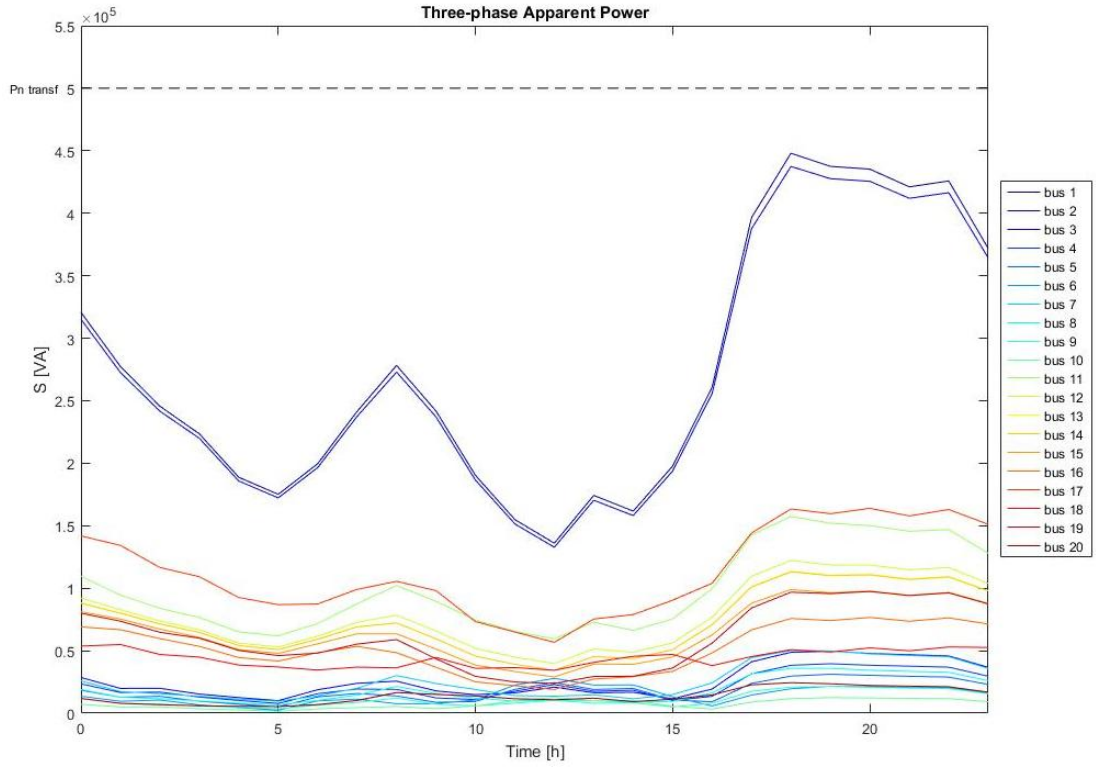

Fig. 3.9.4 S5 - Three-phase Apparent Power

If we compare the results of utilization factor of the distribution transformer shown in Tab. 3.9.4 with those reported in Tab. 3.8.4 of Scenario 4, we can see the same average values, but deeply different maximum values. In fact, in this scenario we obtain hourly utilization factors between 27% and 87%, in Scenario 4 they were between 27% and 107%.

From these results, we can state that EV charging does not negatively affect the daily operation of the electricity network, if the EVs are managed properly to charge their batteries. Indeed, for example, if they charge their batteries during off-peak hours, existing power system could easily withstand the overall power demand, therefore huge investments by system operators are not required.

Tab. 3.9.4 S5 - Transformer utilization factor

Hour	P + jQ	A	Transformer Utilization factor
[h]	[W + jVAr]	[VA]	
0	296995,48 +105428,45i	315153,09	63%
1	252173,06 + 103490,98i	272583,26	55%
2	225161,70 + 87718,10i	241644,89	48%
3	203250,88 + 84053,65i	219945,30	44%
4	170168,51 + 74479,23i	185753,81	37%
5	155363,53 + 74381,82i	172251,22	34%
6	181507,98 + 75095,39i	196429,29	39%
7	218628,80 + 92537,45i	237406,26	47%
8	244649,00 + 120913,10i	272897,62	55%
9	204655,89 + 119649,23i	237065,34	47%
10	150021,00 + 110788,24i	186494,87	37%
11	101204,73 + 112631,41i	151420,71	30%
12	71158,02 + 112022,58i	132712,18	27%
13	119243,62 + 121669,89i	170360,21	34%
14	108165,63 + 115291,59i	158088,44	32%
15	157115,95 + 113386,58i	193757,41	39%
16	224270,70 + 122754,89i	255667,97	51%
17	355358,84 + 154902,85i	387652,94	78%
18	404949,90 + 165415,77i	437432,05	87%
19	398343,87 + 155598,64i	427654,97	86%
20	396638,28 + 154145,66i	425538,26	85%
21	384083,88 + 148865,14i	411923,85	82%
22	387874,11 + 151560,45i	416433,55	83%
23	338392,49 + 135009,12i	364330,82	73%
			54%

At this point, we can focus on the power losses along the network lines. Fig. 3.9.5 below shows the profiles of active power losses in the network lines. Their magnitudes are obviously lower than those of Scenario 4, during the evening, while they are slightly greater during the morning until midday.

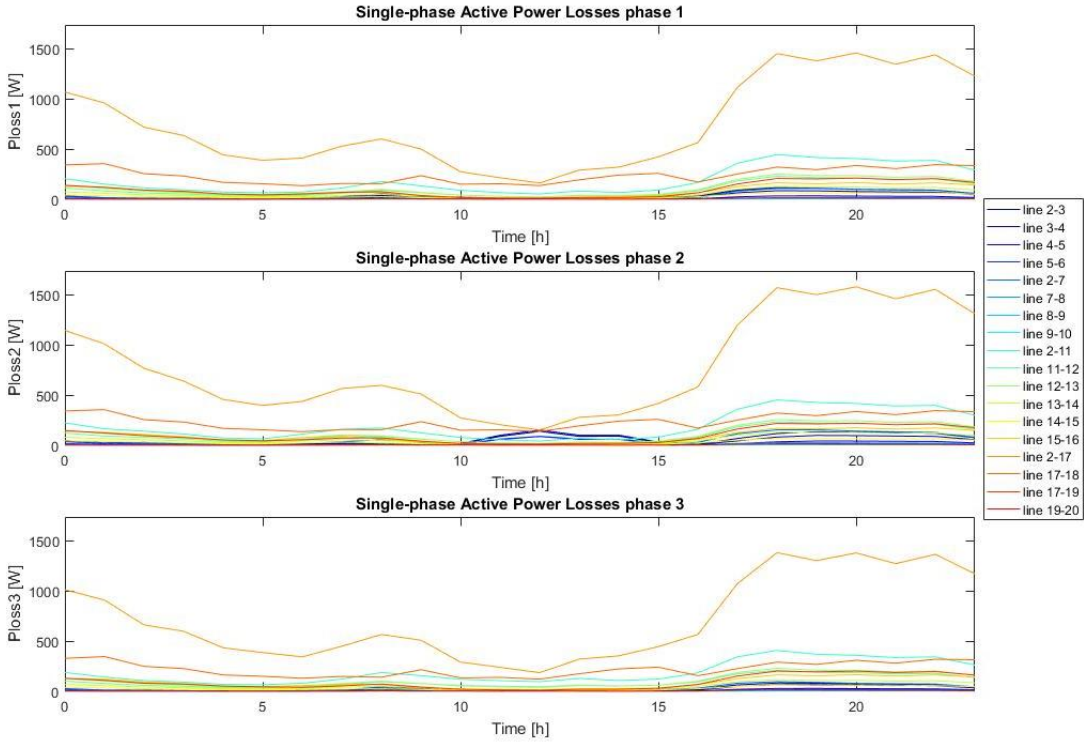

Fig. 3.9.5 S5 - Power losses

For a better understanding of savings related to controlled charging method, we can investigate the economic results provided by the modelling tool. Tab. 3.9.5 reports that the overall operating cost results equal to £ 726.13, while in Scenario 3 it was £ 696.27. Thus, we can evaluate the overall cost incurred to charge all 54 EVs, spread on the electricity grid, subtracting the aforementioned values. The result is £ 29.86, which means that each EV charging costs, on average, about £ 0.55. In Scenario 4, which considered uncontrolled charging, the cost resulted equal to £ 1.30 per each electric vehicle. This reduction is possible thanks to the optimized charging that consumes power in the off-peak hours, when it costs less than in the evening.
In Scenario 5, the cost of energy consumed is £ 707.41, which means more than 97% of the overall cost, and the cost of energy losses is £ 18.72. The latter was equal to £ 20 in Scenario 4, therefore smart charging also allows savings in terms of energy losses of about 10%.
In conclusion, the overall operating cost results 5% lower than the case of uncontrolled charging of Scenario 4.

Tab. 3.9.5 S5 - Economic results

Archetype1	Archetype2	Archetype3	Archetype4	Archetype5	Archetype6	Archetype7	Archetype8	Archetype9	Archetype10
[£]	[£]	[£]	[£]	[£]	[£]	[£]	[£]	[£]	[£]
0,00	18,08	18,01	14,90	18,16	-9,78	23,20	25,20	16,15	1,09
Archetype11	Archetype12	Archetype13	Archetype14	Archetype15	Archetype16	Archetype17	Archetype18	Archetype19	Archetype20
[£]	[£]	[£]	[£]	[£]	[£]	[£]	[£]	[£]	[£]
23,32	45,46	17,49	23,29	43,53	136,22	27,71	126,04	96,07	43,27

ELoss23	ELoss34	ELoss45	ELoss56	ELoss27	ELoss78	ELoss89	ELoss910	ELoss211
[£]	[£]	[£]	[£]	[£]	[£]	[£]	[£]	[£]
0,48	0,39	0,18	0,13	0,46	0,07	0,03	0,02	2,03
ELoss1112	ELoss1213	ELoss1314	ELoss1415	ELoss1516	ELoss217	ELoss1718	ELoss1719	ELoss1920
[£]	[£]	[£]	[£]	[£]	[£]	[£]	[£]	[£]
1,04	1,16	0,59	0,31	0,84	7,67	2,30	0,97	0,05

Total
[£]
726,13

3.10. Scenario 6 (15% of household PV, V2G strategy)

The sixth and last scenario of this case study analyses the operating conditions of the reference electricity distribution network considering the same load configuration as in Scenario 3 (Tab. 3.7.1), but, in this circumstance, it applies V2G technology to perform EV charging.
Therefore, it evaluates the operating conditions expected for the year 2050, if all EV owners will apply Vehicle-to-Grid technology to manage their vehicle charging. It means that all the electric vehicles will be charged in an optimized way in order to minimize charging costs, but this setting also allows power flows from the vehicle to the grid, thus both charge and discharge of EV battery (Sec. 2.2.1).

As explained in section 2.2.1, the modelling tool implements one EV per each smart household, while for smart schools, smart shops, smart industries and smart car parks it considers different numbers of EVs in relation to the percentages reported in Tab. 2.2.1.1. In conclusion, the number of EVs applied on the electricity network is the same of Scenario 5,

but with different charging profiles, because now they are optimized considering V2G technology.
The total number of EVs is 54, 52 related to smart houses and 2 to the smart park.
As in the previous scenarios, not all the EVs related to the smart household loads, are charged at home, in fact, their percentage is an input variable of the modelling tool and it has been set equal to 65%. The remaining 35% charges its batteries in off-home charging infrastructures, along the streets, at charging stations or at work. It has been considered that these charges allow the vehicles to achieve a battery capacity equal to 70% of their ratings.
From a V2G point of view, these off-home charging are the key point to perform a profitable power shifting during the day. Indeed, these EVs can charge their battery exploiting the electricity produced by PV systems during the central hours of the day, along the streets, at charging stations or at work and return energy to the grid during the peak hours, achieving good profits.

As reported in sec. 2.2.1, the minimization algorithm of the modelling tool optimizes EV charging profiles through a cost function, complying with some constraints. Since it also takes into account battery degradation, the resulting profiles are a compromise between profits related to power shifting and costs of battery degradation.
Therefore, the EVs, that charge their battery off-home, can play the role of distributed energy storage systems, allowing delayed green energy consumption: they accumulate solar energy during the daytime and provide it during the other hours of the day. This benefits the operation of electricity grid because it reduces the value of daily peak of power demand. The effect is higher, the more the percentage of off-home charging is high.

Once all the parameters have been set on the modelling tool, we can proceed with the grid analysis. Also in this scenario, we can find EV chargers blocks, which take into account the power consumed to charge the aggregated EVs, inside archetype blocks.
To follow the same scheme as before, the first analysis of the grid is in terms of voltage deviation.
Scenario 6 considers the same distribution transformer as Scenario 3, with same settings and ratings. This because we want to compare the consequences, on the electricity network, caused by different EVs charging strategies.

Fig. 3.10.1 shows the daily profiles of voltage deviations for each phase of grid nodes.
The results related to bus 1, MV node, are not shown because they are basically flat and equal to the value of nominal voltage. In this scenario, as can be seen in figure below, all the profiles are within the imposed limits, contrary to what happened in Scenario 4, and if we analyse the shapes during the evening we can observe they are farer from the lower border than those of Scenario 5. In fact, firstly, the optimization process, performed by the modelling tool, avoids the creation of new peaks in the power demand profiles and moreover V2G technology reduces the power absorbed by the distribution network from the medium voltage connection during the peak hours, which means it reduces the peak value of power demand from the distribution substation point of view.

The implementation of V2G, being a kind of distributed energy storage, can allow extensions, in terms of number of loads and PV generation, of existing distribution networks without affecting the overall operating condition of distribution substations and therefore without requiring significant investments for network enhancements.

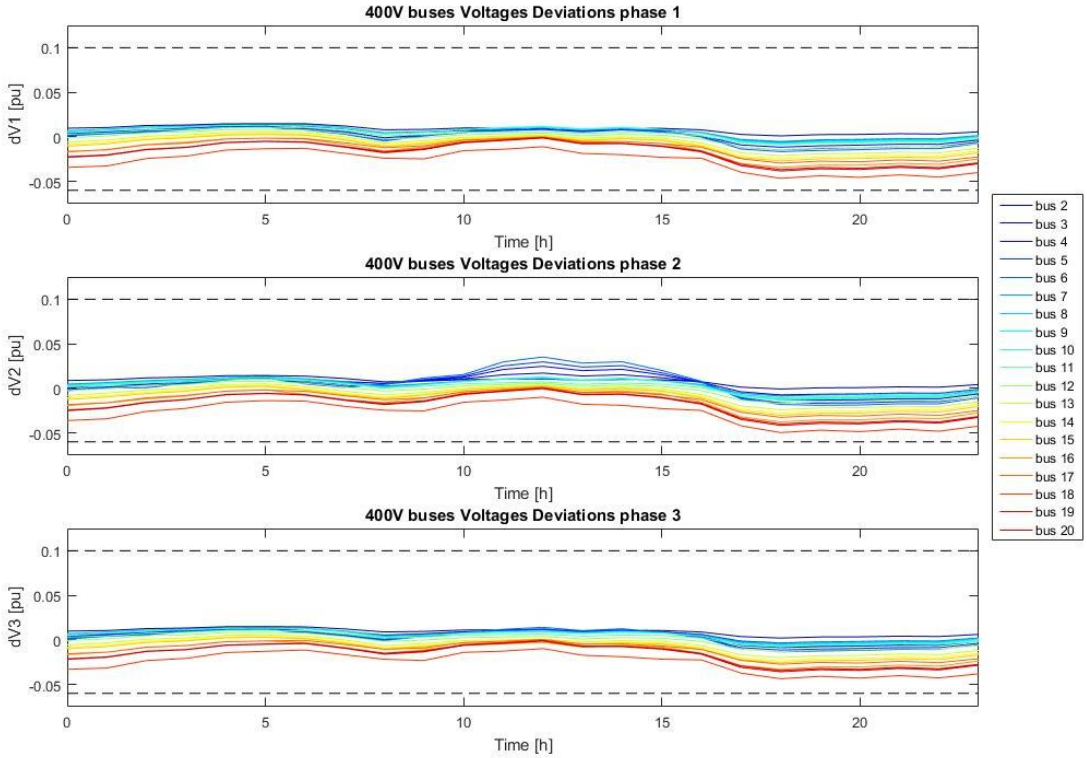

Fig. 3.10.1 S6 - Voltages deviations

Analysing the results in terms of line currents, Fig. 3.10.2 shows their hourly profiles, while following Tab. 3.10.1 reports the maximum measures compared to the lines current rating.

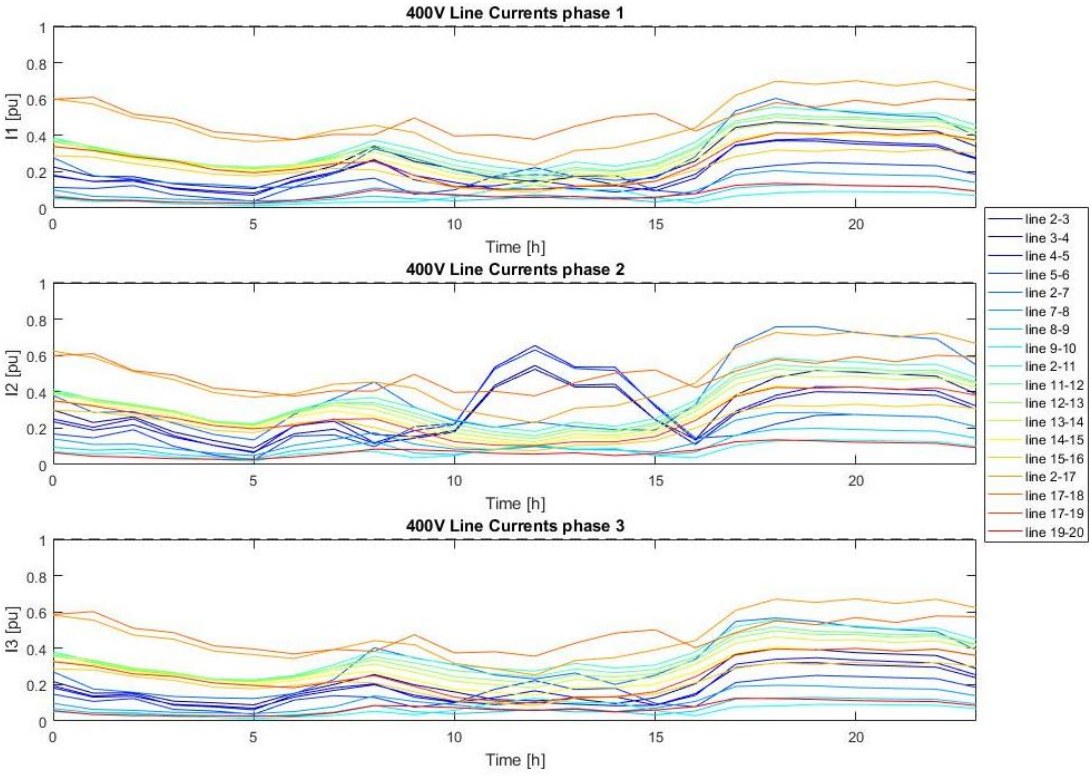

Fig. 3.10.2 S6 - Line Currents

Tab. 3.10.1 S6 - Lines current ratings

Line_2-3	Current rating complied: 81.7031A vs 150A nominal
Line_3-4	Current rating complied: 78.6454A vs 150A nominal
Line_4-5	Current rating complied: 72.036A vs 110A nominal
Line_5-6	Current rating complied: 69.3645A vs 110A nominal
Line_2-7	Current rating complied: 83.4756A vs 110A nominal
Line_7-8	Current rating complied: 62.5014A vs 218A nominal
Line_8-9	Current rating complied: 37.9026A vs 190A nominal
Line_9-10	Current rating complied: 20.508A vs 150A nominal
Line_2-11	Current rating complied: 230.6282A vs 393A nominal
Line_11-12	Current rating complied: 215.6939A vs 393A nominal
Line_12-13	Current rating complied: 179.6898A vs 342A nominal
Line_13-14	Current rating complied: 168.2707A vs 342A nominal
Line_14-15	Current rating complied: 147.0189A vs 342A nominal
Line_15-16	Current rating complied: 113.6785A vs 342A nominal
Line_2-17	Current rating complied: 249.5586A vs 342A nominal
Line_17-18	Current rating complied: 82.3144A vs 135A nominal
Line_17-19	Current rating complied: 146.2331A vs 342A nominal
Line_19-20	Current rating complied: 36.6908A vs 270A nominal

Focusing on current profiles, if we compare Fig. 3.10.2 with Fig. 3.9.2, related to Scenario 5, we can observe some differences during the evening, where some energy is directly provided to the loads by EVs, which have been recharged off-home during the daytime. As explained in sec. 2.2.1, the energy consumed for off-home charging is not taken into account in the operating conditions of the distribution network, but it is considered only in the costs evaluations.

As we could have expected, in Tab. 3.10.1 all current ratings of network lines are complied. This means that EV charging does not negatively affect the overall distribution system, if EVs are properly managed.

Following Tab. 3.10.2 reports the hourly values of line current of each phase of the three-phase branches starting from the distribution substation.
The worst unbalanced conditions in terms of currents are experienced in the line 2-3 as in the Scenario 3 at 12 and 2 p.m.
Comparing Tab. 3.10.2 with Tab. 3.7.3 of Scenario 3 and with Tab. 3.9.2 of Scenario 5, we can notice some differences in the magnitudes of current flowing along grid lines during charging periods. From a macroscopic point of view, we can state that current absorbed by archetypes, after the EVs return home, is generally lower thanks to the contribution of EVs to respond to the power demand.
It is noteworthy that EVs energy discharge causes an increase in current unbalances among the lines of three-phase branches because of the uneven distribution of EVs that charge their battery during the day and consequently they can supply energy to the grid during the peak hours.

Tab. 3.10.2 S6 - Phase currents comparison

Hour	Magnitude I23_ph1	Magnitude I23_ph2	Magnitude I23_ph3	Magnitude I27_ph1	Magnitude I27_ph2	Magnitude I27_ph3	Magnitude I211_ph1	Magnitude I211_ph2	Magnitude I211_ph3	Magnitude I217_ph1	Magnitude I217_ph2	Magnitude I217_ph3
[h]	[A]	[A]	[A]	[A]	[A]	[A]	[A]	[A]	[A]	[A]	[A]	[A]
0	33,99	45,02	32,55	30,51	41,72	29,81	152,02	162,51	149,28	205,15	213,49	199,16
1	26,22	34,72	23,01	19,63	31,56	19,40	131,41	140,84	129,95	195,81	201,02	189,70
2	25,89	39,33	23,23	17,52	32,05	17,34	113,98	129,56	112,78	170,50	175,17	161,85
3	20,08	26,89	16,43	15,03	25,04	14,83	103,70	115,99	104,55	159,43	159,98	153,91
4	17,56	19,73	15,03	14,23	18,23	14,04	92,10	93,50	90,94	133,29	135,41	131,65
5	16,04	13,62	13,32	12,67	14,89	13,59	88,40	87,85	88,89	125,26	126,60	124,79
6	25,97	31,61	22,89	12,72	30,32	16,55	93,47	116,17	98,35	128,74	132,86	117,64
7	35,00	37,49	30,21	20,97	39,94	25,22	116,74	139,12	121,66	146,13	151,17	134,67
8	50,90	24,84	38,41	35,89	49,92	44,31	146,86	144,48	150,70	155,78	155,26	151,17
9	38,51	23,05	29,83	30,00	34,66	38,15	127,14	122,66	137,42	142,04	143,63	143,35
10	32,41	27,97	23,99	23,11	26,47	34,07	103,92	97,49	120,84	105,17	104,92	108,39
11	24,51	65,30	17,71	18,54	22,49	27,82	89,29	81,14	113,56	93,03	90,91	98,22
12	21,92	81,70	16,65	20,33	25,79	25,47	80,08	71,58	107,95	80,96	78,63	86,63
13	25,58	65,39	18,43	19,12	23,02	29,07	99,87	91,40	124,53	108,33	106,04	113,74
14	19,22	66,32	14,34	16,80	21,13	22,11	90,50	82,55	114,32	113,66	110,57	119,40
15	26,20	36,97	19,24	18,16	20,86	27,68	105,29	99,27	121,25	130,61	129,71	134,03
16	38,86	20,62	30,71	31,22	36,30	37,35	142,43	139,08	149,38	150,90	153,23	151,23
17	66,56	57,23	55,36	58,84	72,16	60,26	203,50	208,81	204,17	212,18	219,88	208,12
18	71,07	71,81	59,52	66,42	83,36	62,30	218,65	230,63	218,70	238,72	248,42	229,44
19	69,73	77,51	59,00	60,15	83,48	60,28	211,83	224,19	208,36	232,80	242,99	222,98
20	66,38	76,27	56,40	57,69	79,86	56,95	209,97	221,90	205,43	239,65	249,56	230,08
21	64,95	74,57	55,24	56,11	77,67	55,39	203,37	214,98	198,96	230,22	239,86	220,92
22	63,55	72,97	54,05	54,92	76,03	54,22	205,48	216,83	201,16	238,26	247,70	229,16
23	50,75	58,20	43,23	43,47	60,17	42,91	179,15	188,10	175,72	220,31	227,77	213,11

To evaluate network unbalances, we can calculate the voltage unbalances in the electricity grid. Tab. 3.10.3 shows the measured values of voltage at upstream and downstream nodes of the distribution transformer, bus 1 and bus 2, and the hourly values of voltage unbalances evaluated through the equation 3.5.1 described above.

Tab. 3.10.3 S6 - Phase voltages comparison

Hour	Magnitude E1_ph1	Magnitude E1_ph2	Magnitude E1_ph3	Voltage unbalance	Magnitude E2_ph1	Magnitude E2_ph2	Magnitude E2_ph3	Voltage unbalance
[h]	[V]	[V]	[V]		[V]	[V]	[V]	
0	6338,83	6339,07	6337,17	0,019%	233,17	232,98	233,21	0,061%
1	6339,36	6339,52	6337,82	0,017%	233,35	233,16	233,37	0,058%
2	6341,24	6341,70	6339,30	0,023%	233,87	233,66	233,86	0,060%
3	6341,62	6341,83	6340,34	0,015%	234,01	233,85	234,02	0,046%
4	6342,69	6342,57	6342,06	0,006%	234,32	234,22	234,36	0,033%
5	6342,66	6342,34	6342,51	0,003%	234,33	234,27	234,40	0,027%
6	6342,64	6343,31	6341,00	0,021%	234,33	234,12	234,31	0,058%
7	6340,70	6341,11	6338,95	0,021%	233,75	233,50	233,78	0,077%
8	6337,45	6336,05	6337,56	0,015%	232,77	232,64	233,01	0,086%
9	6337,40	6335,97	6338,75	0,022%	232,87	232,81	233,14	0,085%
10	6338,26	6336,90	6340,56	0,031%	233,23	233,21	233,50	0,082%
11	6337,77	6335,83	6341,92	0,054%	233,21	233,31	233,55	0,083%
12	6337,67	6335,52	6342,69	0,064%	233,26	233,40	233,63	0,086%
13	6336,73	6334,78	6340,90	0,054%	232,92	233,01	233,26	0,085%
14	6337,40	6335,65	6341,54	0,053%	233,13	233,25	233,43	0,070%
15	6337,90	6336,47	6340,41	0,034%	233,13	233,15	233,39	0,070%
16	6337,09	6335,84	6337,87	0,017%	232,76	232,66	232,99	0,079%
17	6333,31	6332,21	6331,98	0,013%	231,56	231,26	231,81	0,124%
18	6332,17	6331,18	6329,63	0,021%	231,19	230,78	231,42	0,152%
19	6333,30	6332,71	6330,43	0,027%	231,52	231,08	231,70	0,153%
20	6333,46	6332,93	6330,56	0,028%	231,56	231,14	231,73	0,147%
21	6334,12	6333,61	6331,30	0,027%	231,75	231,33	231,91	0,143%
22	6333,77	6333,26	6331,00	0,026%	231,66	231,25	231,82	0,140%
23	6335,75	6335,38	6333,57	0,021%	232,25	231,93	232,37	0,109%
				0,026%				0,088%

The average values are 0.026% and 0.088% at 11 kV and 400 V sides, respectively. The first one is the same as in Scenario 5, while the second one is slightly higher because of the aforementioned uneven distribution of EVs that can supply energy to the grid during the peak hours. Indeed, in the LV side of the distribution transformer, the highest values are experienced after 6 p.m.
The maximum values of voltage unbalance follow the trend of the average values and they result equal to 0.064% and 0.153%.

Following Fig. 3.10.3 shows the hourly profiles of single-phase active power at each phase of each grid node.

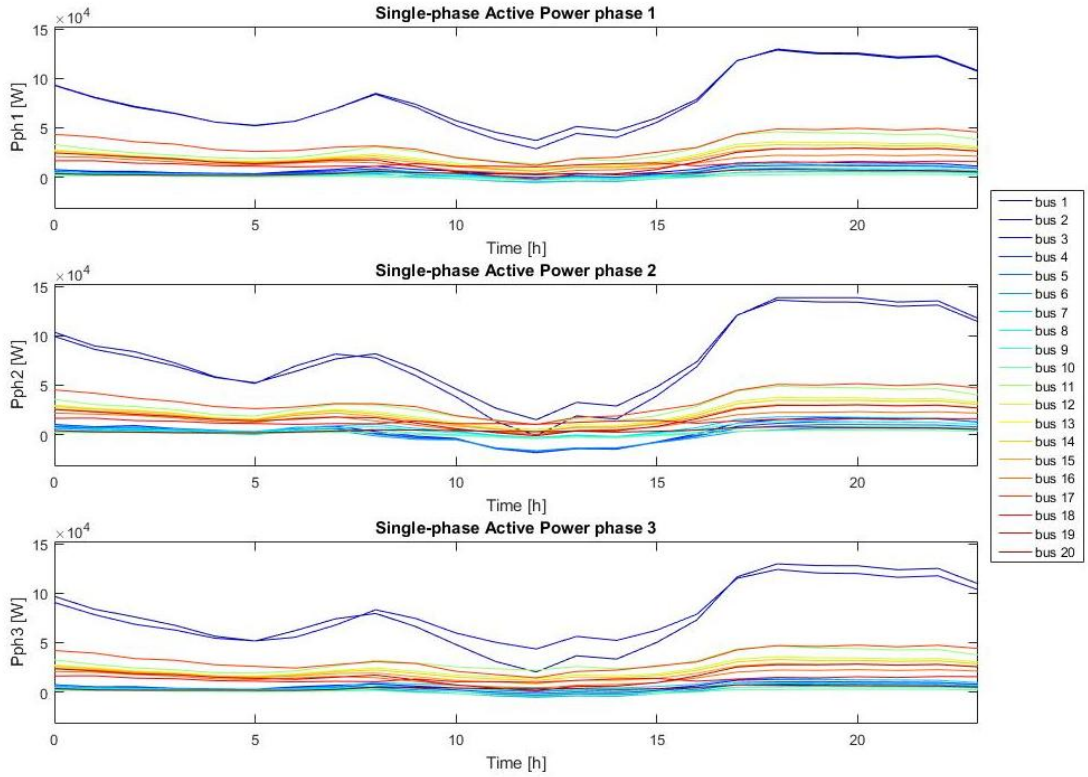

Fig. 3.10.3 S6 - Single-phase Active Power

As has been explained in Scenario 5 analysis, the car park, located at node 6, increases local power consumption of PV generation by limiting reverse power flows. This can be seen in Fig. 3.10.3, in fact, comparing it with Fig. 3.7.3 of Scenario 3, we can observe a decrease of negative power around 10 a.m. Moreover, other differences can be noticed during the evening with a small decrease in absolute values, while the shapes are roughly the same.

In general, from the three-phase apparent power point of view, we can expect that V2G technology leads to an additional decrease in the daily peak of power demand compared to that of Scenario 5, which has considered only smart charging strategy.
Fig. 3.10.4 reports the hourly profiles of three-phase apparent power at each grid node compared to the nominal power rating of the distribution transformer, which is equal to 500 kVA, as usual.
As we could have expected, the power rating of the distribution transformer is suitable to respond to the load demand of the distribution network.

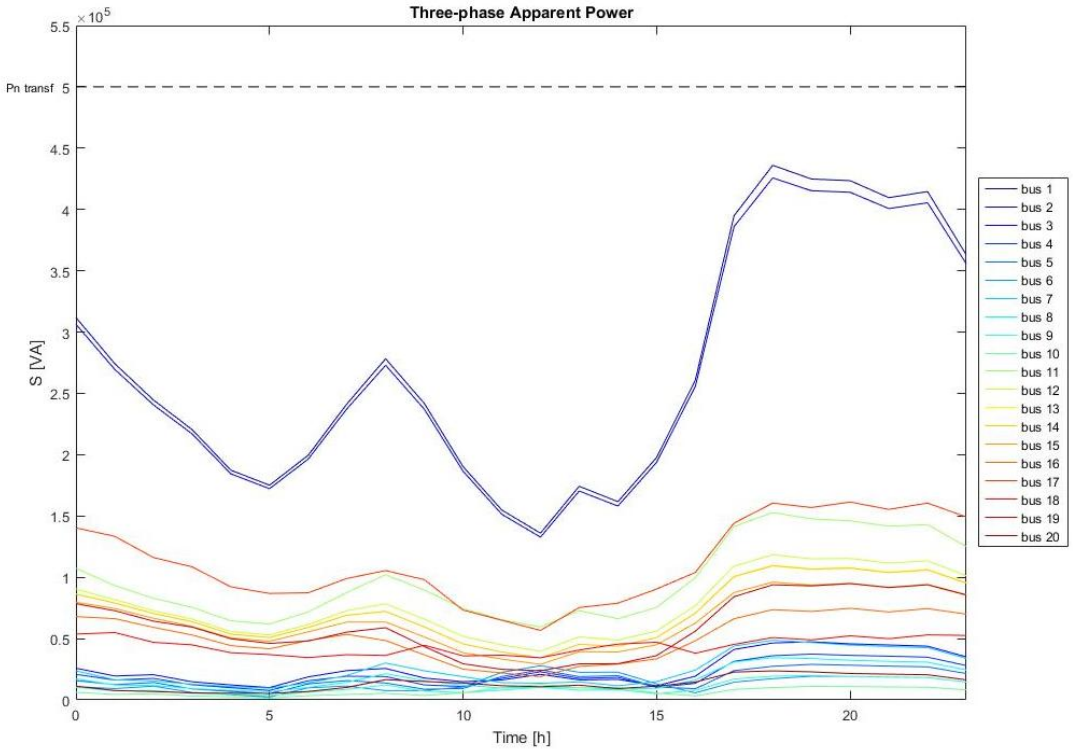

Fig. 3.10.4 S6 - Three-phase Apparent Power

Tab. 3.10.4 shows the hourly values of utilization factor of the distribution transformer. They remain in the range (27 ÷ 85) %, with an average value equal to 53%. Comparing these results with those of Scenario 5, we can state that V2G implementation reduces the highest value by 2%, while the average by 1%.

Tab. 3.10.4 S6 - Transformer utilization factor

Hour	P + jQ	A	Transformer Utilization factor
[h]	[W + jVAr]	[VA]	
0	287438,37 + 106084,77i	306389,94	61%
1	248941,26 + 103438,08i	269575,94	54%
2	224150,16 + 87687,92i	240691,65	48%
3	199993,22 + 84030,34i	216929,45	43%
4	168681,87 + 74465,82i	184387,45	37%
5	155364,71 + 74379,45i	172251,26	34%
6	181507,98 + 75095,39i	196429,29	39%
7	218628,80 + 92537,45i	237406,26	47%
8	244649,00 + 120913,10i	272897,62	55%
9	204655,89 + 119649,23i	237065,34	47%
10	150021,00 + 110788,24i	186494,87	37%
11	101204,73 + 112631,41i	151420,71	30%
12	71158,02 + 112022,58i	132712,18	27%
13	119243,62 + 121669,89i	170360,21	34%
14	108165,63 + 115291,59i	158088,44	32%
15	157115,95 + 113386,58i	193757,41	39%
16	224270,70 + 122754,89i	255667,97	51%
17	353559,33 + 154888,46i	385998,24	77%
18	392395,65 + 165257,69i	425775,12	85%
19	385110,39 + 155414,37i	415287,42	83%
20	384331,47 + 153967,13i	414024,83	83%
21	372098,02 + 148697,79i	400709,33	80%
22	376148,50 + 151395,52i	405472,93	81%
23	329077,93 + 134882,26i	355648,01	71%
			53%

In absolute terms, Scenario 6 (V2G technology) has an highest value equal to 425,78 kVA, Scenario 5 (smart charging) equal to 437,43 kVA.

Focusing now on the hourly power losses along the network branches, Fig. 3.10.5 graphs the profiles of active power losses in the grid lines. Their magnitudes result lower than Scenario 5 because less power and consequently lower currents flow in the distribution network.

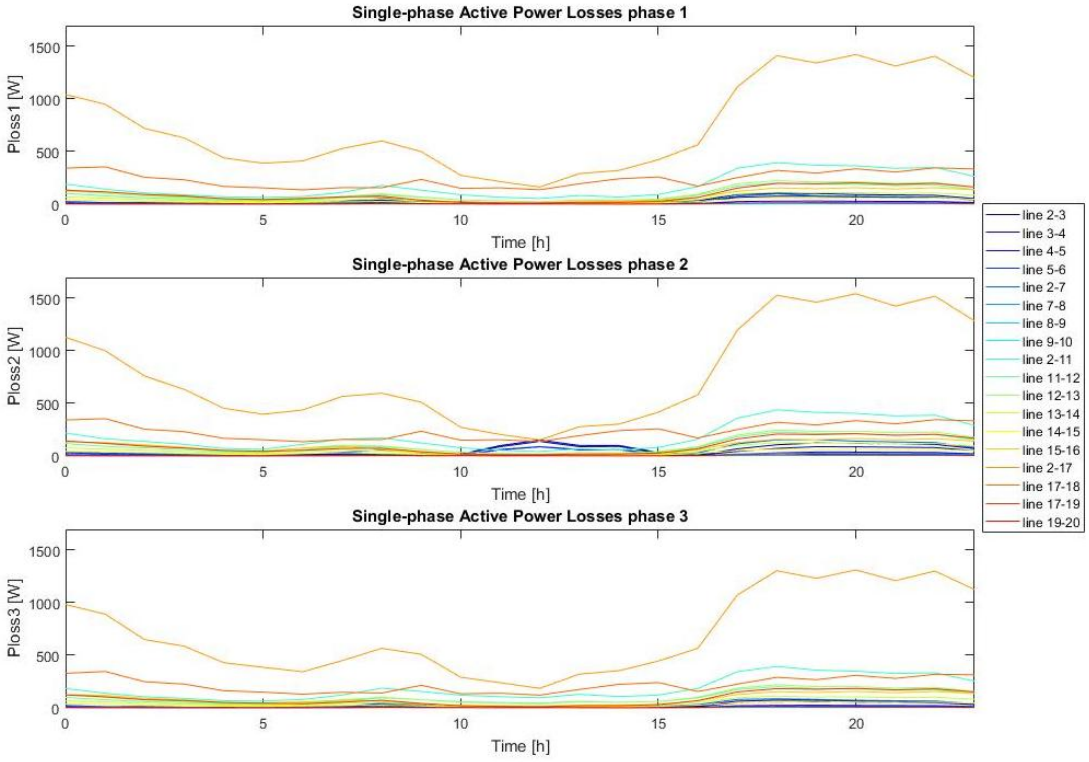

Fig. 3.10.5 S6 - Power losses

At this point, to understand the cost-effectiveness of V2G technology we have to investigate the economic results, evaluated by the modelling tool, reported in the following Tab. 3.10.5.

Tab. 3.10.5 S6 - Economic results

Archetype1	Archetype2	Archetype3	Archetype4	Archetype5	Archetype6	Archetype7	Archetype8	Archetype9	Archetype10
[£]	[£]	[£]	[£]	[£]	[£]	[£]	[£]	[£]	[£]
0,00	18,06	18,01	14,90	18,16	-10,94	22,89	24,89	16,12	0,36
Archetype11	Archetype12	Archetype13	Archetype14	Archetype15	Archetype16	Archetype17	Archetype18	Archetype19	Archetype20
[£]	[£]	[£]	[£]	[£]	[£]	[£]	[£]	[£]	[£]
23,32	45,11	17,49	22,93	43,17	135,13	27,71	126,04	94,99	42,89

ELoss23	ELoss34	ELoss45	ELoss56	ELoss27	ELoss78	ELoss89	ELoss910	ELoss211
[£]	[£]	[£]	[£]	[£]	[£]	[£]	[£]	[£]
0,46	0,36	0,16	0,12	0,43	0,07	0,02	0,02	1,96
ELoss1112	ELoss1213	ELoss1314	ELoss1415	ELoss1516	ELoss217	ELoss1718	ELoss1719	ELoss1920
[£]	[£]	[£]	[£]	[£]	[£]	[£]	[£]	[£]
1,00	1,11	0,57	0,30	0,81	7,52	2,30	0,94	0,05

Total
[£]
719,41

The overall operating cost results equal to £ 719.41, while in Scenario 3, without EVs, it was £ 696.27. Therefore, we can evaluate the overall cost incurred for charging and discharging all 54 EVs, spread on the electricity grid, subtracting the aforementioned values. The result is £ 23.14, which means that each EV incurs a cost of about £ 0.43. In Scenario 5, which considered smart charging strategies, the cost was equal to £ 0.55 per each vehicle. This means that off-home EV charging is more cost-effective than home charging. The resulting value is an average value, therefore the EVs that have been recharged off-home during the daytime have a much lower cost than the others, considering that they are only 35% of the overall number and they reduce the overall cost by more than 20%.
In Scenario 6, the cost of energy consumed is £ 701.20, which means more than 97% of the overall cost, and the cost related to energy losses is £ 18.20. The latter is about 3% less than in Scenario 5. In fact, as we stated above, the overall energy losses are lower than they were in the previous case.
In conclusion, V2G technology leads to a reduction by 1% of the overall operating cost compared to smart charging strategies.

3.11. Relevant results comparison

In the last three scenarios, operating conditions of the reference electricity distribution network have been analysed in order to compare the effects of different strategies of electric vehicles management. The baseline scenario is the number 3, which does not consider EVs on the electricity grid.
In summary, Scenario 4 has considered uncontrolled charging, Scenario 5 smart charging and finally Scenario 6 has considered V2G implementation.
In the following, we will focus on three-phase apparent power profile at the downstream node of distribution transformer and on the network operating costs in order to highlight the pros and cons of each strategy.

Fig. 3.11.1 shows the power profiles at node 2, downstream side of distribution transformer, in the case of Scenario 3 and Scenario 4.

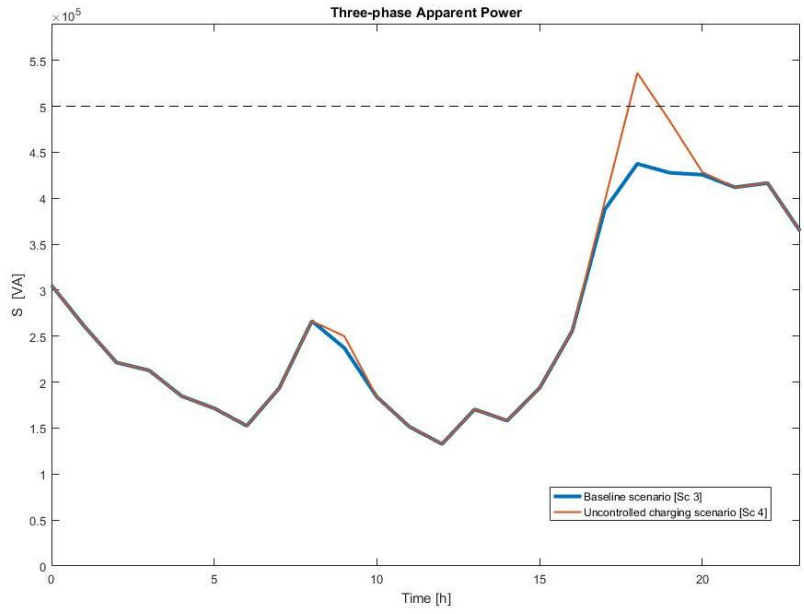

Fig. 3.11.1 There-phase Apparent Power comparison [Sc 3 vs Sc 4]

Fig. 3.11.2 shows the power profiles at node 2, downstream side of distribution transformer, in the case of Scenario 3 and Scenario 5.

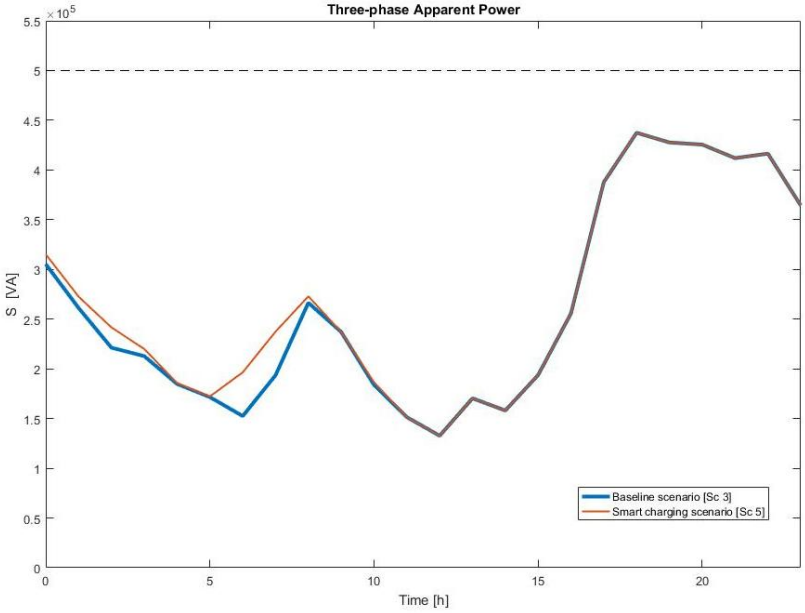

Fig. 3.11.2 There-phase Apparent Power comparison [Sc 3 vs Sc 5]

Fig. 3.11.3 shows the power profiles at node 2, downstream side of distribution transformer, in the case of Scenario 3 and Scenario 6.

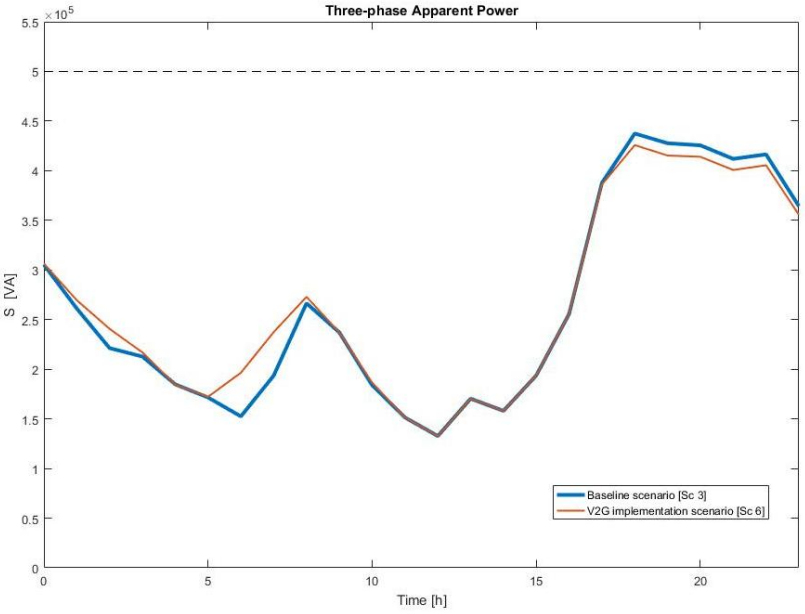

Fig. 3.11.3 There-phase Apparent Power comparison [Sc 3 vs Sc 6]

The daily peak values of load demand result equal to:

- Scenario 3: 437.43 kVA, 87% of transformer power rating;
- Scenario 4: 536.21 kVA, 107% of transformer power rating;
- Scenario 5: 437.43 kVA, 87% of transformer power rating;
- Scenario 6: 425.78 kVA, 85% of transformer power rating.

Following Fig. 3.11.4 summarizes the hourly three-phase apparent power profiles of considered scenarios.

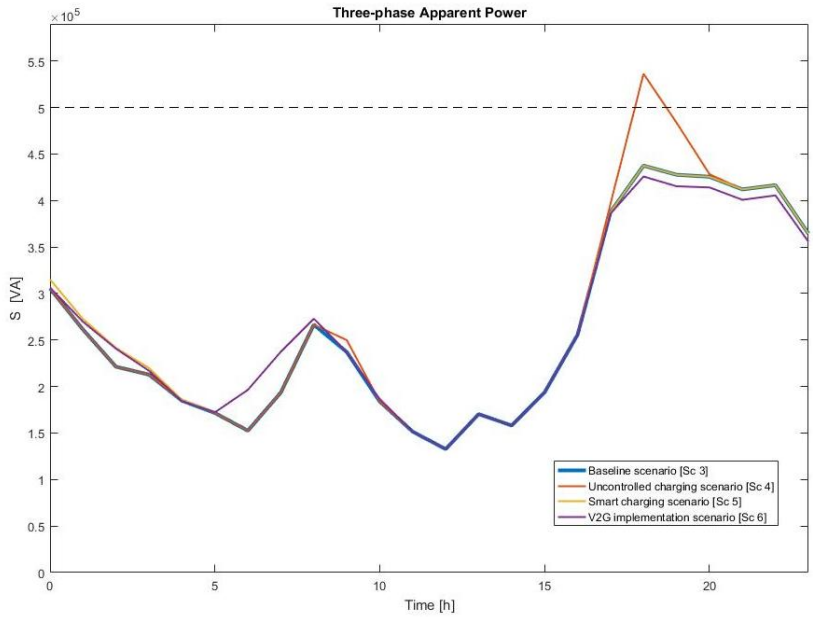

Fig. 3.11.4 There-phase Apparent Power comparison

As explained in the previous chapters, uncontrolled charging is the worst adoptable solution to charge electric vehicles, because most of EV charging occurs when the users get home from work, therefore, in the same hours of the peak of power consumed by household loads. If this strategy will be pursued to charge electric vehicles, huge investments must be planned by distribution system operators to make significant improvements on the electricity grid in order to comply with lines current ratings, transformer power rating and voltage deviation limits.

Smart charging strategy implies an increase of power consumed during the morning, when electricity is cheap, while keeping the same power profile at the other hours of the day.

V2G implementation scenario has an hourly profile very close to that of smart charging during the morning, while it reduces power demand from the distribution transformer during the evening. The EVs, that recharge their battery off-home, supply power to the electricity network in the peak hours, reducing the overall daily power peak. The magnitude of peak shaving depends, of course, on the economic parameters, but also on off-home charging share and reached battery capacity after off-home charging, because they have key roles on the determination of V2G profitability.

Both smart charging and V2G are valley-filling charging strategies because they aim to shift EV charging schedules in order to flat the power load profiles, filling load valley. Therefore, controlled charging increase social welfare, because it involves savings for EV owners and network advantages for system operators.

Tab. 3.11.1 summarizes the economic results assessed by the modelling tool in the different scenarios. Scenario 3, the baseline one, does not consider EVs on the electricity grid; therefore, the related cost of energy consumed is imputable to the operating conditions of only power loads and PV generation, which are implemented on the electricity network.

The last column of table below, reports the average charging cost for each electric vehicle in the case of dumb and smart charging, while it is related to the overall EV battery management, which includes both charging and discharging, in the case of V2G implementation. Let us remember that the number of EVs applied on the electricity grid is 54.

Tab. 3.11.1 Economic results comparison

	Cost of energy consumed [£]	Cost of energy losses [£]	Total operating cost [£]	Average EV operating cost [£]
Scenario 3	677.77	18.50	696.27	/
Scenario 4	747.37	20.00	767.37	1.30
Scenario 5	707.41	18.72	726.13	0.55
Scenario 6	701.20	18.21	719.41	0.43

Scenario 4, that implements dumb charging, involves the highest cost in terms of both energy consumed and energy losses. Indeed, according to what explained before, uncontrolled charging does not make benefits either for EV owners or system operators.
From the results reported in Tab. 3.11.1 above, the most challenging strategy, that is V2G technology, is also the most profitable way to manage EV batteries. It saves about 6% of the overall operating costs compared to uncontrolled charging and it has an average operating cost related to EV charging of about 33% of that of dumb charging, implemented in Scenario 4.
It has been stated that V2G is the most challenging strategy since some difficult tasks must be overcome to achieve its implementation on the electricity networks; for example, global EV charging management system, bidirectional battery chargers and, of course, regulations for EVs implementation on the power system.

CONCLUSION

The purpose of this thesis was to create a Smart Grid Modelling Tool able to model distribution networks and analyse their operating conditions in order to evaluate the impact of different charging strategies of electric vehicles. It has been created a user-friendly GUI that allows the user to manage all the input parameters and output results as planned in the project definition.
This thesis has analysed six different scenarios applied on an existing low-voltage distribution network, simulating current and expected operating conditions in the year 2050; in fact, in the next decades, EV and RES penetration is expected to achieve very high targets, providing many opportunities, but also leading to many challenges for system operators.
The results demonstrate that many local grid issues, such as grid constraints violations, distribution transformer overloading and congestion, can be mitigated performing controlled EV charging, moreover, it is possible to increase the local consumption of renewable generation by charging the vehicles during the daytime.
This project also takes into account V2G implementation, allowing both charging and discharging of EV batteries. This strategy allows the EVs to play the role of dynamic energy storage devices in order to provide several services to the power system, such as peak load shaving, load levelling and as solution for renewable energy shifting in the hours of peak load demand. The thesis describes the cost function optimization processes performed by the tool to define the charging/discharging profiles of EV batteries in both smart charging and V2G modes.
The modelling tool performs a techno-economic assessment of the modelled system applying the considered EV charging strategy and it also takes into account the cost of battery degradation; therefore, has been possible to evaluate the technical and economic feasibility of smart charging and V2G technology.
The results show that the most challenging strategy, that is V2G, is also the most profitable way to manage EV batteries from both EV owners' and system operators' point of view. It saves, in the assessed case study, about 6% of the overall operating costs of the electricity network, compared to the uncontrolled charging scenario, but considering only the costs related to EV management, V2G allows saving about 33% of those of uncontrolled charging.
As aforementioned, the case study considers a real distribution network, but all the information has been provided in confidential way, therefore anything that could allow an identification has been omitted in the thesis.
The modelling tool, as described in chapter 2 is based on some preliminary assumptions to define the characteristics of grid loads, for example, a "smart house" consists of one EV charger, one PV system and the power consumption. To establish the expected framework in the year 2050, the forecasted evolution of PV generation and number of houses in the UK have been considered as reference. Therefore, since the projections to the year 2050 in the UK state that the penetration of household PV will be around 15% and the number of houses will increase by around 17%, the number of EVs, taken into account in the electricity grid, is implicitly determined by those percentages. In summary, the EV implementation is directly related to the share of smart houses. A possible improvement in the tool could be to break this correlation and consider another input parameter to define the number of EV chargers installed in each grid load.
Moreover, another assumption considered by the tool is about the SOC of the EV batteries. Indeed, it is maintained between 30% and 80%, in order to preserve battery lifetime, as explained in the introduction chapter.

This tool evaluates the hourly availability of each electric vehicle at its charger, taking into account its daily trip schedule. In fact, an input parameter defines the share of household EVs that charge their battery at home, while the remaining EVs charge their battery in off-home charging infrastructures during the day, which means along the streets, at charging station or at work, before getting home from work. These off-home charges do not affect the electricity grid from an energy point of view, because it is impossible to decide in which nodes they are performed, due to the unpredictability of the trips. Therefore, it has been considered that this share of EVs charges the battery in nodes of other distribution networks; nevertheless, charging costs are taken into account in the economic assessment.

A possible improvement could be to consider the hourly space distribution of each vehicle in order to take accounts of more interactions with the electricity grid, but obviously, this requires much more information.

In the cases of smart charging and V2G strategy, the tool applies to each charger the optimized charging profile, without taking into account that the standard charging infrastructures currently in use cannot provide continuously controllable charging power, especially because of battery requirements. Therefore, another possible improvement could be to consider proper charging patterns in order to meet the batteries needs in terms of smooth DC voltage and current.

The modelling tool allows many other comparisons, which are not considered in this thesis, by changing the values of input parameters. For instance, an interesting assessment could be to investigate the variation of profitability caused by different shares of home charging or different levels of initial and final battery capacity and that reached after off-home charging.

It is important to stress that this tool is composed by several blocks, which are Matlab scripts; therefore, future work could easily allow the implementation of new features, such as advanced ancillary services, and system components, such as different typologies of generation.

In conclusion, Smart Grid Modelling Tool meets all initially planned goals of this thesis project, providing several opportunities to model and analyse different electricity grids in order to investigate the technical and economic feasibility of their operating conditions, considering three different EV charging strategies: uncontrolled, smart and V2G technology.

ACKNOWLEDGMENT

This thesis is the result of the work done during my Erasmus period at University of Northumbria at Newcastle upon Tyne, UK; an experience that will always remain alive in my heart for the several friendships born, for the chances and social realities I encountered, but also for the difficulties I had to face.
For this reason, I would like to thank all the people who welcomed me and helped me in this adventure. Above all, Prof. Ghanim Putrus, for giving me the opportunity to collaborate in an international working environment, then Dr. Yue Wang and Dr. Ridoy Das for their technical and moral support and, not least, the precious bond created during these months lived together.
A particular thank to Prof. Roberto Turri for his extraordinary helpfulness and trust in me and because, by offering us students the chance to live these important abroad experiences, allows us to grow not only from a professional and technical point of view, but also from a personal point of view.

RINGRAZIAMENTI

Questa tesi è frutto del lavoro svolto durante il periodo Erasmus presso Northumbria University di Newcastle upon Tyne, Inghilterra; un'esperienza che resterà sempre viva nel mio cuore per le numerose amicizie nate, per le opportunità e realtà che ho incontrato, ma anche per le difficoltà che ho dovuto affrontare.
Per questo desidero ringraziare tutte le persone che mi hanno accolto e che mi hanno aiutato in questa avventura, in primis il Prof. Ghanim Putrus, per avermi dato l'opportunità di collaborare in un ambito di lavoro internazionale, poi la Dr.ssa Yue Wang e il Dr. Ridoy Das per il loro sostegno tecnico e morale e, non ultimo, per il prezioso legame creatosi durante questi mesi trascorsi assieme.
Ringrazio in particolar modo anche il Prof. Roberto Turri per la sua straordinaria disponibilità e fiducia nei miei confronti e perché, offrendo a noi studenti l'opportunità di vivere queste importanti esperienze all'estero, ci permette di crescere non solo dal punto di vista professionale e tecnico, ma anche personale.

Un enorme grazie va a tutte quelle persone che in questi anni mi hanno incoraggiato nelle molteplici esperienze vissute e che non hanno mai smesso di camminare al mio fianco, dagli amici ai parenti, dai conoscenti agli insegnanti, dai più piccoli ai più esperti di vita.
Un affettuoso pensiero va a quanti hanno contribuito a scrivere importanti pagine della mia vita, ma che, purtroppo, oggi non possono essere qui per brindare a questo mio, ma anche loro, meraviglioso traguardo.
Il ringraziamento più speciale, che con le sole parole non è semplice da esprimere, va alla mia famiglia che mi ha educato e cresciuto con valori molto solidi, che mi impegno a mantenere vivi ogni giorno. A mamma Sandra e papà Gianfranco che, con notevoli sacrifici, mi hanno sempre appoggiato e sostenuto nel raggiungimento di importanti obiettivi, come questa laurea in Ingegneria; e a mia sorella Erika per i suoi preziosi consigli e pareri e per l'instancabile presenza.

Questi mesi passati all'estero, lontano dalla mia quotidianità, mi hanno permesso di capire ancora più profondamente quanto sono fortunato ad avere nella mia vita persone così meravigliose, grazie a tutti!!!

REFERENCES

[1] U.S. Energy Information Administration (EIA), "International Energy Outlook 2016," *International Energy Outlook 2016*, 2016. [Online]. Available: https://www.eia.gov/outlooks/ieo/pdf/0484(2016).pdf.

[2] J. Munkhammar, J. D. K. Bishop, J. J. Sarralde, W. Tian, and R. Choudhary, "Household electricity use, electric vehicle home-charging and distributed photovoltaic power production in the city of Westminster," *Energy Build.*, vol. 86, pp. 439–448, 2015.

[3] J. Zhong *et al.*, "Coordinated control for large-scale EV charging facilities and energy storage devices participating in frequency regulation," *Appl. Energy*, vol. 123, pp. 253–262, 2014.

[4] H. L. Ferreira, R. Garde, G. Fulli, W. Kling, and J. P. Lopes, "Characterisation of electrical energy storage technologies," *Energy*, vol. 53, pp. 288–298, 2013.

[5] R. E. P. N. for the 21st C. (REN21), "Renewables 2017," *Renewables 2017*, 2017. [Online]. Available: http://www.ren21.net/wp-content/uploads/2017/06/GSR2017_Full-Report.pdf.

[6] European Commission, "A Roadmap for moving to a competitive low carbon economy in 2050," *A Roadmap for moving to a competitive low carbon economy in 2050*, 2011. [Online]. Available: http://eur-lex.europa.eu/legal-content/EN/TXT/PDF/?uri=CELEX:52011DC0112&from=EN.

[7] P. Codani, P.-L. Le Portz, P. Claverie, M. Petit, and Y. Perez, "Coupling local renewable energy production with electric vehicle charging : a survey of the French case," *Int. J. Automot. Technol. Manag.*, vol. 16, no. x, pp. 1–11, 2016.

[8] K. M. Tan, V. K. Ramachandaramurthy, and J. Y. Yong, "Integration of electric vehicles in smart grid: A review on vehicle to grid technologies and optimization techniques," *Renew. Sustain. Energy Rev.*, vol. 53, pp. 720–732, 2016.

[9] J. Wu, J. Ekanayake, and K. Samarakoon, "Frequency response from electric vehicales," *Communications*, no. c, pp. 148–152, 2011.

[10] International Energy Agency (IEA), "Global EV Outlook 2017: Two million and counting," *Global EV Outlook 2017*, 2017. [Online]. Available: https://www.iea.org/publications/freepublications/publication/GlobalEVOutlook2017.pdf.

[11] Q. Wang, X. Liu, J. Du, and F. Kong, "Smart Charging for Electric Vehicles: A Survey from the Algorithmic Perspective," *IEEE Commun. Surv. Tutorials*, vol. 18, no. 2, pp. 1500–1517, 2016.

[12] L. Mihet-popa, "Minimization of Load Variance in Power Grids—Investigation on Optimal Vehicle-to-Grid Scheduling," *Energies*, no. November, 2017.

[13] X. Luo, J. Wang, M. Dooner, and J. Clarke, "Overview of current development in electrical energy storage technologies and the application potential in power system operation," *Appl. Energy*, vol. 137, pp. 511–536, 2015.

[14] E. Bentley, G. Putrus, and G. Lacey, "A modelling tool for distribution networks to demonstrate smart grid solutions," *2014 IEEE Veh. Power Propuls. Conf. VPPC 2014*, 2014.

[15] G. A. Putrus, P. Suwanapingkarl, D. Johnston, E. C. Bentley, and M. Narayana, "Impact of Electric Vehicles on Power Distribution Networks," *2009 IEEE Veh. Power Propuls. Conf.*, no. September, pp. 827–831, 2009.

[16] R. H. Ashique, Z. Salam, M. J. Bin Abdul Aziz, and A. R. Bhatti, "Integrated photovoltaic-grid dc fast charging system for electric vehicle: A review of the architecture and control," *Renew. Sustain. Energy Rev.*, vol. 69, no. November 2016, pp. 1243–1257, 2017.

[17] C. Weiller and A. Neely, "Using electric vehicles for energy services: Industry

perspectives," *Energy*, vol. 77, pp. 194–200, 2014.
[18] W. Kempton and J. Tomić, "Vehicle-to-grid power fundamentals: Calculating capacity and net revenue," *J. Power Sources*, vol. 144, no. 1, pp. 268–279, 2005.
[19] D. Connolly, H. Lund, B. V. Mathiesen, E. Pican, and M. Leahy, "The technical and economic implications of integrating fluctuating renewable energy using energy storage," *Renew. Energy*, vol. 43, pp. 47–60, 2012.
[20] V. V. Viswanathan and M. Kintner-Meyer, "Second use of transportation batteries: Maximizing the value of batteries for transportation and grid services," *IEEE Trans. Veh. Technol.*, vol. 60, no. 7, pp. 2963–2970, 2011.
[21] J. Schmalstieg, S. Käbitz, M. Ecker, and D. U. Sauer, "A holistic aging model for Li(NiMnCo)O2 based 18650 lithium-ion batteries," *J. Power Sources*, vol. 257, pp. 325–334, 2014.
[22] J. D. K. Bishop, C. J. Axon, D. Bonilla, M. Tran, D. Banister, and M. D. McCulloch, "Evaluating the impact of V2G services on the degradation of batteries in PHEV and EV," *Appl. Energy*, vol. 111, pp. 206–218, 2013.
[23] F. Mwasilu, J. J. Justo, E. K. Kim, T. D. Do, and J. W. Jung, "Electric vehicles and smart grid interaction: A review on vehicle to grid and renewable energy sources integration," *Renew. Sustain. Energy Rev.*, vol. 34, pp. 501–516, 2014.
[24] S. Han, S. Han, and K. Sezaki, "Estimation of achievable power capacity from plug-in electric vehicles for V2G frequency regulation: Case studies for market participation," *IEEE Trans. Smart Grid*, vol. 2, no. 4, pp. 632–641, 2011.
[25] N. Shaukat *et al.*, "A survey on electric vehicle transportation within smart grid system," *Renew. Sustain. Energy Rev.*, vol. 81, no. February 2016, pp. 1329–1349, 2018.
[26] H. Shareef, M. M. Islam, and A. Mohamed, "A review of the stage-of-the-art charging technologies, placement methodologies, and impacts of electric vehicles," *Renew. Sustain. Energy Rev.*, vol. 64, pp. 403–420, 2016.
[27] B. Soares M.C. Borba, A. Szklo, and R. Schaeffer, "Plug-in hybrid electric vehicles as a way to maximize the integration of variable renewable energy in power systems: The case of wind generation in northeastern Brazil," *Energy*, vol. 37, no. 1, pp. 469–481, 2012.
[28] K. Shimizu, T. Masuta, Y. Ota, and A. Yokoyama, "Load frequency control in power system using vehicle-to-grid system considering the customer convenience of electric vehicles," *2010 Int. Conf. Power Syst. Technol. Technol. Innov. Mak. Power Grid Smarter, POWERCON2010*, pp. 1–8, 2010.
[29] European Union, "Interreg Europe." [Online]. Available: https://www.interregeurope.eu/.
[30] European Union and North Sea Region, "SEEV4-City," 2014. [Online]. Available: http://www.northsearegion.eu/seev4-city/.
[31] MathWorks, "MATLAB & Simulink R2016a." Natick, MA, USA, 2016.
[32] Department of Trade and Industry, "Guidance on The Electricity Safety, Quality and Continuity Regulations 2002," *Rep. Number URN 02/1544*, no. October, pp. 1–47, 2002.
[33] C. Deziel, "How to Convert Distances From Degrees to Meters," *Sciencing*, 2018. [Online]. Available: http://sciencing.com/convert-distances-degrees-meters-7858322.html.
[34] MathWorks, "User's Guide," *MathWorks documentation*, 2018. [Online]. Available: https://it.mathworks.com/help/simulink/.
[35] G. Lacey, G. Putrus, E. Bentley, D. Johnston, S. Walker, and T. Jiang, "A modelling tool to investigate the effect of electric vehicle charging on low voltage networks," *2013 World Electr. Veh. Symp. Exhib.*, pp. 1–7, 2013.
[36] V. Monteiro, H. Goncalves, and J. L. Afonso, "Impact of electric vehicles on power quality in a Smart Grid context," *Proceeding Int. Conf. Electr. Power Qual. Util.*

EPQU, no. September, pp. 660–665, 2011.
[37] UK Government, "Solar Photovoltaics Deployment in the UK."
[38] R. Gough, P. Speers, and V. Lejona, "Evaluating the Benefits of Vehicle-to-Grid in a Domestic Scenario," *EVS30 Symp.*, 2017.
[39] Vehicle Certification Agency, "The Worldwide Harmonised Light Vehicle Test Procedure (WLTP)," 2017. [Online]. Available: http://www.dft.gov.uk/vca/fcb/wltp.asp.
[40] E. Apostolaki-Iosifidou, P. Codani, and W. Kempton, "Measurement of power loss during electric vehicle charging and discharging," *Energy*, vol. 127, pp. 730–742, 2017.
[41] ICF Consulting Services, "Overview of the Electric Vehicle Market and the Potential of Charge Points for Demand Response," *ICF Consult. Serv.*, no. March, pp. 1–32, 2016.
[42] Office for National Statistics, "Households in the UK," *Freedom of Information*, 2016. [Online]. Available: https://www.ons.gov.uk/aboutus/transparencyandgovernance/freedomofinformationfoi/householdsintheuk.
[43] National Grid, "Future Energy Scenarios - July 2017," *Futur. Energy Scenar.*, 2017.
[44] P. D. United Nations, Department of Economic and Social Affairs, "UK Population Pyramids," 2017. [Online]. Available: https://www.populationpyramid.net/united-kingdom/.

APPENDIX

Tab. A.1 Workspace variables

- Costs_arch: total electricity operational costs in each network node
- Costs_PLoss: power loses costs in each network line;
- Costs_sh: electricity operational costs of smart households in each network node;
- Costs_sind: electricity operational costs of smart industries in each network node;
- Costs_sp: electricity operational costs of smart car parks in each network node;
- Costs_ss: electricity operational costs of smart shops in each network node;
- Costs_ssc: electricity operational costs of smart schools in each network node;
- Costs_th: electricity operational costs of traditional households in each network node;
- Costs_tind: electricity operational costs of traditional industries in each network node;
- Costs_tot: total electricity network operational costs;
- Costs_ts: electricity operational costs of traditional shops in each network node;
- Costs_tsc: electricity operational costs of traditional schools in each network node;
- dpuE: hourly line to ground voltage deviation (pu) matrix per phase of each network node;
- dV: hourly voltage drop matrix in each network line;
- Ebuses: hourly line to ground voltage matrix per phase of each network node;
- EVi_ind: total Industries' EVs (single-phase and three-phase) in each network node;
- EVi_p: total car parks' EVs (single-phase and three-phase) in each network node;
- EVph_h: matrix of total single-phase household EVs per phase of each network node;
- EVph_ind: matrix of single-phase industries' EVs per phase of each network node;
- EVph_p: matrix of single-phase car parks' EVs per phase of each network node;
- EVph_s: matrix of single-phase shops' EVs per phase of each network node;
- EVph_sc: matrix of single-phase schools' EVs per phase of each network node;
- EVtri_ind: number of three-phase industries' EVs in each network node;
- EVtri_p: number of three-phase car parks' EVs in each network node;
- Ibranches: hourly line current matrix per phase of each network branch;
- Ipu: hourly line current magnitude (pu) matrix per phase of each network branch;
- magE: hourly line to ground voltage magnitude matrix per phase of each network node;
- magI: hourly line current magnitude matrix per phase of each network branch;
- magV: hourly line to line voltage magnitude matrix per phase of each network node;
- maxI: vector of maximum current magnitudes per each network line;
- nEVph_h: matrix of single-phase household EVs, which charge at home, per phase of each network node;
- nEVph_nh: matrix of single-phase household EVs, which charge off-home, per phase of each network node;
- nPVph_h: matrix of single-phase household PV per phase of each network node;
- nPVph_p: matrix of single-phase car parks' PV per phase of each network node;
- nPVph_s: matrix of single-phase shops' PV per phase of each network node;
- nPVtri_h: number of three-phase household PV in each network node;
- nPVtri_ind: matrix of three-phase industries' PV in each network node. First row is related to the number of 25 kW PV, second row of 60 kW PV.
- nPVtri_p: number of three-phase car parks' PV in each network node;
- nPVtri_s: number of three-phase shops' PV in each network node;

- nPVtri_sc: matrix of three-phase schools' PV in each network node. First row is related to the number of 10 kW PV, second row of 12 kW PV.
- PEV23_ind: hourly industries' 23 kW EV's charger power matrix per phase of each node;
- PEV23_p: hourly car parks' 23 kW EV's charger power matrix per phase of each node;
- PEV3_h: hourly household 3 kW EV's charger power matrix per phase of each node;
- PEV3_sc: hourly schools' 3 kW EV's charger power matrix per phase of each node;
- PEV50_p: hourly car parks' 50 kW EV's charger power matrix per phase of each node
- PEV7_h: hourly household 7 kW EV's charger power matrix per phase of each node;
- PEV7_ind: hourly industries' 7 kW EV's charger power matrix per phase of each node;
- PEV7_p: hourly car parks' 7 kW EV's charger power matrix per phase of each node;
- PEV7_s: hourly shops' 7 kW EV's charger power matrix per phase of each node;
- PEV7_sc: hourly schools' 7 kW EV's charger power matrix per phase of each node;
- PEV_h: overall hourly household EV's charger power matrix per phase of each node;
- PEV_ind: overall hourly industries'' EV's charger power matrix per phase of each node;
- PEV_p: overall hourly car parks' EV's charger power matrix per phase of each node;
- PEV_s: overall hourly shops' EV's charger power matrix per phase of each node;
- PEV_sc: overall hourly schools' EV's charger power matrix per phase of each node;
- PEVtri23_p: hourly car parks' 23 kW EV's charger power matrix of each node;
- PEVtri50_p: hourly car parks' 50 kW EV's charger power matrix of each node;
- PEVtri_ind: hourly industries' EV's charger power matrix of each node;
- PEVtri_p: overall hourly car parks' EV's charger power matrix of each node;
- phiE: hourly line to ground voltage phase matrix per phase of each network node;
- phiI: hourly line current phase matrix per phase of each network branch;
- phiV: hourly line to line voltage phase matrix per phase of each network node;
- puE: hourly line to ground voltage magnitude (pu) matrix per phase of each network node;
- P: hourly three-phase active power matrix of each network node;
- Ploss: hourly active power losses matrix per phase of each network branch;
- Psph: hourly phase's active power matrix per phase of each network node;
- Pwbuses: hourly phase's apparent power matrix per phase of each network node;
- PwPVph46_h: single-phase household PV's power matrix per phase of each node;
- PwPVph46_s: single-phase shops' PV's power matrix per phase of each node;
- PwPVph8_p: single-phase car parks' PV's power matrix per phase of each node;
- PwPVtri12_h: three-phase household PV's power matrix of each node;
- PwPVtri12_s: three-phase shops' PV's power matrix of each node;
- PwPVtri16_p: three-phase car parks' PV's power matrix of each node;
- PwPVtri_ind: three-phase industries' PV's power matrix of each node;
- PwPVtri_sc: three-phase schools' PV's power matrix of each node;
- Q: hourly three-phase reactive power matrix of each network node;
- Qsph: hourly phase's reactive power matrix per phase of each network node;
- S: hourly three-phase apparent power matrix of each network node;
- smarthouseph: matrix of smart houses per phase of each network node;
- tradhouseph: matrix of traditional houses per phase of each network node;
- Vbuses: hourly line to line voltage matrix per phase of each network node;
- XEV23_ind: hourly EVs availability matrix at 23 kW industries' EV chargers per phase of each node;

- XEV23_p: hourly EVs availability matrix at 23 kW car parks' EV chargers per phase of each node;
- XEV3_h: hourly EVs availability matrix at 3 kW household EV chargers per phase of each node;
- XEV3_sc: hourly EVs availability matrix at 3 kW schools' EV chargers per phase of each node;
- XEV50_p: hourly EVs availability matrix at 50 kW car parks' EV chargers per phase of each node;
- XEV7_h: hourly EVs availability matrix at 7 kW household EV chargers per phase of each node;
- XEV7_ind: hourly EVs availability matrix at 7 kW industries' EV chargers per phase of each node;
- XEV7_p: hourly EVs availability matrix at 7 kW car parks' EV chargers per phase of each node;
- XEV7_s: hourly EVs availability matrix at 7 kW shops' EV chargers per phase of each node;
- XEV7_sc: hourly EVs availability matrix at 7 kW schools' EV chargers per phase of each node;
- XEV_h: overall hourly EVs availability matrix at household EV chargers per phase of each node;
- XEV_ind: overall hourly EVs availability matrix at industries' EV chargers per phase of each node;
- XEV_p: overall hourly EVs availability matrix at car parks' EV chargers per phase of each node;
- XEV_s: overall hourly EVs availability matrix at shops' EV chargers per phase of each node;
- XEV_sc: overall hourly EVs availability matrix at schools' EV chargers per phase of each node.

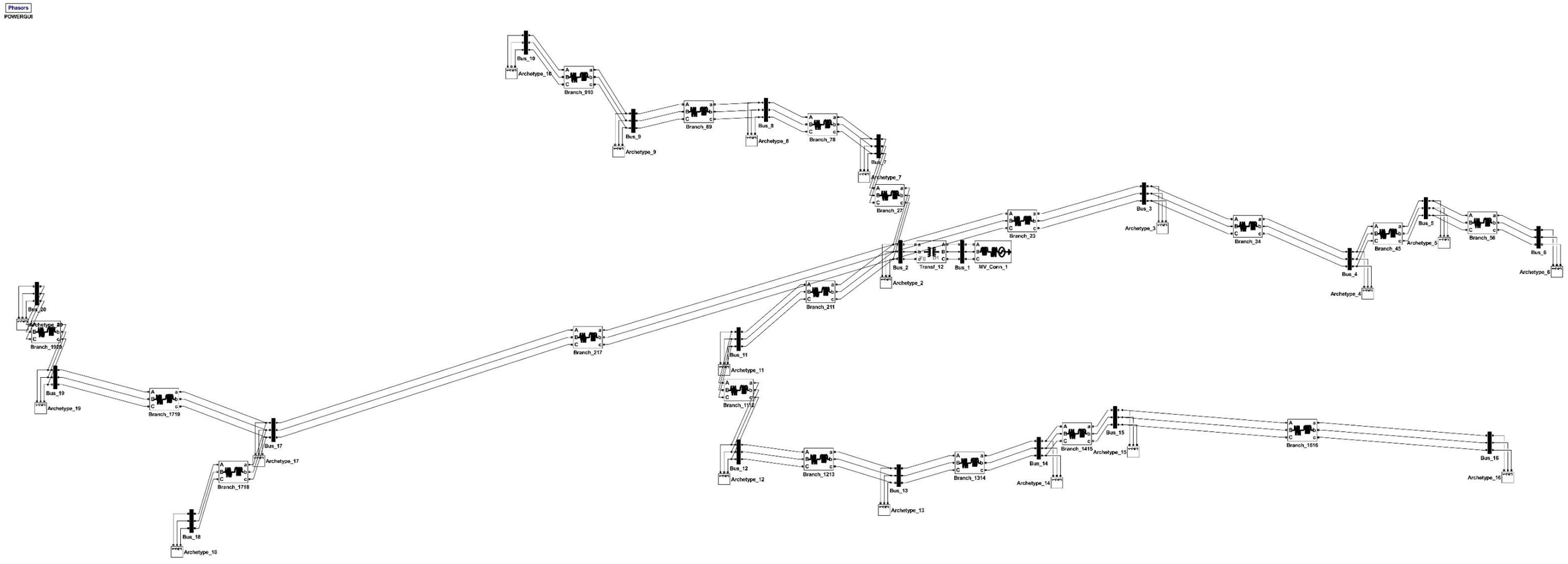

Fig. A.1 Simulink representation of the Electricity grid